TAMPEREEN TEKNILLINEN YLIOPISTO
TAMPERE UNIVERSITY OF TECHNOLOGY

JAAKKO PAAVOLA

PREDICTING A FLYBACK CONVERTER'S RADIATED EMISSIONS BASED ON MEASUREMENTS OF ITS NEAR FIELD AND TRANSFORMER

Master of Science Thesis

Examiner: Professor Teuvo Suntio
Examiner and topic approved in the Faculty of Computing and Electrical Engineering Council meeting on
4 May 2011

ABSTRACT

TAMPERE UNIVERSITY OF TECHNOLOGY
Master's Degree Programme in Electrical Engineering
PAAVOLA, JAAKKO: Predicting a Flyback Converter's Radiated Emissions Based on Measurements of its Near Field and Transformer
Master of Science Thesis, 98 pages, 21 appendix pages
July 2013
Major: Power Electronics
Examiner: Professor Teuvo Suntio
Keywords: EMC, electromagnetic compatibility, EMI, interference, SMPS, switch mode power supply, switching converter, flyback, pre-compliance measurement, radiated emissions test, radiation, noise, disturbance

Chargers and power supplies of household appliances almost always incorporate switched mode power supply technologies, such as the flyback topology. An inherent problem with electric products using power switching technologies is their inadvertent generation of electromagnetic emissions. Also, there may be great variation in the levels of electromagnetic emissions between different specimens of a given product. This variation is normally due to variation in the physical structure and materials of the electric product's components, that is, due to variation in its components' homogeneity. Such variation in the quality of the switching converter's transformer component can account for much of the variation in the electromagnetic emissions.

The true levels of a given product's electromagnetic emissions can be determined using standard electromagnetic emissions tests. However, these tests are not suitable for screening out sub-standard specimens in the manufacturing process because they are time-consuming and require expensive measurements. Instead, indirect methods of predicting electromagnetic emissions must be used for such screening purposes. The research described in this paper aims to discover a quick and inexpensive method for predicting the radiated emission levels of a flyback charger equipped with a given transformer.

The research showed that the use of certain indirect measurements in the transformer's association could be used to predict the true radiated emission levels with some accuracy. I analyzed the measurement readouts of four near-field probes, two of which were magnetic-field probes measuring the magnetic field near the transformer and the other two current probes measuring the magnetic field around the input and the output conductors of the charger. I also analyzed an assortment of electrical and physical properties' measurement readouts measured directly from the transformer. The analysis was mainly correlation computations between the readouts of the above measurements and those of the standard radiated emissions test for the same charger and transformer combination. The analysis revealed that the measurements of all four near-field probes and of various electrical properties all showed a clear correlation with the radiated emissions. The strongest correlation was obtained with the current probe measurements, as was expected from the literature.

Nevertheless, the discovered results are difficult to apply in practice, such as a production line test that screens out sub-standard transformers. This is because although correlations are evident from the results, their degree is not sufficient for creating a general rule for rejecting specimens based on fixed tolerance limits. Successful development of such a quality control procedure calls for a follow-up research focusing on enhancing the measurement accuracy and more elaborate data analysis methods.

TIIVISTELMÄ

TAMPEREEN TEKNILLINEN YLIOPISTO
Sähkötekniikan koulutusohjelma
PAAVOLA, JAAKKO: Predicting a Flyback Converter's Radiated Emissions Based on Measurements of its Near Field and Transformer
Diplomityö, 98 sivua, 21 liitesivua
Heinäkuu 2013
Pääaine: Tehoelektroniikka
Työn tarkastaja: Professori Teuvo Suntio
Avainsanat: EMC, sähkömagneettinen yhteensopivuus, EMI, häiriö, hakkuri, konvertteri, teholähde, flyback, pre-compliance, säteilevät häiriöt, emissiot, häiriötestit

Kotitalouksien sähkölaitteiden teholähteet ja laturit hyödyntävät lähes aina hakkuriteknologioita, kuten esimerkiksi flyback-topologiaa, toiminnassaan. Hakkuriteknologioille ominainen ongelma on niiden sivutuotteenaan synnyttämät merkittävät sähkömagneettiset emissiot. Lisäksi yhden hakkureita käyttävän sähkölaitteen eri yksilöiden tuottamat emissiot voivat erota suuresti toisistaan. Yleensä erot johtuvat vaihtelusta sähkölaitteen komponenttien fyysisessä rakenteessa ja materiaaleissa, eli vaihtelusta sen komponenttien tasalaatuisuudessa. Tällainen vaihtelu hakkurin muuntajakomponentin laadussa voi suurelti selittää sähkölaitteen yksilöiden väliset erot sähkömagneettisissa emissioissa.

Sähkölaitteen sähkömagneettiset emissiot voidaan määrittää standardinmukaisilla sähkömagneettisten häiriöiden testeillä. Nämä testit eivät kuitenkaan sovi seulomaan heikkolaatuisia yksilöitä tuotantoprosessissa, sillä ne vaativat aikaavieviä ja kalliita mittauksia. Niiden sijaan seulontaan täytyy käyttää epäsuoria menetelmiä ennustaa sähkömagneettisia emissioita. Tässä paperissa esiteltävän tutkimuksen tavoitteena on kehittää nopea ja edullinen menetelmä ennustaa flyback-laturin säteileviä emissioita sen mukaan mikä muuntajayksilö siihen on kytkettynä.

Tutkimus osoitti, että muuntajan yhteydessä tehdyt tietyt epäsuorat mittaukset voivat ennustaa säteileviä emissioita tiettyjen tarkkuuksien rajoissa. Tutkimuksessa analysoitiin mittauslukemia neljästä lähikenttäanturista, joista kaksi oli muuntajan lähellä magneettikenttää mittaavia magneettikenttäantureita ja kaksi laturin sisäänmeno- ja ulostulokaapelien ympäriltä magneettikenttää mittaavia virta-antureita. Tutkimuksessa analysoitiin myös suoraan muuntajasta mitattujen sähköisten ja fyysisten ominaisuuksien mittauslukemia. Analyysi oli etupäässä edellämainittujen mittausten ja samalla laturi-muuntaja -yhdistelmällä mitatun standardinmukaisen säteilevien häiriöiden testin mittauslukemien korrelaatioiden määrittämistä. Analyysi osoitti, että kaikkien neljän lähikenttäanturin sekä useiden muuntajan sähköisten ominaisuuksien mittauslukemilla oli selvää korrelaatiota säteilevien emissioiden kanssa. Voimakkain korrelaatio saatiin virta-anturimittauksilla, kuten lähdekirjallisuudesta saattoi olettaa.

Havaittuja tuloksia on silti vaikeaa soveltaa käytäntöön esimerkiksi tuotantolinjan varrella sijaitsevan, heikkolaatuisia muuntajia seulovan testin muodossa. Nimittäin vaikka tutkimuksen tulokset selvästi todistavat korrelaatioista, korrelaatioiden aste ei ole tarpeeksi suuri, jotta voitaisiin suoraan luoda yleispätevä sääntö, joka seuloo muuntajayksilöitä toleranssirajoihin perustuen. Tällaisen laadunvalvontaprosessin onnistunut kehittäminen vaatii jatkotutkimusta, joka keskittyy parantamaan mittaustarkkuutta ja data-analyysimenetelmiä.

PREFACE

Firstly, I would like to thank the two people who most influenced this work, the supervisor and the examiner. I would like to thank my supervisor from Salcomp, VP of R&D Juha Raussi who signed me up for this job. He also provided the research problem, test equipment and facilities, and sent me to Shenzhen, China to build samples and to conduct the radiated emissions tests. I would like to similarly thank my examiner from Tampere University of Technology, Prof. Teuvo Suntio, for helping with the starting points of the research and for encouragement during the writing process, which was prolonged significantly due to my acceptance of a full-time post in Salcomp in 2012.

Secondly, there are many others that influenced the work. I would like to thank the people in Salcomp Shenzhen: Jarkko for being the local facilitator for my work, Aman's magnetic engineering team for the help with the measurement box and the transformers, Aung's lab team for conducting the radiated emissions tests, sourcing team for helping with the transformer suppliers and samples, Christopher's prototype team for building charger samples, Leon's R&D team for helping to define the transformer property measurements and Lily's IQC team for conducting them. The R&D guys in Salcomp Salo helped me a lot especially with the near-field probe measurements, thanks Jarmo, Jani and others. Thanks go also to HR and administrative people for all the arrangements and also to all those colleagues who showed curiosity toward my work and encouraged me along the way on those coffee and lunch breaks, and in the shared commuter car. Also thanks to Mikko and Jope for the help with the data handling and the algorithms.

I absolutely must thank my parents, Pirkko and Pekka, my grandfather Aimo, and the rest of my family for the great support and encouragement during the writing process. Kalle and other friends, thanks for taking my mind off the thesis when I needed it, and also for the peer support. Thanks to Benjamin for proofreading and curiosity toward the paper. Finally a special thanks to Wei Wei for enduring numerous weekends at home, keeping me company during the writing of the paper.

Jaakko Paavola
26th July 2013

CONTENTS

ABBREVIATIONS AND NOTATION

μ, μ_0, μ_R	Permeability, the permeability of free space, and the relative permeability normalized to μ_0, respectively. Unit *H/m*.
ε, ε_0, ε_R	Permittivity, the permittivity of free space, and the relative permittivity normalized to ε_0, respectively. Unit *F/m*.
σ	Conductivity. Unit *S/m*.
ϕ	Magnetic flux. Unit *Wb*.
Ω	Ohm, the unit of impedance.
ω, f	Angular frequency, unit rad/s, and frequency, unit *Hz* or *cycles*/*s*, respectively.
$\bar{E}$/*E*, $\bar{D}$/*D*	Electric field strength, unit *V/m*, and electric flux density, unit C/m^2, respectively.
$\bar{H}$/*H*, $\bar{B}$/*B*	Magnetic field strength, unit *A/m*, and magnetic flux density, unit *T* or Wb/m^2, respectively.
capacitive coupling/ electric coupling	A type of electromagnetic coupling that is associated with electric fields.
characteristic wave impedance	The ratio of an electric and a magnetic field quantity or circuit quantity in a given homogenous material.
circuit analysis/lumped element analysis	A collection of simplifying techniques of the comprehensive theory of electromagnetism suitable for analysing circuits at low frequencies.
common-mode	Voltage or current that exists with regard to the ground reference.
conducted emissions	Electromagnetic emissions that are conveyed to a “victim” conductor through near-field coupling.
conductive coupling	Near-field coupling that happens through movement of charge carriers and associated electric and magnetic fields.
desired signal	An electromagnetic signal with only the ideal, intended content, as opposed to a noise signal.
dielectric material	Material that is ”favorable” for electromagnetic energy to reside and propagate in as electric field energy.
differential-mode	Voltage or current that exists with regard to intentional conductors of the given current loop.
displacement current	A manifestation of current in an electrodynamic situtation in addition to moving charge carriers of conductive currents.
DM-to-CM conversion	In an unbalanced circuit, a phenomenon that creates common-mode electromagnetic energy from differential-mode electromagnetic energy.
electrical length	A length equal to or longer than the conductor’s physical length due to the effect of inductance or capacitance.

electrodynamic	Electromagnetic field's state in which the field's history must be known to be able determine the state of a conductor within it at a given point in time.
electromagnetic emissions	Electromagnetic energy that is created and spread into the surroundings by a source/emitter.
electromagnetic compatibility (EMC)	A discipline or a collection of rules that aim to prevent malfunction of devices due to electromagnetic energy.
electromagnetic disturbance/noise	Electromagnetic energy that forms a noise signal in a receptor/receiver; originates from external source/emitters or from the receptor/receiver's intrinsic sources.
electromagnetic energy	A manifestation of energy that can be explained by photons and quantum physics.
electromagnetic interference (EMI)	Malfunction caused by electromagnetic disturbance/noise and the associated noise signals.
electrostatic	Electromagnetic field's state in which the field's history does not need to be known to be able to determine the state of a conductor within it at any point in time.
electromagnetic coupling	Transfer of electromagnetic energy through electric and/or magnetic field.
electromagnetic far-field coupling	Transfer of electromagnetic energy through electromagnetic plane wave/transverse electromagnetic wave.
electromagnetic near-field coupling	Transfer of electromagnetic energy through electric and/or magnetic near field.
electromagnetic wave	Fluctuation of the electric and/or the magnetic field and their bound energy in electrodynamic or quasi-electrostatic state.
extrinsic capacitance	Capacitance between charges, that is, mutual capacitance.
extrinsic inductance	Inductance between conductors, that is, mutual inductance.
extrinsic coupling/ mutual coupling	Electromagnetic coupling through extrinsic capacitance or extrinsic inductance.
far field	The part of electromagnetic field far enough from its source/emitter so that the electromagnetic energy in it has "broken free" from its sphere of influence.
flyback topology	A switching mode converter design popular in chargers.
full wave analysis	A collection of techniques for comprehensive analysis of electromagnetic phenomena at any frequency.
fundamental frequency	A waveform's lowest frequency component, which in switching converters equals the switching frequency.
ground loop	A current loop for noise driven by a noise voltage normally caused by a stray ground current in the ground reference; often "closed" by a capacitive path to the ground reference.

ground reference	From a current loop's standpoint, all unintentional conductors collectively within its near field.
harmonics/sinusoidal components	A waveform's "building blocks" or components, which superimposed together form the waveform.
inductive coupling/ magnetic coupling	A type of electromagnetic coupling that is associated with magnetic fields.
intrinsic capacitance/ inductance	Capacitance/inductance that a conductor always has, even by itself, regardless of other conductors in its surroundings.
magnetic material	Material that is "favorable" for electromagnetic energy to reside and propagate in as magnetic field energy.
near field/induction field/induction region	Electromagnetic field so close to its source/emitter that the electromagnetic energy in it is bound to the source/emitter.
noise signal	An electromagnetic signal with only unintentional noise content from noise sources, as opposed to a desired signal.
parasitic impedance	A manifestation of an unintentional near-field coupling path within a given entity (component, circuit, device, system).
receptor/receiver	An object/device that receives electromagnetic emissions.
resonance/anti-resonance	A phenomenon resulting from a standing wave, in which a transmission line's input impedance is rendered zero (resonance) or infinite (anti-resonance).
return conductor	A current loop's conductor that connects the electricity source to the load on the high-potential side.
send/go conductor	A current loop's conductor that connects the electricity source to the load on the low-potential side.
signal integrity (SI)	A discipline that observes non-idealities of a signal when they travel from the electricity source to the load.
source/emitter	An object/device that produces electromagnetic emissions.
stray impedance	A manifestation of an unintentional near-field coupling path between a given entity and its surroundings.
switch mode power supply (SMPS)	A power supply based on switching mode operation by its switching devices.
switching device	A component that can switch its impedance rapidly between very low and very high, for example a transistor or a diode.
switching transformer	A transformer used in switching mode power supplies.
transmission line analysis	A collection of techniques used for high-frequency analysis of a current loop.
transverse electromagnetic (TEM) wave	Electromagnetic wave that has assumed a plane wave mode of propagation; usually interchangeably used with "electromagnetic plane wave" or just "plane wave".
wave impedance	The ratio of an electric and a magnetic field quantity or circuit quantity at any given point.

1 INTRODUCTION

The past one hundred years has seen a proliferation of electric and electronic devices, and the pace of their growth in the contemporary world is ever faster. Not only does the number of these devices around us increase, but the electric circuits and components are also packed ever more densely and operated with ever higher frequencies to attain a higher performance and a smaller size. This is generally considered positive progress, because the direction is towards a future in which technology provides us with more entertainment, welfare, comfort, emancipation from routine tasks, and even healthier and longer lives. However, this progress also undisputedly affects the environment.

In addition to the obvious impacts of the electric and electronics industry on the environment in the form of particle emissions, waste production, and consumption of natural resources, there is also a less-known impact: *electromagnetic* (EM) *emissions* caused on the *electromagnetic environment*. The EM environment is a concept that pertains to the *EM net field*, the totality of all the *electromagnetic energy* – intentional and unintentional, natural and man-made – in our surroundings. The preferred state of the EM environment is the "natural" one, that is, as it exists without man-made emissions, apart from intentional emissions at regulated frequencies and power levels, such as communications broadcasts and other signals that serve a purpose and are under regulatory control.

Man-made EM emissions are mainly created by operation of electrical appliances. All electrical, electromechanical and electronic activities always involve *propagation of EM energy*, and consequently they always cause EM emissions, which are usually unintentional. Some electrical appliances, such as radio transmitters and radars, produce intentional EM emissions as a fundamental part of their operation, but part of their emissions are also unintentional. There are also natural sources of EM emissions, such as solar and lightning radiation. *Intrinsic noise sources*, such as *thermal noise* and *shot noise*, which arise from random *fluctuations* of charge carriers within conductive structures, are also a natural source of EM emissions [**1**]. Fluctuation means motion that is constantly changing state: accelerating, breaking, and/or changing direction. When a charge carrier fluctuates, there always are fluctuating electric and magnetic fields associated with it. Fluctuating fields, in turn, imply that some EM energy is detached from the charge carriers' sphere of influence by radiating into the surroundings.

Switch mode power supplies (SMPS's) are today's power supplies of choice in most DC voltage-fed applications. During the past decades, SMPS's have effectively made the old-fashioned *linear power supplies* obsolete in all but the cheapest and most low-

power applications. This is due to the unbeatable *efficiency ratio* and the compact size of SMPS's, as compared with those of linear power supplies, for dealing with wattages of common domestic appliances or higher.

However, the SMPS's advantages come with a price: higher EM emissions. As Armstrong [**2**] states: "all power switching technologies generate a lot of electrical 'noise', from their basic switching frequency and all of its various harmonics up to radio frequencies". Once we realize that "almost every (electrical) product, system, vehicle or installation now contains at least one switch-mode or PWM (pulse width modulated power switching) converter, even the tiniest iPod, and a typical cellphone or notebook computer has several" [**2**], we begin to understand the impact of power switching technologies on the EM environment.

SMPS's are inherently emission generative. This stems from the intrinsic nature of switched mode operation, in which pulsating current and voltage waveforms at the frequency of the switching action play a central part. Pulsating waveforms implies that there are fast current and voltage *transients*, and further, significant high-reaching harmonic content, that is, high-order multiples of the fundamental switching frequency, also called high-frequency components. Significant high-frequency current and voltage components are prone to produce EM emissions into the surroundings, as will be explained later in this paper.

This paper concerns a study on the EM emissions of a commercial *flyback* cell phone charger as a commission from its manufacturer, *Salcomp PLC*. Flyback is a transformer-isolated *switch mode converter topology* that is commonly used in cell phone chargers. The manufacturer assumed the transformer component, the *switching transformer*, to be the most decisive component in causing deviation in measured EM emissions between different charger specimens. The assumption was based on the fact that switching transformers inherently contain emission-producing structural properties which are likely to exhibit significant variation in the transformer manufacturing process. Appendix A shows X-ray pictures of the studied transformer samples, demonstrating the structural variation.

Regulatory authorities' *electromagnetic compatibility* (EMC) standards define exact requirements for EMC test set-ups and results, including those of EM emissions tests. By successfully meeting the regulatory authorities' requirements, an electric or electronics product is eligible to be marketed and sold in the regulated market area [**3**]. There are a number of different standard EM emissions tests, but the two main ones, the conducted and the radiated emissions test, are usually the minimum requirements and often the sticking point for a consumer electronics product. The standard EM emissions tests, especially the radiated emissions test, require an expensive arrangement of test equipment and construction of controlled testing premises (for example a *radio-frequency anechoic chamber*). In addition to the costs, the standard EM emissions tests take a long time to perform: the radiated emissions test takes several tens of minutes for one *device under test* (DUT). As a result, the usage of standard EM emissions tests is

usually limited to testing the compliance of a prototype or a sample before production ramp-up and to running occasional sample based quality control tests.

The goal of this research was to find a quick and inexpensive method to predict a given charger specimen's standardly measured radiated emissions from any combination of its EM, electrical, and physical properties either entirely or predominantly dependent on the switching transformer. This approximate prediction method for the charger or transformer should be suitable to use in mass-scale testing at both the production line and the incoming quality check for the device. The premise was to study the correlation between near-field probe measurement readouts and radiated emissions, as well as the correlation between transformer's electrical and physical properties' measurement readouts and radiated emissions. The final prediction method would then be developed based on the findings from the analyses of these correlations.

Existing studies that are most closely related to this research have made the following findings:

1) Radiated emissions can be predicted by measuring common-mode current [**4**,**5**].
2) Conducted emissions can be predicted by simulating the operation of SMPS with lumped element models [**6**,**7**,**8**,**9**]; even individual properties alone, such as leakage inductance [**10**], can be used for the prediction.
3) Near-field measurement results can give an overall "feel" of radiated emissions, but they cannot be directly extrapolated into far-field measurement results due to near field's complexities [**11**,**12**].

This research aimed to repeat the first finding, to extend the second finding to the prediction of radiated emissions from individual properties, and to challenge the third finding by identifying individual frequency points at which extrapolation from near field to far field is possible.

This paper is divided into two major parts. The first part is the theory, which covers chapters 2-5 and is essential for fully understanding the second part. The second part is the experiments and results, which covers chapters 6-8.

Chapter 2 presents the EM phenomena behind EM emissions and *electromagnetic interference* (EMI), as well as some essential concepts and terminology related to them. Chapter 3 gives a thorough account of *impedance*, including its connection with EM phenomena, as well as modeling and analysis. Chapter 4 describes the various natures of EM emissions, and how their levels can be measured. Chapter 5 applies the concepts from the preceding chapters in the context of a generic flyback charger, highlighting any of its measurable properties that may have a direct impact on the emissions. The theory part aims to give a clear motive for the measurements that were conducted in this research's experiments in order to find a prediction method for radiated emissions.

Chapter 6 presents the three different types of measurements carried out on the chargers and the transformers: near-field probe, electrical and physical property, and standard radiated emissions measurements. Lastly, the chapter reflects on the ability to repeat and reproduce the measurements. Chapter 7 gives an overview on the collected measurement data and describes its subsequent processing and analysis. Chapter 8

presents the findings of the data analysis, categorizing the discovered correlations into strong, weak, and no correlation. The experiments and results part aims to give a detailed account of what was measured, how it was measured, and why it was measured. Moreover, this part describes how the collected data was utilized, what conclusions were drawn out of it, and on what grounds.

Finally, chapter 9 concludes the outcome of the research and reflects on how the set targets were met, what sources of inaccuracy and error there were, and where subsequent research could improve upon the research presented here.

2 ELECTROMAGNETIC ENERGY AND COMPATIBILITY

The comprehensive, "raw", theory of electromagnetism is often difficult and arduous to apply to practical problems. Fortunately simplifications and simplifying models come to help. For example, conventional *circuit analysis* uses simplifying models of the comprehensive EM field and wave theory to facilitate modeling and designing electronic circuits.

On the other hand, simplifications can sometimes obscure essential aspects of the comprehensive theory. For example, circuit analysis draws critique for omitting the existence of magnetic and electric fields altogether by merely modeling them with two *circuit elements*: capacitance and inductance [**13**]. In fact, the magnetic field and the electric field are the very essence of any kind of EM energy; all the associated phenomena, such as currents and voltages, are only their byproducts [**14**]. As Armstrong states [**15**], most educational establishments have the weight of electrical engineering students' training in the circuit analysis way of thinking, which in many cases is a misleading or an outright flawed approach, especially if the circuits under scrutiny operate at high operating frequencies.

This and the next three chapters aim to give a good overview, primarily to a reader who is familiar with the circuit analysis way of thinking, on the fundamental role of *EM fields and waves* in electrical devices' operation and byproduct phenomena. The chapters attempt to achieve this without involving rigorous mathematical descriptions, but still implicitly keeping the fundamental laws and clauses of classic electromagnetism as the foundation for everything that is claimed.

2.1 Electromagnetic Waves and Fields

An *EM wave* is fluctuation of the *electric field component* and the *magnetic field component* of total *EM field*. If there is no fluctuation of the field, then there is no EM wave. But if there has been no fluctuation of fields at some point in time, there also cannot be any EM fields. The electric and the magnetic field must have accumulated at some point, and that requires fluctuation. In any case, EM energy is always bound in electric and magnetic fields, whether fluctuating or not. Fluctuation, in fact, alters the bound energy in the electric and in the magnetic field.

One can conceive EM waves as a means of conveying information regarding the state of its "source/emitter", usually a conductor in man-made applications, to the

surroundings. When the state of the source/emitter remains constant, there are no EM waves. In such a case the EM field is *static*, that is, remains constant, as opposed to *dynamic*, that is, time-varying. Correspondingly, we speak of *electrostatic* and *electrodynamic* EM fields. A static EM field can convey EM energy to a load as well as a dynamic one, *if* there is a conductively intact current loop, that is, an intact *transmission line*, between the source and the load.

Electric fields can be the result of two different causes, or of a combination of both. The first cause is the *static cause*, which creates an electric field from positive charges to negative charges. One can conceive that these fields are created between every positive and every negative charge in existence. But distance mitigates the field strength proportional to its square, which is why a detectable field between two given points, or accruals of charge, is only created both when enough positive and enough negative charge is accrued at those points, and when these points are close enough to each other. An electric field created in this way is *conservative*, meaning that a *contour integral* within it always yields a zero. Let us consider a "test charge" which we can freely move in a given electric field, and which provides us with the electric field potential in its respective location. In a conservative field, the potential of the test charge always returns to its starting value as it moves back to its starting point, regardless of the path it has taken. In other words, the path or the locational history of the test charge in a conservative field does not affect its potential value. [**14**]

The second cause of electric fields is the *dynamic cause*, which is due to time-dependent magnetic fields. This cause is a consequence of *Faraday's law*, which states that a time-varying *magnetic flux* creates an electric field that is *non-conservative*. In other words, a contour integral in such an electric field yields a non-zero result, meaning that a voltage is induced along the contour; moving a test charge around in a non-conservative field and then returning it to its starting point in the electric field does not return its potential to its starting value. Moreover, the path that the test charge has taken affects the potential value that it has at a given point in the field. [**14**]

In contrast, magnetic fields can only result from one cause: currents [**14**]. But one can conceive currents to be of two different types: 1) *conductive currents*, in which charge carriers move along the current's path and 2) *displacement currents*, in which charge carriers do not move along the current's path, but charge is "carried virtually" by a time-varying electric field [**14**]. Thus, displacement currents can only occur in situations with dynamic, that is, AC or time-varying, fields, whereas conductive currents can occur both in static and dynamic situations. Displacement currents should be regarded as currents just like conductive currents; the conventional definition of current as an *amount of charge through the cross-section of a conductor per second* covers only conductive currents and should be replaced with a more general definition that includes displacement currents: *the change in electric flux in the cross-section of a conductor per second*. According to Ampere's law, displacement currents even contribute to the magnetic field around the conductor, same as conductive currents. [**14**]

EM fields and waves are more fundamental manifestations of EM energy than voltages and currents [**14**]. It is conventional to think that "electrical energy is carried by conductors", but in fact conductors only "guide" EM waves and EM energy associated with EM fields. In man-made applications, EM waves are made to travel alongside conductors, which have plenty of free electrons to function as charge carriers. When a conductor guides an EM wave, its free electrons move around in response to the wave, generating voltages and currents. But the electrons' velocity is only about 3 kilometers per hour, whereas the EM wave is moving at the speed of light, implying that moving electrons cannot be the fundamental essence of EM energy. A good analogy is a "bucket fire brigade", a line of people passing water buckets onwards towards the flames. Similarly, electrons are just "passing water buckets", that is, EM energy, onwards towards the circuit's load [**16**]. Also, an electric field and a magnetic field can exist without any associated voltages and currents, that is, without any charge gradients or varying electric or magnetic fluxes in a conductor's association, for example in an *EM plane wave*, but no voltages or currents can exist without any associated electric fields and magnetic fields. Thus, EM fields and waves are the more fundamental essence of EM energy than currents and voltages, which are mere side effects created by EM waves. [**13**,**14**]

As mentioned, conductors have an ability to "guide" EM waves and EM energy; however, EM energy does not reside inside the conductors themselves, but in the *dielectric*, for example plastic, rubber or air, around it. The distribution of EM energy becomes clear when we observe EM energy per unit time, that is, *EM power*, expressed by $\bar{S} = \bar{E} \times \bar{H}$, the *Poynting vector*, in which $\bar{E}$ is the *electric field strength*, $\bar{H}$ the *magnetic field strength*, and $\bar{S}$ the EM power vector [**14**]. The electric field inside a conductor is nearly insignificant due to *electric influence*, a phenomenon covered in the next chapter, which renders the electric field inside the conductor infinitesimal. In contrast, a significant magnetic field exists inside the conductor at low frequencies, but when the frequency increases, even the magnetic field becomes weaker due to the canceling effect of *eddy currents*. Consequently, very little EM energy is concentrated inside the conductor, even if a large current flows along it. In contrast, the dielectric alongside the conductor has a high *E* and a high *H* and thus carries most of the EM energy when the conductor conducts current, as per Poynting's expression [**14**].

The electric and the magnetic field components of an EM field can be illustrated by field lines, which are similar to contour lines on a map. With contour lines, the denser the lines are at a given point on a map, the steeper the elevations on the terrain. Similarly with field lines, the denser the lines are at a given point in space, the stronger is the field there [**14**]. The tangent of a field line at any given point gives the direction of the field at that point, and *flux* is the amount of field lines going through a given surface. The flux through a *differentially small* surface perpendicular to the field lines at a given point and divided by its surface area gives that point's *flux density*, which is proportional to the *field strength*.

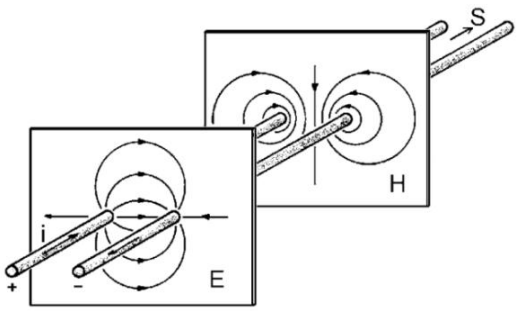

Figure 2.1. *An illustration of field lines; electric and magnetic field lines around the send/go and the return conductor of a conducting circuit, depicted on two cross-sections of space [**14**].*

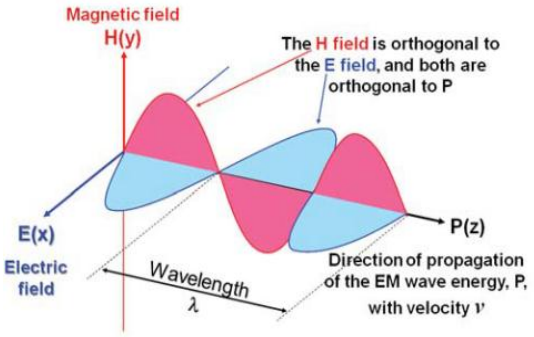

Figure 2.2. *An illustration of a TEM wave's propagation direction and the directions of its electric and magnetic field components [**13**].*

Figure 2.1 illustrates the electric and the magnetic field lines on two cross-sections of space around the *send/go* and the *return conductor* of a conducting circuit, and figure 2.2 visualizes how the propagation direction of an EM wave (the Poynting vector), the electric field, and the magnetic field component are all orthogonal to each other in a *transverse electromagnetic* (TEM) *wave*. "TEM wave" is often interchangeably used with "EM plane wave" to denote an EM wave that has broken free from its source/emitter's sphere of influence and thus has a different nature than those within the influence. The electric and the magnetic field components always have the same frequency in a given EM wave, and the EM wave has the frequency X, when its electric and magnetic field components have the frequency X, and vice versa. But the electric and the magnetic field components' amplitudes, and the ratio of those varies depending on the nature of the source/emitter and the medium of propagation.

2.2 Technical Glossary

EMC terminology has many terms coinciding with one another and is thus misleading and confusing from time to time. Grasping the key terms is crucial in order to talk and understand the same language with EMC literature and the experts of the field.

2.2.1 Electromagnetic Emissions

All electrical, electromechanical, and electronic devices receive EM energy in the form of EM emissions from the EM environment and also produce EM emissions themselves. EM energy that has been "picked up" by a device and that can potentially cause interference in its operation is called *electromagnetic disturbance* [**2**]. *Electromagnetic noise*, or just *noise*, is a commonly used term to mean more or less the same as EM disturbance. Ott [**1**] defines EM noise as "any electrical signal present in a circuit other than the *desired signal*". He also adds that *signal distortion* produced in a circuit due to *nonlinearities* is excluded from this definition, unless the distortion is coupled into

another part of the circuit [**1**]. Sometimes "noise" may also exclusively refer to intrinsic noise, such as thermal noise, instead of noise caused by EM energy originating from outside the circuit.

Electromagnetic interference, EMI, refers to the errors and malfunctions that a circuit will experience when the EM energy it receives exceeds critical levels for the circuit. EMI is often erroneously used to mean the same as EM emissions or EM disturbances and EM noise [**2**]. Ott [**1**] defines EMI as "the undesirable effect of noise". He says: "Noise cannot be eliminated, but interference can. Noise can only be reduced in magnitude, until it no longer causes interference."

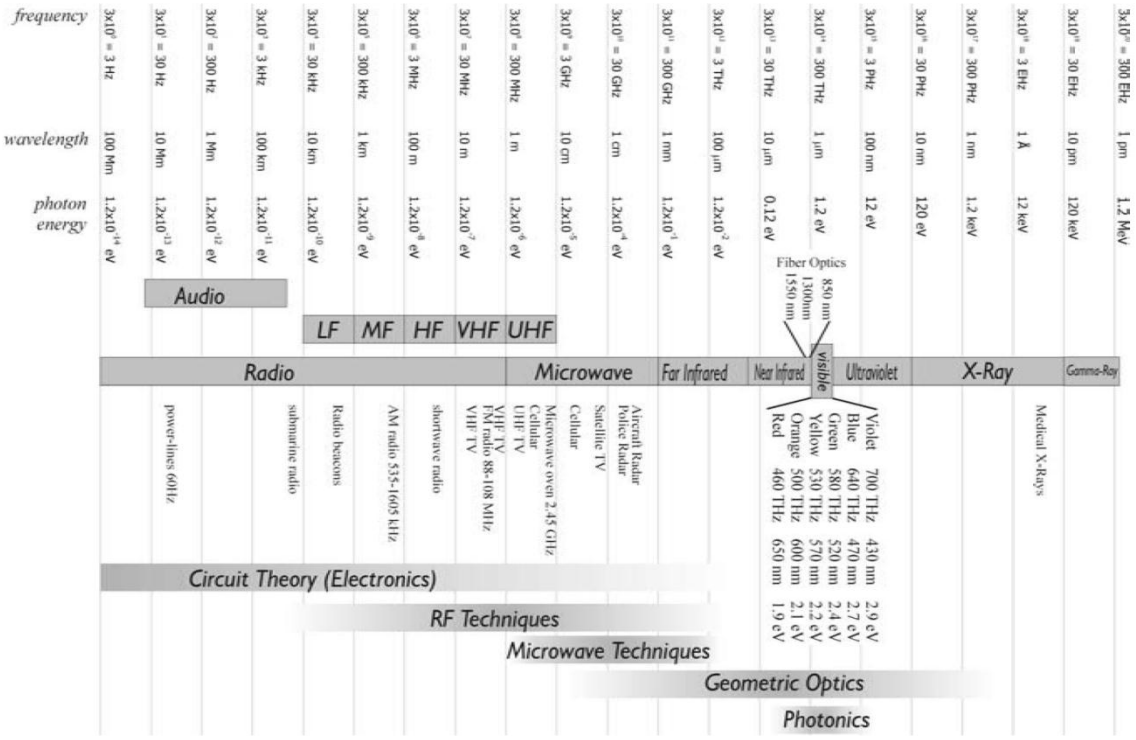

Figure 2.3 *The spectrum of EM energy [**16**].*

There is an umbrella of EMC terms beginning with the word pair *radio-frequency* (RF). These include *RF energy*, *RF emissions*, *RF disturbance*, *RF noise* and *RF interference*. Montrose [**17**] defines RF as "The frequency range within which coherent electromagnetic radiation is useful for communication purposes – roughly from 10 kHz to 100 GHz. This energy may be generated intentionally, as by a radio transmitter, or unintentionally as a by-product of an electronic device's operation." According to the American regulatory authority *Federal Communications Commission* (FCC), "a radio-frequency device is any device which in its operation is capable of emitting radio-frequency energy by radiation, conduction or other means [**18**]." FCC defines RF energy as "electromagnetic energy at any frequency in the radio spectrum between 9 kHz and 3,000,000 MHz (3,000 GHz) [**19**]".

One can understand RF as referring to high-frequency EM energy, as opposed to low-frequency or "infra-RF" (<9 kHz) EM energy, for example *harmonic pollution*, which can also create but is usually not a pivotal cause of EMI, unlike RF EM energy,

which usually is a major cause. In any case, both RF and infra-RF EM phenomena are considered part of EMC. But if the frequency is increased to "ultra-RF" (>3000 GHz) frequencies, then the EM energy reaches infrared, visible light, ultraviolet, X-ray and gamma-ray ranges, which generally do not pose a threat to electronic devices' operation in the same way and are thus not considered part of EMC.

Figure 2.3 illustrates the EM spectrum, but note that it does not follow the FCC definition of the RF range. The bottom of the figure also shows what different simplifications of the comprehensive theory of electromagnetism, that is, techniques or disciplines, can be used in each frequency range.

2.2.2 Electromagnetic Compatibility

Electromagnetic compatibility is a discipline concerned with controlling EMI. It covers three main aspects: 1) *emissions*, 2) *self-compatibility*, and 3) *susceptibility*. These three aspects are the cornerstones of EMC's purpose, which is to ensure 1) that every system's EM emissions are low enough so as to cause no EMI in other systems or the system itself, and 2) that their immunity against EM disturbances is high enough so as to be able to operate in an EM environment that has acceptable levels of EM emissions. These three points are the criteria for a system to be *electromagnetically compatible*. [**1**,**2**,**20**]

Armstrong defined susceptibility as "the capability of a device or circuit to respond to unwanted electromagnetic energy (i.e. noise)" [**1**]. As mentioned, EMI occurs only if the received EM energy causes the *receptor/receiver* to behave in an undesired manner. EMI can be anything between mildly impaired functionality to physical damage to the device. As Paul [**20**] says: "The unintentional transfer of energy causes interference only if the received energy is of sufficient magnitude and/or spectral content at the receptor/receiver input to cause the receptor/receiver to behave in an undesired fashion". Thus, existence of EMI depends on the receptor/receiver's response on received EM energy, that is, on its susceptibility.

If a device is susceptible to the EM environment, it is often evident to the user and as a reaction they might not continue using or purchasing that product. Susceptibility is self-regulating, because it is a crucial matter for a product's sales and profits whether the product can withstand the EM environment or not. In contrast, emissions are often not self-regulating. Emissions of a product may not affect the functionality of that product itself, only other products in its surroundings. This is why regulatory authorities must stipulate EMC regulations covering all electric products and stating at least the maximum allowable EM emission levels. [**1**]

2.2.3 Near Field and Far Field

When near to a circuit that has fluctuating voltages and currents, the corresponding electric and magnetic fields form complex patterns with field strengths that vary as functions of $1/r^3$, $1/r^2$ and $1/r$, where r is the radial distance from the source/emitter.

This region is called *near field*, and also *induction field* or *induction region*. The EM phenomena in the near field can often be presented using capacitances, inductances, and conductances, that is, the ways that circuit analysis uses for modeling *capacitive*, *inductive*, and *conductive coupling*. However, not all EM phenomena in the near field can be modeled using circuit analysis techniques, as Van der Laan [**14**] highlights.

At every point in space, EM waves have a given ratio of *E* and *H*, that is, the *wave impedance* $Z_{wave} = E/H$, which depends on the distance from the source/emitter. A predominantly electric field originates from fluctuation of voltage in a circuit that has a *high impedance*, whereas a predominantly magnetic field originates from fluctuation of current in a circuit that has a *low impedance*. However, as the distance from the source/emitter increases, the *E/H* ratio approaches a specific value characteristic to the medium, the *characteristic wave impedance*, as depicted in figure 2.4. In a vacuum or *free space*, the value of the characteristic wave impedance is $120\pi\ \Omega \approx 377\ \Omega$. In medium other than free space the characteristic wave impedance is calculated by:

$$Z_{wave} = \sqrt{\mu_0 \cdot \mu_R / \varepsilon_0 \cdot \epsilon_R}\ \Omega = 120\pi \sqrt{\mu_R / \varepsilon_R}\ \Omega\,, \qquad (2.1)$$

in which μ_0 is the permeability of free space, μ_R the relative permeability normalized to μ_0, ε_0 the permittivity of free space, and ε_R the relative permittivity normalized to ε_0.

Once an EM wave reaches such a distance from its source/emitter that its wave impedance equals the characteristic wave impedance of the medium, the EM wave is no more in the near field, but in the *far field*. In the far field, the distribution of fields in space follows that of a TEM wave, the field strengths only varying as a function of *1/r*. In other words, an EM wave in the far field takes the form of a TEM wave depicted in figure 2.2.

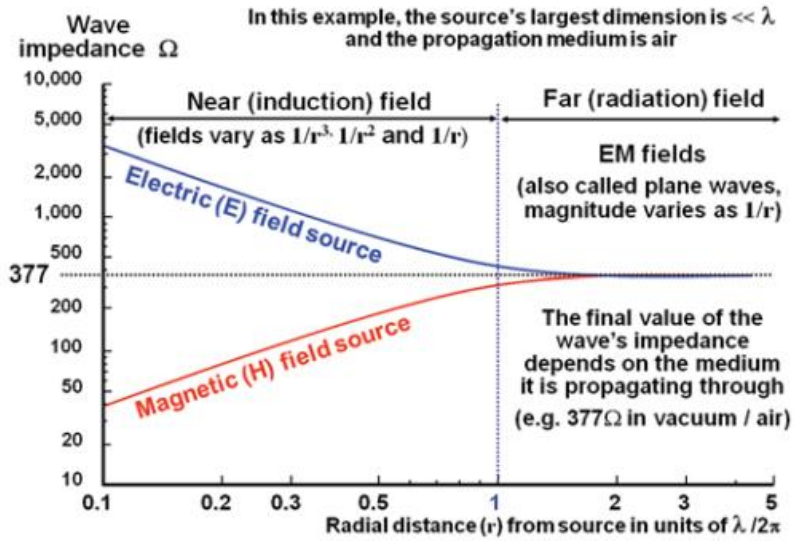

Figure 2.4. *Wave impedances in the near field and in the far field [**13**].*

For a source/emitter with longest dimensions much less than a wavelength, the *boundary distance* between the near field and the far field lies approximately where the distance *r* from the source/emitter is $\lambda/2\pi$. For a source/emitter with longest dimensions not much less than a wavelength, the boundary distance is given by $r = 2D^2/\lambda$, where *D*

is the largest dimension of the source/emitter. However, the transition from near field to far field is gradual, not abrupt, and thus the resulting EM field exhibits mixed properties of the two in the *transition region* between them.

2.3.4 Electromagnetic Coupling

EM coupling is a phenomenon in which two points in space connect so that EM energy can be transferred between them. *EM near-field coupling* happens through capacitive, magnetic, or conductive "EM near-field interaction". Capacitive or *electric coupling* refers to propagation of EM energy through an electric field, inductive *or magnetic coupling* to that through a magnetic field, and conductive coupling to that through the flow of charge carriers. In contrast, *EM far-field coupling*, interchangeable with the term radiated coupling, refers to transfer of EM energy through the far field as a TEM wave.

The *EMC coupling problem* describes the fundaments required for the generation of EMI. They are: 1) the source/emitter that produces the EM emissions, 2) the *transfer/coupling path* that transfers the EM energy, and 3) the receptor/receiver to which the EM energy is transferred and in which the possible detrimental effects come out. For EMI to exist, all three of these must be present. If even one of the three is removed, there is no EMI. These fundaments form the basic framework of *design for EMC*, because they suggest that there are three ways to prevent EMI: 1) by suppressing EM emissions at their source/emitter, 2) by making transfer/coupling paths as inefficient as possible, and 3) by making the receptor/receiver less susceptible to EM emissions. [**17**,**20**]

2.3.5 Harmonic Content and Pollution

Fourier's theorem states that repeating waveforms of any shape can be "constructed" from the superimposition of sinusoidal waves of specific amplitudes and specific frequencies. A selection of sinusoidal waves that constitute a given waveform when superimposed together can be called the waveform's *harmonics*, *sinusoidal components*, or just *components*. As a rule, the more discontinuous a waveform is, that is, the sharper edges it has, the larger the amplitudes of its high-frequency sinusoidal components. Also, the larger *rates of change* a waveform has, the larger the amplitudes of its high-frequency sinusoidal components are. Therefore, *on/off type* waveforms, such as digital or *pulse width modulated* (PWM) signals, are "rich in high-order harmonics" or "have a high *harmonic content*", that is, have sinusoidal components with large amplitudes at high frequencies. Figure 2.5 shows an on/off waveform with 2-ns *rise and fall times* at the *fundamental frequency* of 16 MHz Fourier's theorem states that the frequencies of a waveform's sinusoidal components are the fundamental frequency's multiples, which are all odd multiples for a square-wave and for a rectangular wave. Figure 2.6 shows the harmonic content of the waveform of figure 2.5. [**15**]

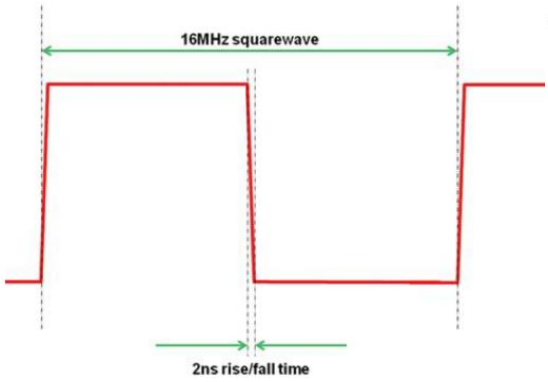

Figure 2.5. *A 16-MHz squarewave with 2-ns rise and fall times, that is, a trapezoidal wave [**15**].*

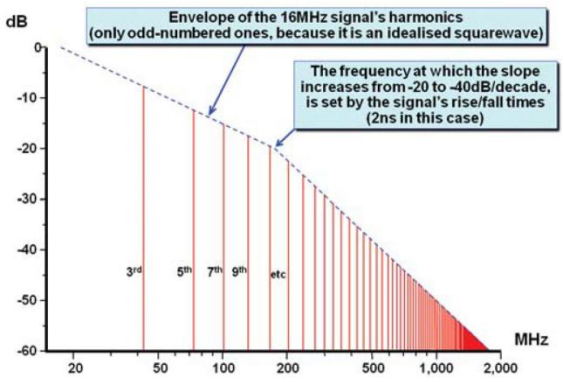

Figure 2.6. *The frequency spectrum of the 16-MHz trapezoidal wave with 2-ns rise and fall times [**15**].*

Harmonic pollution refers to the harmonic content in the mains supply's output current and voltage at multiples of the mains supply's 50- or 60-Hz fundamental frequency. Harmonic pollution is a problem both of *power quality*, a subset of EMC, and of the supply authorities, whose obligation is to provide a high-quality supply of electricity. At the very source of the electricity, for example a power plant, the mains voltage waveform is generated as a pure sine wave. However, the mains supply is not an ideal zero-impedance voltage source, and so *reactive impedance* of the distribution network together with non-linear loads, which create harmonics at multiples of the mains current's frequency, cause the voltage waveform to distort. Usual causes for the mains supply's non-linear loading are power converters and electronic power supplies. [**1**,**21**]

Although harmonic pollution is considered a subset of EMC, it usually does not cause EMI, which instead tends to happen in the RF range. Harmonic pollution is not considered RF EM emission, because EMC regulations define the upper limit of harmonic pollution rather low, in *IEC-61000-3-2* [**21**] at 2 kHz, the 40th harmonic of 50 Hz.

2.3.6 Signal Integrity

Signal integrity (SI) is a way to describe the "quality" of a desired signal's waveform in a circuit. SI describes how unchanged or constant the shape of the desired signal has remained having reached from the source/driver to the load/receiver.

Figure 2.7 shows the waveform from figure 2.5 when it has traveled in a real-life conductor, a 200-mm-long PCB trace, and reached the end or the load. When an oscilloscope measures the waveform at the end, it shows the red waveform, which is what is left of the desired signal and thus of the EM energy. The blue waveform is the EM energy that has been radiated into the surroundings. If the red and the blue waveform are superimposed, the result is the original desired signal in green. [**13**]

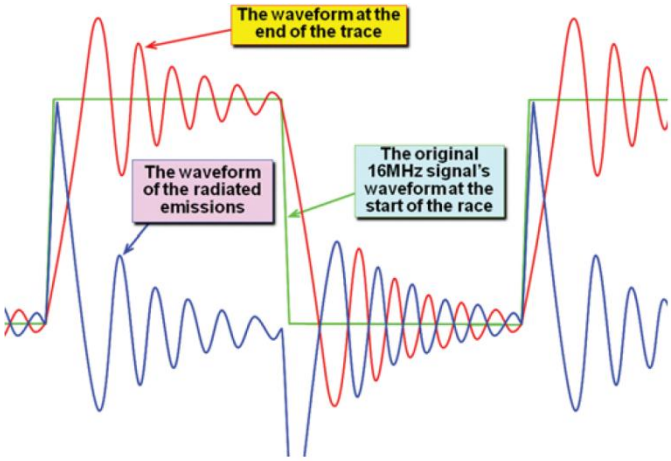

Figure 2.7. *The original signal (green) on a 200-mm-long PCB trace is made up of the superimposition of the waveform at the end of the trace (red), and the waveform of the radiated emissions (blue) [**13**].*

Figure 2.7 illustrates degradation of SI due to far-field coupling, but unintentional near-field coupling causes similar degradation of SI. *Capacitive coupling* and *inductive coupling* from a circuit's conductor to another conductor of the same or a different circuit, that is, *capacitive crosstalk* and *inductive crosstalk*, are examples of this. In circuit analysis way of thinking, capacitive or inductive crosstalk allows high-frequency components of current to "break away" from the conductor, impairing the desired signal's waveform. In field and wave analysis way of thinking, an electric or a magnetic field encountering a conductor induces voltages and/or currents in it and, consequently, transfers EM energy to it. Near-field coupling also introduces new *resonance frequencies* on top of those ones exhibited by the intentional circuit alone, possibly also further hampering the SI.

SI is a subset of EMC, because the greater the noise signal added to the desired signal is, the higher are the EM emissions emitted to the surroundings. Thus, measures of SI enhancement will also enhance EMC. The loss of EM energy associated with degraded SI affects the intentional circuit's voltages and currents by impairing their waveforms before they reach the load, that is, adds a *noise signal* to the desired signal. Similarly, the EM energy received by a *victim conductor* produces a noise signal in the *victim circuit* and also adds it up with the victim's desired signal, if such is present, degrading the SI in the victim. [**13**]

SI analysis is normally used to judge the quality of digital signals, that is, ideally perfectly rectangular waveforms, and can then be referred to as *digital signal integrity* (DSI) analysis. Real digital signals are not perfectly rectangular: they have finite rise and fall times, and they exhibit, for example, *oscillations* (*ringing*), *overshoot*, *undershoot*, and *shelves* (*non-monotonic behavior*), which are all forms of degraded SI. Figure 2.8 shows different kinds of non-idealities in digital signals. Although the voltage and the current waveforms in switching converters cannot be called digital, they are similarly on/off waveforms, to which DSI type analysis can be applied.

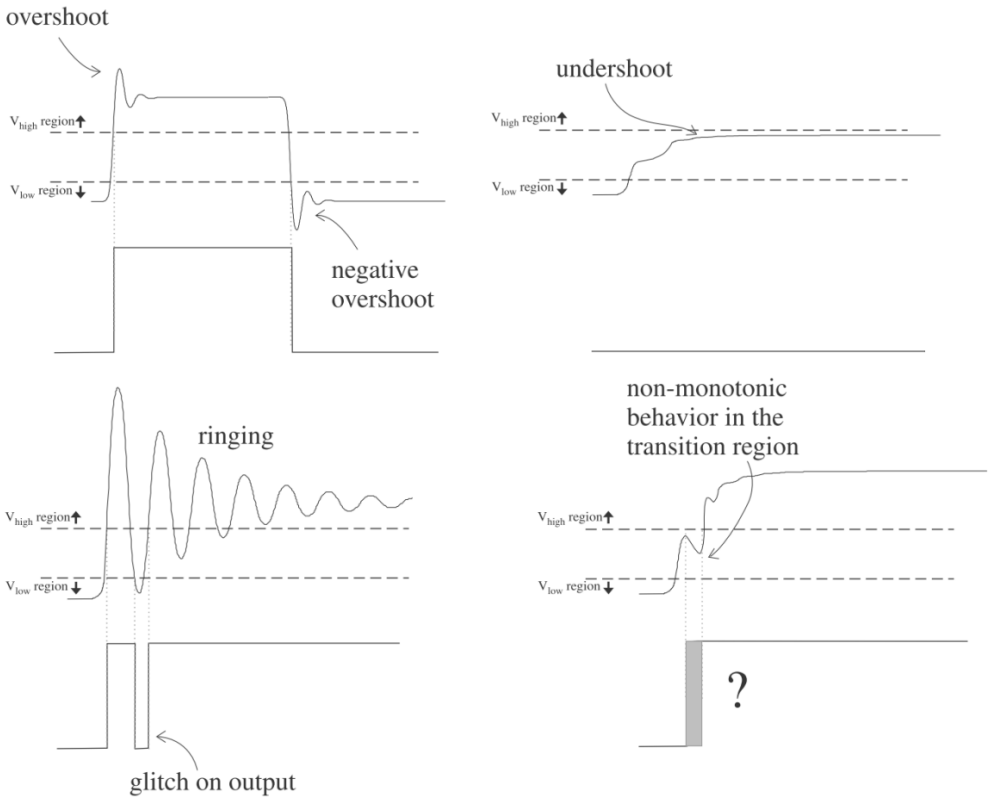

Figure 2.8. *Non-idealities of a digital waveform. [**16**]*

2.3.7 Ground Reference

Understanding the concept *ground reference* is important in comprehending EMI phenomena. Ground reference collectively refers to all conductors that do not belong to a given intentional current loop, but that still have "near-field coupling interaction" with it. In other words, ground reference is collectively made up of all conductors in the given current loop's surroundings other than its intentional send/go conductor, its intentional return conductor, and its intentional load.

The ground reference for a current loop may change, and usually does, when the current loop is moved around. Thus, the circuit designer can never accurately account for the ground reference, even if some predominant components of it are constant, such as a metal casing or the conductors of other current loops in the circuit.

Ground reference is not *equipotential*; not all points in it are in the same potential. Depending on the given current loop, it may be possible to divide its ground reference into different subsets, such as *circuit ground*, *chassis ground* and *earth ground*, between which potential differences can be very large. But no single subset of any current loop's ground reference is an equipotent either, essentially because there is no such thing as a *perfect conductor*.

3 IMPEDANCE

Every point in all media and materials has three *point-specific EM properties*: *conductivity*, *permittivity* and *permeability*. Permittivity is associated with electric fields, permeability with magnetic fields, and conductivity, the reciprocal of which is *resistivity*, with the conversion of EM energy into heat. When a given medium is homogenous in terms of its EM properties, that medium has a *characteristic conductivity*, a *characteristic permittivity*, and a *characteristic permeability*. One may call such characteristic EM properties *material-specific*.

Characteristic permittivity tells how "favorable" a propagation path a given material is for the electric field component of an EM wave, while characteristic permeability tells how "favorable" a propagation path a given material is for the magnetic field component of an EM wave. Characteristic conductivity tells how "favorable" a propagation path a given material is for the flow of charge carriers caused by an EM wave. A simple way to put this is: a material with a high permittivity *guides electric flux well*, a material with a high permeability *guides magnetic flux well*, and a material with a high conductivity *guides charge carriers well*.

The three material-specific EM properties – characteristic permittivity, permeability, and conductivity – dictate the wave impedance, that is, the ratio of a TEM wave's electric and magnetic field components' magnitudes, which the wave will have in the given material. This wave impedance is called the material's characteristic wave impedance. The wave impedance at a given point in a material can differ from the material's characteristic wave impedance, if the point is within the near field of the EM wave's source/emitter, where the wave impedance has not yet settled to the material's characteristic wave impedance.

From a material's characteristic wave impedance one can derive the *lumped element impedance* between two coupling points on a volume of that material. The lumped element impedance dictates the ratio of magnitudes of a given voltage and an associated current between the two coupling points. A lumped element impedance can be broken down into three components: *inductance, capacitance, and conductance*, which are similarly defined as properties affiliated with two coupling points on a volume of material. Capacitance is associated with electric fields, inductance with magnetic fields, and conductance with the conversion of EM energy into heat between the two points on the volume of material.

3.1 Modeling and Analysis of Impedance

An ideal circuit analysis circuit element has the same potential at every point and experiences the same current flow through every cross-section along its entire length. However, since EM energy travels as EM waves consisting of limited-length waves of electric and magnetic fields, both the electric and the magnetic field have differing magnitudes at different points along a *real* circuit component at any given moment. Thus, the potential and the current have differing magnitudes at different points along a real circuit component at any given moment. This must be taken into account when analyzing or modeling a circuit.

When analyzing or modeling a circuit, the ratio between the EM wave's wavelength and the dimensions of the circuit in question is crucial, because it determines both the sufficient level of accuracy and the best method of impedance modeling. One must choose one of three methods of analyzing a circuit and modeling the impedances in it. The methods, together with corresponding rules-of-thumb on when to use them, are:

1) When the dimensions of an EM wave's source/emitter are "much less" than $\lambda/2\pi$, use *lumped element analysis*.
2) When any dimension of an EM wave's source/emitter is not "much less" than $\lambda/2\pi$, use *transmission line analysis*.
3) When two or three dimensions of an EM wave's source/emitter are "not much less" than $\lambda/2\pi$, use *full wave analysis*. [**13**]

3.1.1 Lumped Element Analysis

Lumped element analysis is the simplest EM field and wave analysis and modeling method. It uses *lumped impedances* to model the impact of objects (or volumes of medium/media) within the near field of an EM wave source/emitter, for example the impact of objects in an electric circuit's association, on EM waves and fields. Lumped element analysis is effectively a *circuit analysis and modeling method*. A lumped impedance is for modeling the impedance between an object's two given coupling points, through which one can envision EM energy to propagate. The insides of the object can be regarded as a "black box": the object may consist of a number of different materials in complex shapes and concentrations, but as long as the impedance between those two coupling points is known, the internal composition of the black box is insignificant. In practice, the lumped impedance between two coupling points is usually determined by measuring it.

Lumped element analysis is the normal circuit analysis way of modeling a circuit, in which one uses resistances, inductances, and capacitances lumped into two-port circuit elements, whereas the rest of the circuit is modeled as if consisting of ideal conductors and insulators. Resistances, inductances, and capacitances are circuit analysis's fundamental "building blocks" of modeling EM phenomena. Basically, all phenomena that circuit analysis is expected to deal with can be modeled using them, because they model all three of EM waves' fundamental properties in the near field: formation of heat,

and energy in magnetic field and electric field. However, many real-life components' behavior is very difficult to model using only these three circuit elements, because real-life components may be, for example, *non-linear* or *anisotropic* (direction-dependent) by nature. Thus, it is smart to use special circuit elements for modeling, for example, semiconductor devices and mechanical switches.

One can use lumped element analysis when the dimensions of the circuit under analysis are "much smaller" than $\lambda/2\pi$ of the EM wave propagating in it. The distance between the objects' given two coupling points, across which lumped impedances are modeled, should be small enough so that the EM wave's phase difference between the coupling points does not cause the magnitudes of current and voltage to be "skewed", consequently rendering the lumped impedance ambiguous. EMC design-wise lumped element analysis is accurate only if one also takes into account all the significant *stray* and *parasitic* inductances, capacitances, and conductances that exist within and around the circuit and models them with corresponding two-port circuit elements. [**13**]

3.1.2 Transmission Line Analysis

Transmission line analysis is an EM field and wave analysis and modeling method that uses the characteristic impedance of a transmission line to model the impact of the whole EM wave's near-field propagation path on EM fields and waves; not only discrete objects within the source/emitter's near field. In other words, transmission line analysis does not assume conductors and insulators to be ideal, but takes their real-life behavior into account.

A transmission line is a structure that transfers an EM wave from the source/driver to the load/receiver; any current loop forms a transmission line. One can conceive the transmission line model as an extension of the electrostatic, or low-frequency, model of a current loop made up of an ideal send/go conductor, an ideal return conductor, and an ideal dielectric between them. This transmission line extension also covers electrodynamic, or high-frequency, situations. In other words, transmission line analysis is more generally applicable than lumped element analysis, though more arduous as well.

In an electrodynamic situation, new factors that affect the behavior of an electric circuit arise compared with an electrostatic situation. These factors are conductor inductances, capacitances between conductors through the dieletric, increasing conductor resistances due to *skin effect* and *proximity effect* and, furthermore, *resonances* due to a suitable ratio of the EM wave's wavelength and the *electrical length* of the transmission line. Transmission line analysis takes these factors into account by modeling them with respective circuit elements, also the resistances, which can be modeled with a capacitor and an inductor in parallel, as section 4.8.2 will later explain.

When a source/driver injects a signal into a current loop, it in fact sends an EM wave propagating along the associated transmission line, creating fluctuations of voltages and currents in the current loop in the process. At the source/driver end, the

EM wave has the impedance of the source/driver, and at the load/receiver end the impedance of the load/receiver. When a sufficient distance away from both the source/driver and the load/receiver the impedance of the propagating EM wave is dictated by the characteristic impedance of the transmission line, a quantity that tells the transmission line's impedance per unit length. Thus, a lumped element impedance for a transmission line can be calculated by multiplying its characteristic impedance by the length of the transmission line. [**13**]

Transmission line analysis must be used instead of lumped element analysis when any one (and only one) dimension of the EM wave's source/emitter is "not much less" than $\lambda/2\pi$ of the EM wave; otherwise the accuracy of the analysis is not sufficient. This dimension is usually the direction from the source/driver to the load/receiver. [**13**]

The characteristic impedance Z_0 of a transmission line is given by:

$$Z_0 = \sqrt{\frac{R + j\omega L}{G + j\omega C}}\ , \tag{3.1}$$

in which R is the resistance and L the inductance of the conductors, and G and C the conductance and the capacitance through the dielectric, respectively. These transmission line parameters are depicted in figure 3.1. [**1**]

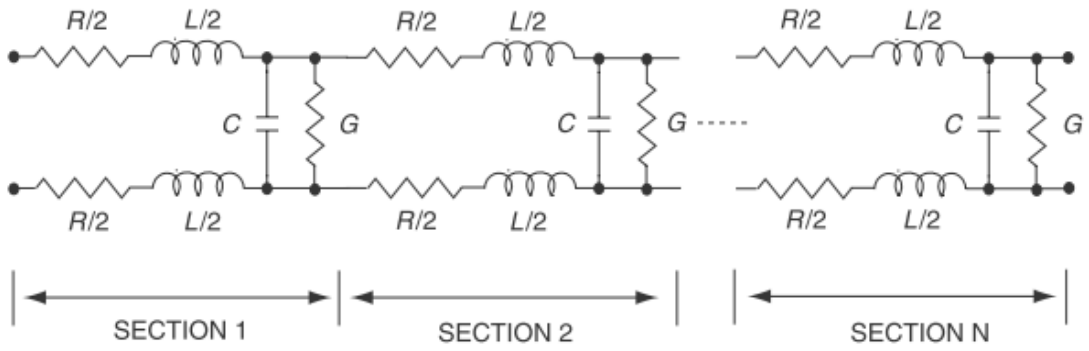

Figure 3.1. *A transmission line model with transmission line parameters [**1**].*

3.1.3 Full Wave Analysis

Full wave analysis is the most complex and thus the most generally applicable EM field and wave analysis and modeling method. It uses characteristic wave impedances of materials to model the impact of objects (or volumes of medium/media) on EM fields and waves. It requires knowing the exact arrangement of materials and their characteristic wave impedances, dimensions, and concentrations. The method is thus laborious, but the upside is that once one has constructed a full wave model of an object or a setting, one can, for example, readily find out the lumped impedance between any two points covered by the model without a need to make impedance measurements. Also, with a full wave model one is not tied to analyzing EM phenomena only in the near field of a circuit, but can, for example, simulate TEM waves' behavior in the far field. Therefore, full wave analysis is not plainly a circuit analysis method, but can be used to analyze and model EM phenomena more generally.

Full wave analysis must be used instead of transmission line analysis or lumped element analysis, when two or three dimensions of the EM wave's source/emitter are "not much less" than $\lambda/2\pi$ of the EM wave; otherwise the accuracy of the analysis is not sufficient [**13**]. Furthermore, as Van der Laan [**14**] points out in his book's appendix titled *Conflicts between Kirchoff and Maxwell*, there are situations in which results given by lumped element or transmission line analysis are confusing or outright incorrect, and in which full wave analysis must thus be used. For instance, only full wave analysis takes into account the resonances of an EM wave's source/emitter in every possible dimension.

Full wave analysis of any real-life electric or electronic device requires such complexity that it is only practical when using computer-based simulation. Full wave analysis using "pen and paper" is practical only in very simple situations, such as when analyzing a flat conductive plate or an empty conductive box. [**13**]

3.2 Intrinsic and Extrinsic Impedance

Impedances can be broken down into *intrinsic*, or *self-coupling* type, and *extrinsic*, or *mutual coupling* type. As mentioned, inductance, capacitance, and conductance can be regarded as the "components" of impedance; thus, let us cover them next.

3.2.1 Intrinsic and Extrinsic Inductance

Intrinsic inductance of a pair of coupling points is defined as the *magnetic flux per one ampere of current* associated with that magnetic flux and flowing between those coupling points. In other words, inductance defines the relationship between the magnitudes of magnetic flux and current associated with a given pair of coupling points:

$$L = \frac{\Phi}{I}, \tag{3.2}$$

in which L is the intrinsic inductance of two coupling points with current flow I that is associated with magnetic flux ϕ through a given area. Figure 3.2 depicts a stretch of conductor with a current flow and the associated magnetic field. For a current loop, the magnetic flux is defined through the loop's area. However, also a mere stretch of conductor that does not form a current loop equally has an intrinsic inductance; one can conceive the magnetic flux associated with its inductance to be defined through an infinite plane that is parallel with the stretch of conductor and splits its cross-section into two, as figure 3.3 depicts.

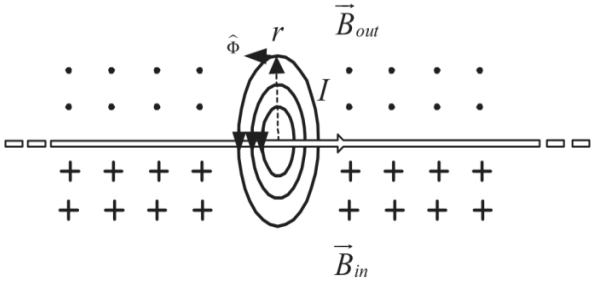

Figure 3.2. *A stretch of conductor with a current flow I and an associated magnetic field [**22**].*

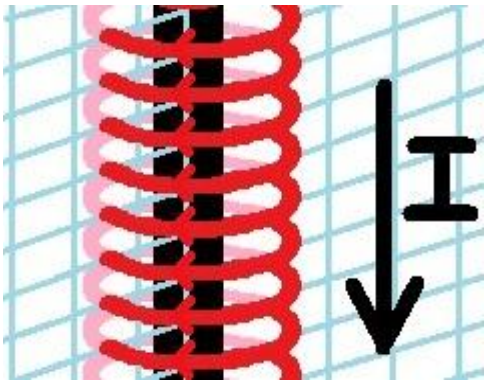

Figure 3.3. *The infinite plane through which the intrinsic inductance of a stretch of conductor is defined.*

Extrinsic inductance of a pair of coupling points is also defined as the ratio of magnetic flux and current:

$$M_{12} = \frac{\phi_{12}}{I_1}. \tag{3.3}$$

As opposed to the magnetic flux ϕ in the expression of intrinsic inductance, the one in the expression of extrinsic inductance, ϕ_{12}, is not directly associated with the current in the expression, I_1. The magnetic flux ϕ_{12} is a subset of the total magnetic flux ϕ, which is the one directly associated with the current I_1; ϕ_{12} is the share of ϕ that *couples mutually* with a given external conductor, the "mutually-coupled counterpart". It follows that the maximum extrinsic inductance of a conductor is equal to its intrinsic inductance. In such a case all the magnetic flux produced by the given current flow through the conductor is mutually coupled with the counterpart. In other words, extrinsic inductance is effectively a subset of intrinsic inductance.

Extrinsic inductance forms a coupling path through which EM energy can propagate between its two coupling points on two different conductors or circuits. The current I_1 in the extrinsic inductance's expression is located on one coupling point's side and the mutually-coupled counterpart on the other coupling point's side.

With ideal conductors, the intrinsic and extrinsic inductances are stipulated only by the affiliated conductor's distances and geometries and not by any electrical quantities of the setting. Thus, even if there is no current or voltage present in a conductor, it still has as valid and as equal inductances associated with it as when currents and voltages are present.

An equivalent circuit of mutual coupling through extrinsic inductance is depicted in figure 3.4; let us next understand why the equivalent circuit is such. Let us have two circuits coupling mutually through extrinsic inductance, and let us refer to the "induction culprit" circuit as the *primary circuit* and to the "induction victim" circuit as the *secondary circuit*. Let us refer to the primary circuit's pair of coupling points whose intrinsic inductance is involved in the mutual coupling as the *primary side* and that of the secondary circuit as the *secondary side*. The situation is that of a transformer with only a primary and a secondary winding, as depicted in figure 3.5.

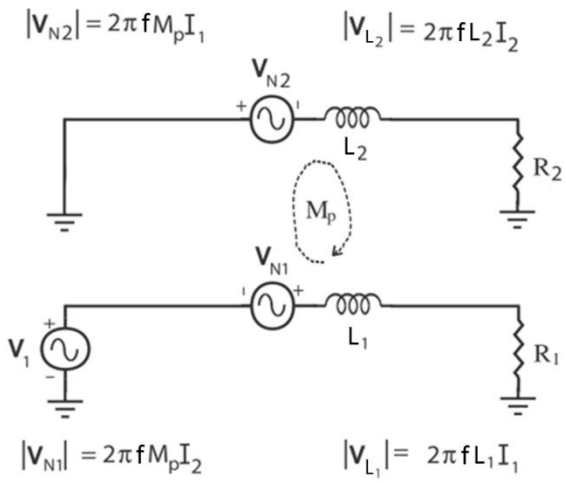

Figure 3.4. *An equivalent circuit of inductive coupling through extrinsic inductance, that is, through mutual inductive coupling [**16**].*

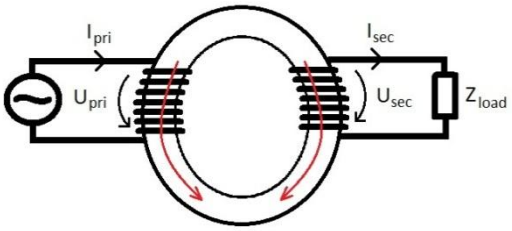

Figure 3.5. *A transformer with the windings wound in opposite directions. The red arrows illustrate the magnetic field and the satisfaction of Lenz's law.*

Using two overlapping squares that represent the primary and the secondary side magnetic fluxes, figure 3.6 illustrates what happens in mutual inductive coupling of two circuits. The overlapping proportion of the squares, that is, the area with black background, represents the mutually-coupled magnetic flux and the remaining areas with gray background the self-coupled magnetic fluxes of the primary and the secondary side. The share of the mutually-coupled magnetic flux dictates the proportion of the extrinsic inductance with regard to the intrinsic inductance, and the shares of the self-coupled magnetic fluxes dictate those of the primary and the secondary side *leakage inductances*. The red square represents the maximum secondary side flux induced by the primary side with the given primary current. The whole primary side magnetic flux with the given primary side current dictates the magnitude of the primary side intrinsic inductance and the maximum secondary side magnetic flux dictates the magnitude of the secondary side intrinsic inductance.

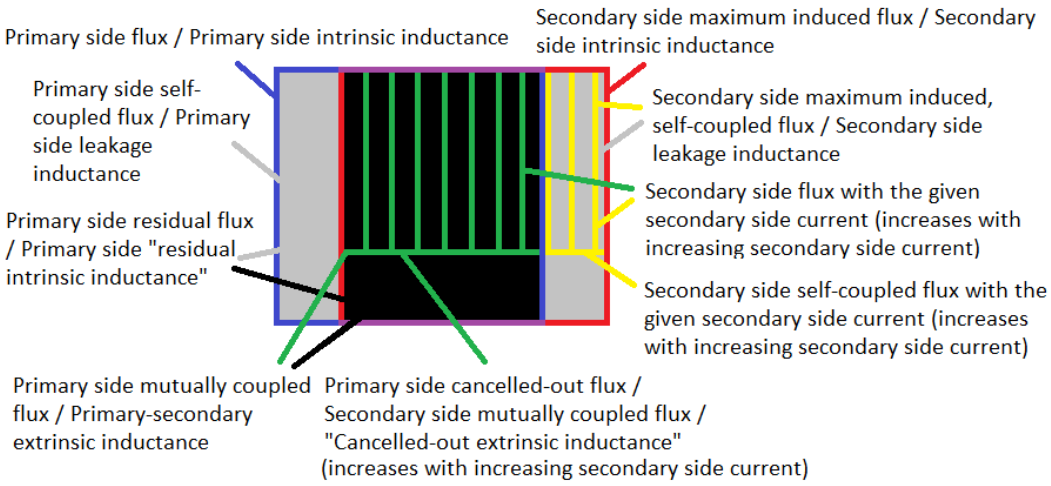

Figure 3.6. *An illustration of inductances and magnetic fluxes in the mutual inductive coupling of a dominant primary and a submissive secondary winding.*

It depends on the primary side current's frequency and on the geometries and distances of the primary and the secondary side as to what share of the primary side flux effectively couples mutually with the secondary side and vice versa. In other words, figure 3.6 is a valid representation only with a given physically fixed configuration of the primary and the secondary side at a fixed frequency. Moving the two sides in relation to each other or changing the primary side current's frequency would change the effective mutually coupling flux and thus move the representative squares in the figure in relation to one another. In the case of perfect mutual coupling the squares would be perfectly overlapping. It follows that by definition inductance is always only stipulated by geometries and distances, not by any electrical quantities.

Figure 3.6's surface areas can also be associated with the induced voltages in figure 3.4:

1) the blue square with the voltage V_{L1} across the primary side intrinsic inductance
2) the red square with the maximum voltage $V_{L2,max}$ across the secondary side intrinsic inductance (when the induced secondary side current is at its maximum)
3) the striped area (both green and yellow stripes) with the voltage V_{L2} across the secondary side intrinsic inductance
4) the black-background area with the voltage V_{N2} across the secondary side extrinsic inductance
5) the green-striped area with the voltage V_{N1} across the primary side extrinsic inductance.

Lenz's law states the directions of the induced voltages: "Changing magnetic fluxes induce an induction voltage in such a direction that the induction current, if it can flow, opposes the original flux change [**14**]." In figure 3.5, the induced current on the secondary side satisfies Lenz's law by cancelling the whole *rate of change* of the mutually-coupled flux.

In figure 3.6, the striped area (both green and yellow) represents the secondary side flux that is associated with the given induced secondary side current, normalized to the secondary side intrinsic inductance. The magnitude of the induced secondary side current is directly proportional to the magnitude and the frequency of the primary side current, and inversely proportional to the load impedance of the secondary circuit. As mentioned, the striped area can be associated with the voltage V_{L2}, which is a voltage that opposes the voltage V_{N2} induced across the secondary side extrinsic inductance by the primary side current. The green-striped area represents the share of the induced secondary side flux that couples mutually with the primary side, cancelling out an equal amount of primary side flux. In figure 3.4, this can be associated with the voltage V_{N1}, which is a voltage that opposes the voltage V_{L1} self-induced across the primary side intrinsic inductance by the primary side flux. At maximum, the voltage V_{N1} can equal the voltage V_{N2} across the secondary side extrinsic inductance; this happens when the induced secondary side current is at its maximum, that is, large enough to fully cancel out the share of the primary side flux that couples mutually with the secondary side.

The area inside the blue square without green stripes represents the primary side's "residual magnetic flux", the share of the primary side flux that does not get cancelled out by the secondary side flux. This flux can be associated with the voltage $V_{L1} - V_{N1}$ in figure 3.4. If $V_{N1} = V_{N2}$, the green stripes fill the whole black-background area, leaving only the gray-background area uncovered inside the blue square. In such a case, the primary side residual flux stipulates the primary side leakage inductance, which is associated with the voltage $V_{L1} - V_{N1,max} = V_{L1} - V_{N2}$.

The area inside the red square with only yellow stripes represents the secondary side's residual magnetic flux, the share of the secondary side flux that does not couple mutually with the primary side. In figure 3.4, this flux can be associated with the voltage $\frac{V_{N1}}{V_{N2}} \cdot (V_{L2,max} - V_{N2})$. If $V_{N1} = V_{N2}$, the whole gray-background area inside the red square is covered by yellow stripes. In such a case, the secondary side residual flux stipulates the secondary side leakage inductance, which is associated with the voltage $V_{L2,max} - V_{N2} = V_{L2,max} - V_{N1,max}$.

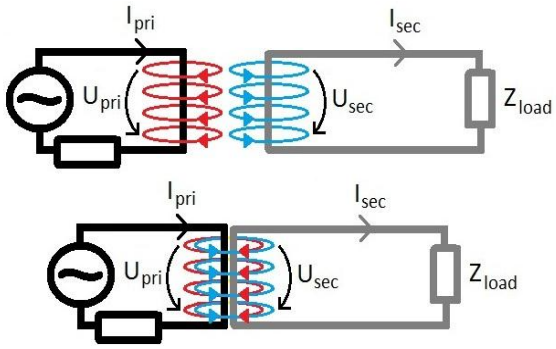

Figure 3.7. *The directions of a primary and a secondary side's magnetic fields between (top picture) and around (bottom picture) two coupling circuits.*

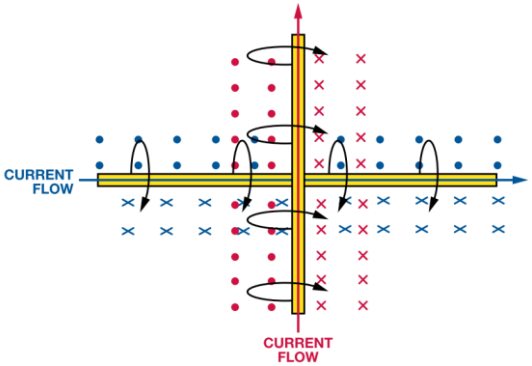

Figure 3.8. *Perpendicular conductors do not couple magnetically [**23**].*

Inductive Coupling between an Active Primary and a Passive Secondary Circuit

Figure 3.7 shows an "active" (an electricity source attached) current-driven primary circuit and a "passive" (no electricity source) secondary circuit with their primary and secondary side conductors, between which mutual coupling through extrinsic inductance occurs. The result of mutual inductive coupling is an induced voltage, which tends to drive an induced current. According to Lenz's law, the direction of an induced current is such that *around* both the primary and the secondary side conductor, that is, inside both the primary and the secondary circuit, its magnetic field "tries" to cancel out any change in the magnetic field of the current that causes the induction. The cancellation happens through superimposition of the magnetic fluxes of the primary and the secondary side, making the fluxes either to add up or subtract.

Figure 3.7 also illustrates the directions of a primary and a secondary side conductor's magnetic fields both between and around the conductors. Between the

conductors the magnetic fluxes add up and around them they subtract. Where the magnetic fluxes subtract, they contribute to both the extrinsic and the intrinsic inductances of the conductors. Where the magnetic fluxes add up, they contribute only to their intrinsic inductances. Thus, the closer the primary and the secondary side conductors are to each other, the less self-coupled flux and the stronger the mutual coupling between, that is, the larger the extrinsic inductance of, the two conductors.

The inductance associated with self-coupled flux, which we can call "residual intrinsic inductance", is always smaller than or equal with the conductor's actual intrinsic inductance; in terms of associated voltages of figure 3.4 we can express this as $V_{L1} - V_{N1} \leq V_{L1}$ and $V_{L2} - V_{N1} \leq V_{L2}$. This implies that when mutual inductive coupling takes place, the voltage drops across the primary and the secondary side conductors are lower than when the same currents are driven in them without any mutual inductive coupling. The effect is as if the intrinsic inductance was reduced on both the primary and the secondary side conductor. But since we have earlier defined inductance as something that only depends on the physical setting, the phenomenon must be seen as an ostensible reduction of intrinsic inductance caused by cancellation of magnetic fluxes. Thus, residual intrinsic inductance is not a real inductance.

If the primary and the secondary side conductors were perpendicular to each other, there would be no mutual inductive coupling and thus no extrinsic inductance between them [**23**]. This is because the secondary side conductor can have no induced current with such a magnetic field that would cancel out any of the magnetic field associated with the primary side's current. This, in turn, is because two perpendicular current flows do not have any parallel current flow components, as shown in figure 3.8. However, in reality, some inductive coupling would occur and result in eddy currents being created in the secondary side conductor. The magnetic field of these eddy currents would cancel out some of the primary side current's magnetic field, and thus, by definition, cause mutual inductive coupling and extrinsic inductance to exist between the primary and the secondary side.

Inductive Coupling between an Active Primary and an Active Secondary Circuit

The secondary side of mutual inductive coupling is not always passive, but may have a current driven by some electricity source of its own, as in inductive crosstalk between conductors of two different circuits – or between different conductors of one single circuit. When also the secondary side is active, differentiating which one is the primary and which one the secondary side becomes ambiguous, but we shall stick to this designation.

Let us consider two parallel current-carrying conductors, one of which is an active primary and the other one an active secondary side. When the conductors' magnetic field lines are superimposed, depending on the currents' directions, the field lines either 1) subtract around and add up between them, as in figure 3.9 with currents flowing in opposite directions or 2) subtract between and add up around them, as in figure 3.10 with currents flowing in the same direction.

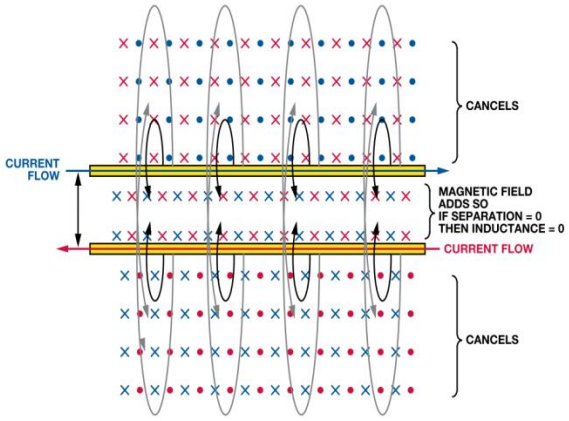

Figure 3.9. *Parallel conductors with currents flowing in opposite directions [**23**].*

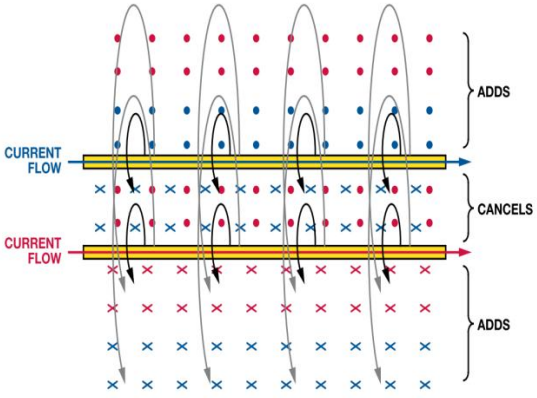

Figure 3.10. *Parallel conductors with currents flowing in the same direction [**23**].*

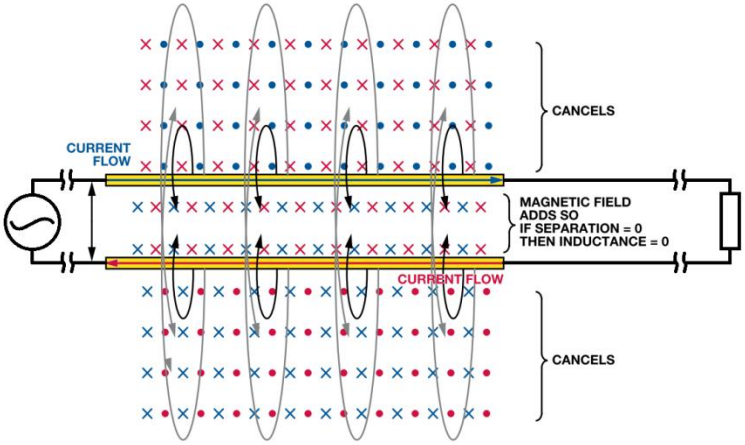

Figure 3.11. *Magnetic coupling between parallel send/go and return conductors in a single current loop [**23**].*

Figure 3.11 illustrates a current loop in which magnetic coupling between its send/go and return conductors can effectively be seen similarly as in inductive coupling between an active primary and an active secondary in which the currents are equal in magnitude, but opposite in direction. Due to the equal but opposite current flow on the send/go and the return conductors, all the mutually coupling magnetic flux is fully cancelled out. If the send/go and the return conductor are very close to each other, mutual coupling between them is perfect, that is, all their magnetic flux couples mutually because all the magnetic flux encircles both the send/go and the return conductor and none pass in between them. As a consequence, the mutually induced voltages V_{N1} and V_{N2} fully cancel out the self-induced voltages V_{L1} and V_{L2}, and thus the conductors appear as if they had no intrinsic inductance.

One EMC design principle, placing the send/go and the return conductor close to each other, is based on this ostensible reduction of their intrinsic inductances. A reduced intrinsic inductance enhances a circuit's SI and mitigates its near-field magnetic and far-field radiated coupling, both as the source/emitter and the receptor of EM energy [**24**].

Ideally, the send/go and the return conductor are twisted around each other, because twisting further enhances the cancellation of flux when the distance of the conductors is already the shortest attainable [**1**]. The circuit analysis way of explaining this is that "the voltage induced in each small twist area is approximately equal and opposite to the voltage induced in the adjacent twist area [**22**]", and thus the voltages cancel each other out.

It depends also on the electrical length of a current loop as to how well the voltages that are self-induced across the intrinsic inductances of its send/go and return conductor at a given frequency cancel out when the conductors are placed at a given distance from each other. If the conductors' distance is infinitesimally small and the current loop's electrical length much smaller than the wavelength at the given frequency, Lenz's law is always satisfied, and there is no self-induced voltage across the intrinsic inductance of the send/go or the return conductor. In contrast, if the conductors' distance is infinitesimally small, but the current loop's electrical length is not much smaller than the wavelength at the given frequency, the current's magnitude varies as a function of position along the current loop, because the frequency component of the current is a sinusoidal waveform. Thus, the current and its associated flux between two inductively coupled points, one on the send/go and the other one on the return conductor, have a phase difference. Consequently, Lenz's law is not fully satisfied, and voltages across the primary and the secondary side's intrinsic inductances do occur.

When Lenz's law is not satisfied by currents initially driven in the primary and the secondary sides, mutual induction attempts to satisfy it by inducing voltages that drive such currents that compensate for the difference in the initial currents' magnitudes between given two inductively coupled points. As a result, there is a net transfer of EM energy between the send/go and the return conductor, that is, a share of the EM energy "takes a short-cut" past the load. Such inadvertent mutual inductive coupling is an instance of inductive crosstalk.

3.2.2 Intrinsic and Extrinsic Capacitance

Intrinsic capacitance of an object is its total charge per one volt of the object's potential. According to *Gauss's law for electric fields*, the object's *total electric flux per one volt of its potential* means essentially the same and conveniently makes the definition more equivalent with that of intrinsic inductance. An object's total electric flux is the electric flux penetrating a closed surface enclosing the object, its total charge the amount of "unpaired" charge, that is, charge that does not have an opposite-sign counterpart within the closed surface, and its potential the average density of its unpaired charge.

Intrinsic capacitance is the minimum capacitance that an object always has regardless of how other objects are situated in relation to it. This is because intrinsic capacitance is the summation of *capacitance with infinity* and *capacitance with external charges*. Capacitance with infinity is called *free space capacitance*, and thus we shall call charge that is associated with free space capacitance as *free space charge*.

Capacitance with external charges, *extrinsic capacitance*, is directly proportional to the total electric flux that couples mutually with external charges, or flux that has its starting or termination points in external charges. Analogically with inductance, an object's maximum extrinsic capacitance is equal to its intrinsic capacitance in a given setting of charges and geometries; an object attains its maximum extrinsic capacitance when its free space capacitance is zero, and thus all its intrinsic capacitance is then capacitance with external charges.

Similarly with inductance, the extrinsic type capacitance of an object is stipulated only by the distances and geometries of the given object and the external charges in its surroundings, not by any electrical quantities, assuming the object is an ideal conductor. The capacitance value of all three types of capacitance, that is, capacitance with infinity, capacitance with external charges, and intrinsic capacitance, dictates the ratio of the associated charge and potential in the given capacitive coupling instance:

$$C = \frac{Q}{V}, \tag{3.4}$$

in which Q is the amount of charge involved in the given coupling instance and V the voltage between the coupling points, that is, the difference in their average unpaired charge densities or potentials. Note that one coupling point of a given capacitive coupling instance must always have a positive charge $+Q$ and the other one an equal but negative charge $-Q$.

Capacitive Coupling between Conductive Objects

Let us review some fundamentals of electrostatics for ideal conductors to better explain what was stated above.

Capacitance is associated with electric fields, and in the static and the *quasi-static* cases, electric fields are created by charges. A positive charge is traditionally illustrated having field lines beginning from it and a negative charge having field lines terminating in it, as shown in figures 3.12-3.14. In conductors, electrons are the negative charge carriers and protons the positive ones. Protons are confined to reside in their atom nuclei in solid conductors, but electrons are free to move around, making electrons the reason why conductors conduct.

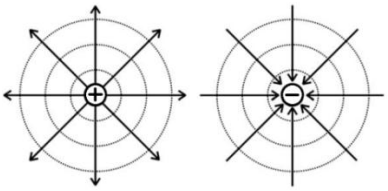

Figure 3.12*. Electric field lines of a positive and a negative charge [**16**].*

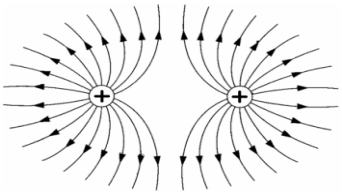

Figure 3.13. *Electric field lines of two like-signed charges [**25**].*

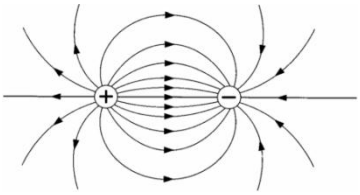

Figure 3.14. *Electric field lines of two opposite-signed charges [**25**].*

A conductor is *neutral* if it meets two conditions: 1) it has the same overall quantity of protons and electrons, and 2) it has them all *recombined*, or paired, and none *anti-recombined*, or unpaired.

If the first condition is violated, the conductor has a total charge, which can be negative due to an "excess" of electrons or positive due to a "shortage" of electrons with regard to the number of protons. In either case, the negative or the positive total charge tends to distribute itself on the surface of the conductor so that the charges are as far away from each other as possible, rendering the conductor's interior equipotential, as in the charged conductor in figure 3.15. When associated with the given conductor's free space capacitance, a total charge can build up in the conductor entirely irrespective of other objects in its surroundings, dependent only upon the conductor's own surface area. Charges on the surface of a conductor are called *surface charges*. The *surface charge density*, or rather its average, dictates the potential of a given conductor. The average surface charge density of a conductor is equal to its *average charge density of anti-recombined charges*, because in an ideal conductor all anti-recombined charges reside as surface charges.

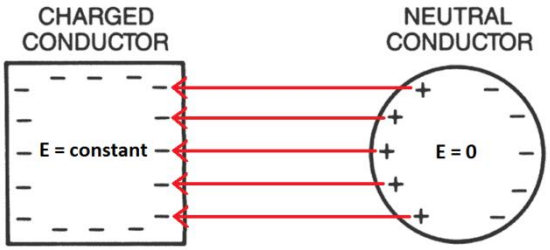

Figure 3.15. *A charged conductor causes anti-recombination and redistribution of charge in a neutral conductor [**1**].*

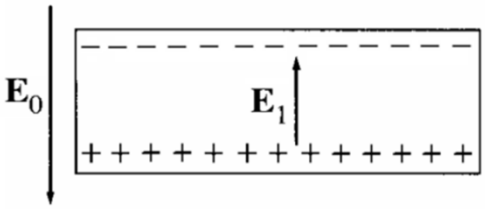

Figure 3.16. *An external electric field causes anti-recombination and redistribution of charge in a neutral conductor [**25**].*

If the second condition is violated, the conductor's charge is *polarized* due to an external electric field causing *electric induction* or *electric influence*, a manifestation of capacitive coupling. Electric induction may be caused by a near-by charged object, as in figure 3.15, or by some disembodied charges in the ambience, as in figure 3.16, apparent only from the electric field they produce. In either case, charges in the "victim" conductor start to anti-recombine and electrons start to flow in the direction of the electric field, effectively causing a current flow that redistributes the charges of the conductor. Consequently, an internal electric field is created within the conductor. The conductor's charge distribution tends toward a state in which the internal electric field is equal in magnitude with, but opposite in direction to, the external electric field that caused the electric induction. Only when such a charge distribution is reached, the conductor's charge distribution remains in equilibrium.

Surface charge densities on two conductors dictate if electric induction takes place between them and how strong it is, not the total charge on them per se. If two conductors with an identical size and shape, an equal non-zero total charge, and an equal size are brought close together, no electric induction occurs. This is equivalent to bringing close together just two neutral conductors. If two conductors with an equal total charge, but unequal size and/or shape are brought close together, electric induction

may take place, because the surface charge densities on them may differ due to geometrical differences. With two conductors of identical geometry, but unequal total charge, electric induction takes place inevitably.

Figures 3.17-3.20 depict electric induction between a conductor with a negative total charge and a conductor that 1) has an equal positive total charge, 2) is neutral, 3) has a smaller negative total charge, and 4) has a smaller positive total charge. In capacitive coupling, one coupling point must always have a positive charge $+Q$ and the other one an equal but negative charge $-Q$. If one side lacks enough charge of the needed sign, electric induction causes electrons and protons to *anti-recombine*, that is, become unpaired, and further electrons to flow in the direction of the electric field until equilibrium is reached.

When the extrinsic capacitance of a conductor is equal to its intrinsic capacitance, all of its anti-recombined charge is engaged in capacitive coupling. It follows that the maximum amount of charge possible to be engaged in capacitive coupling is the total charge of the involved conductor that has a larger total charge.

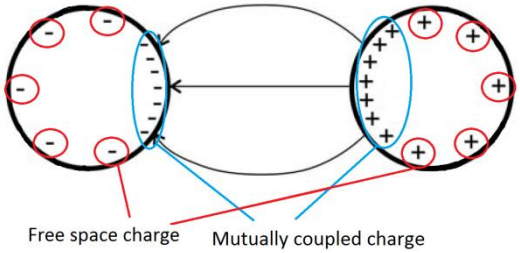

Figure 3.17. *Two conductors with an equal total charge but opposite sign.*

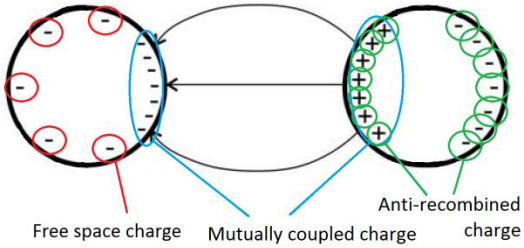

Figure 3.18. *A negative and an originally neutral conductor.*

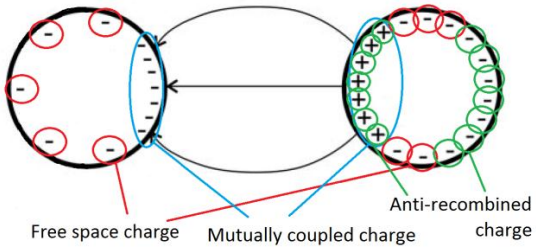

Figure 3.19. *Two conductors with unequal negative total charges.*

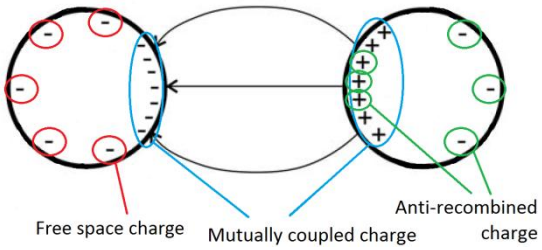

Figure 3.20. *Two conductors with unequal and opposite total charges.*

3.2.3 Intrinsic and Extrinsic Conductance

As for conductance, classification into its intrinsic and extrinsic forms could be done following similar logic as with inductance and capacitance, but because it would be somewhat contrived and would not yield much additional insight, we shall disregard such categorization and simply consider conductance to be of only one type.

3.3 Impedance in Storing, Transferring and Converting Electromagnetic Energy

Lumped impedance's "components", namely capacitance, inductance, and conductance/resistance, define a given modeled object's capability to store, to transfer, and to convert EM energy that it is exposed to through given two coupling points in it into heat. As a side note, conductance and resistance are each other's reciprocals, and even though resistance is more often used as a lumped circuit element in circuit analysis, it is more apt to equal expressly conductance with inductance and capacitance when EM coupling is concerned. Thus, we talk about conductance instead of resistance in this connection.

Inductance and capacitance cause separate points in space to *couple together* through magnetic and electric fields, respectively, enabling EM energy to propagate through the created *EM coupling path*. With inductance, this coupling phenomenon is called inductive coupling, and with capacitance capacitive coupling of EM energy. An instance of inductive or capacitive coupling can be interpreted as a phenomenon that either stores or transfers EM energy, although such a division is often trivial because in the end, both are just manifestations of EM coupling.

Conductance is different from inductance and capacitance in that it creates its associated coupling phenomenon, that is, *conductive coupling* of EM energy, through moving charge carriers between the given coupling points, not through EM fields directly. But moving charge carriers require an electric field to move them, and moving charge carriers themselves generate a magnetic field around them. Thus, conductance is, in fact, affiliated with both electric and magnetic field, but in an indirect way.

Added conductance in an electric field can be regarded as something that "transforms" an electric field's energy into a magnetic field's energy, or even charge carriers' "potential energy" into charge carriers' "kinetic energy", although such terminology is not correct in this context. The conductance of a conductive coupling path also governs the conversion of associated EM energy into heat; the higher the conductance, the less of the associated EM energy is converted into heat in it.

Although higher conductance was just claimed to mean less heat conversion, added conductance in an electric field, in fact, often increases the generated heat. This can be seen from a basic expression for power: heat loss in a resistive load, $P = U^2/R$; when conductance increases, resistance R decreases, and consequently power P increases. The explanation is that added conductance does not necessarily mean smaller *absolute* but instead smaller *relative* conversion of associated EM energy into heat. Added conductance increases the total associated EM energy in the conductive coupling path, because it becomes a more likely propagation path for EM energy than the surrounding medium, but a smaller *relative share* of the EM energy is converted into heat in it. The resulting total heat energy generated may be either less or more with the added conductance than without it, depending on certain additional factors.

3.3.1 Impedance in Electrodynamic Situations

From the above description of conductance's effect in an electric field it may seem that the nature of electric field is to store energy and the nature of magnetic field is to transfer it. This may apply to *electrostatic* situations, but in *electrodynamic* situations the roles are often quite the opposite. In fact, at high enough frequencies conductance's/resistances become negligible both because electric fields *transfer* all EM energy across insulators through *displacement currents*, and because magnetic fields *store* all EM energy around conductors through *self-induction*. Thus, in very high-frequency electrodynamic situations mainly the magnetic fields associated with intrinsic inductances store EM energy, and mainly the electric fields associated with extrinsic capacitances transfer EM energy. However, also the magnetic fields associated with extrinsic inductances transfer EM energy, and also the electric fields associated with free space capacitances store it in electrodynamic situations.

One can picture the storing of EM energy in magnetic fields through the notion of "energy feedback" and the transferring of it via electric fields through the notion of "energy feed-forward". Intrinsic inductance stores EM energy in a stretch of conductor's affiliation through an energy feedback, in which a current's associated magnetic field energy is converted into an induced voltage's associated electric field energy through self-induction. The self-induction continually "feeds back" EM energy into the stretch of conductor, preventing the EM energy from leaving it. Conversely, extrinsic capacitance transfers EM energy past a stretch of conductor through an energy feed-forward, in which a current's associated magnetic field energy is converted into a displacement current's associated electric field energy through electric induction. The capacitive coupling continually "feeds forward" EM energy past the stretch of conductor, preventing the EM energy from entering it. As the frequency rises, the feedback and the feed-forward strengthen. Eventually, the intrinsic inductance of the stretch of conductor feeds back all the EM energy that has entered into it, and the extrinsic capacitance of the stretch of conductor feeds forward all the EM energy that arrives into its affiliation. This behavior is best understood by reviewing the high-frequency behavior, or parasitic impedances, of different electric circuit elements.

3.4 Parasitic and Stray Impedance

Unwanted impedances are called *parasitic* or *stray* impedances. At a given frequency, if there are no other conductive objects within the near field of a given object, all its unintentional impedances are parasitic impedances, that is, undesired inductances, capacitances, and conductances which couple its distinct points together. But if other conductive objects exist within the given object's near field, it also has stray impedances, which couple it together with those other objects. In some literature, stray impedances are regarded a subset of parasitic impedances and are therefore called *stray parasitic impedances*. But in this paper we consider them two mutually exclusive types

of *unintentional EM coupling* which exist between and within different parts of components/devices/systems, such as conductor leads, wires, traces, pads, planes, platings, shields, heat sinks, racks, cases, and enclosures.

A component model with only parasitic impedances, that is, with only the component's internal composition determined, is a decent estimation of its real-life behavior. However, yet a better model takes into account also the stray impedances, requiring consideration of the component's surroundings' impact, that is, that of the whole circuit, the whole system, and the entire EM environment. But differentiating between parasitic and stray impedance is not always easy, as the boundaries of a single object are not explicit, and so it depends on the scope of observation whether a given unwanted impedance is stray or parasitic.

3.4.1 Conductor's Hidden Schematic

In circuit analysis, conductors are normally considered ideal: having no resistive losses, intrinsic or extrinsic inductances, or intrinsic or extrinsic capacitances. However, no real-life conductor has a zero impedance; especially at high frequencies resistances, inductances, and capacitances come into play substantially.

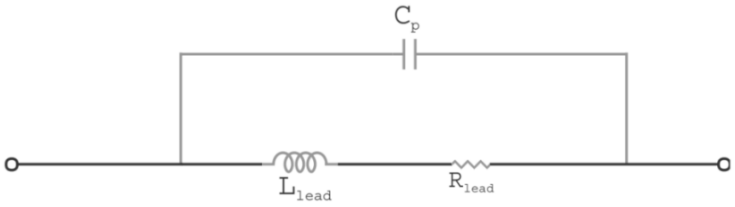

Figure 3.21. *A high-frequency equivalent circuit of a stretch of conductor [**16**].*

A high-frequency equivalent circuit showing parasitic impedances of a stretch of conductor is illustrated in figure 3.21. At low frequencies, the resistance is the sole "decisive" parasitic impedance, that is, the only one that needs to be considered, due to its significant impedance value. But at higher frequencies, the inductance becomes decisive too, as per the expression for *inductive reactance*, $X_L = \omega L$, and eventually even more that than the resistance. When the frequency is yet higher, the capacitance also becomes significant by providing a path for current to bypass the inductance and the resistance, as per the expression for *capacitive reactance*, $X_C = 1/\omega C$. Eventually, at high enough frequencies, the inductive reactance is very high and the capacitive reactance very low in value. Now the earlier description of energy feedback and feed-forward in a stretch of conductor is more understandable.

In addition to reactive impedance, or inductive and capacitive reactance, *resistive impedance* also changes with increasing frequency due to skin effect, which forces current to flow closer to conductor's surface. Skin effect decreases the conductor's cross-sectional area in which the current is able to flow and therefore increases the resistance in the current's path. This phenomenon does not happen in electrostatic situations; it is exclusive to electrodynamic ones. *Skin depth* gives the depth into the

conductor by which *current density* has reduced to *1/e*, where *e* is *Euler's number*. Skin depth is denoted with δ and defined as

$$\delta = \frac{1}{\sqrt{\pi \cdot f \cdot \mu_0 \cdot \mu_R \cdot \sigma}}, \tag{3.5}$$

in which σ is the conductivity of the conductor material. Each skin depth further into the conductor reduces the current density by another *1/e*. The higher the frequency is, the less the depth into the conductor and the smaller the cross-sectional area below the conductor's surface in which the current can flow and, consequently, the higher the resistance that the conductor appears to have.

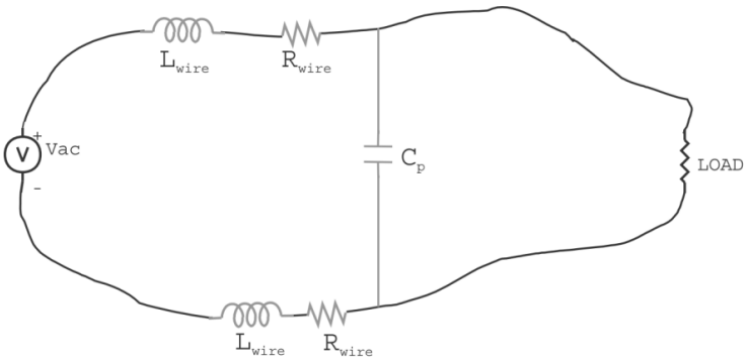

***Figure 3.22**. A high-frequency equivalent circuit of a current loop [**16**]*.

Figure 3.22 shows a high-frequency equivalent circuit of a current loop: the parasitic intrinsic inductances and the resistances of the send/go and the return conductors and the extrinsic capacitance between them. High-frequency equivalent circuit analysis of a current loop is, in fact, more or less similar with transmission line analysis, as one can see when comparing figure 3.22 with figure 3.1.

A current loop's high-frequency equivalent circuit can be used for analyzing crosstalk within the current loop. Capacitive coupling through extrinsic capacitance between the send/go and the return conductor is a source of capacitive crosstalk. Figure 3.22 does not present inductive coupling through extrinsic inductance between the send/go and the return conductor, but as long as the distance between the conductors is within near field's limits, also extrinsic inductance and consequent mutual inductive coupling occurs. Inductive coupling through extrinsic inductance between the send/go and the return conductor is a source of inductive crosstalk.

3.4.2 Resistor's Hidden Schematic

A high-frequency equivalent circuit of a resistor component is essentially the same as that of a stretch of conductor. The main difference is that the resistor's resistance value is not a parasitic impedance, but an intentional resistive impedance and thus usually much larger by its absolute value and in relation to the parasitic inductance and capacitance values than in the case of a stretch of conductor's parasitic resistance. Another difference is that the parasitic inductance resides mainly in the association of the component leads and the parasitic capacitance between the component leads. Figure

3.23 shows a resistor's high-frequency equivalent circuit, in which the larger resistance value is emphasized with a larger font and a larger circuit element symbol.

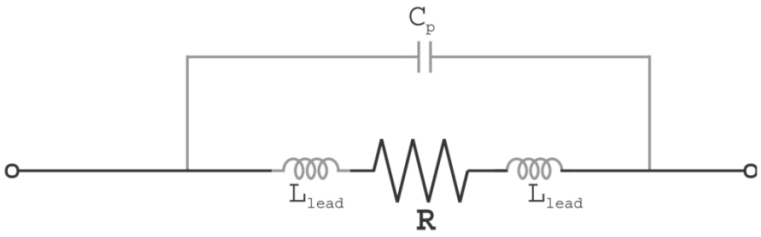

Figure 3.23. *A high-frequency equivalent circuit of a resistor* ***[16]***.

3.4.3 Inductor's Hidden Schematic

High-frequency equivalent circuit of an inductor component is similar to those of a stretch of conductor and a resistor component. The main difference is that an inductor's inductance, which is mainly not parasitic, resides in the association of an *inductor winding*, adjoined by the component leads. This inductance is larger by absolute value and in relation to parasitic resistances and capacitances than in the case of the former ones. A second difference is that the *inductor core* provides a conductive coupling path in parallel with the inductance. Thirdly, the absolute value of an inductor's parasitic capacitance is likely to be larger than that of a conductor or a resistor, because the inductor winding's turns constitute plenty of parallel conductive surface area, between which large extrinsic capacitances can be formed. Figure 3.24 shows a high-frequency equivalent circuit of an inductor with the inductor winding's inductance, the inductor core's parasitic conductance/resistance, and the parasitic resistances of the component leads.

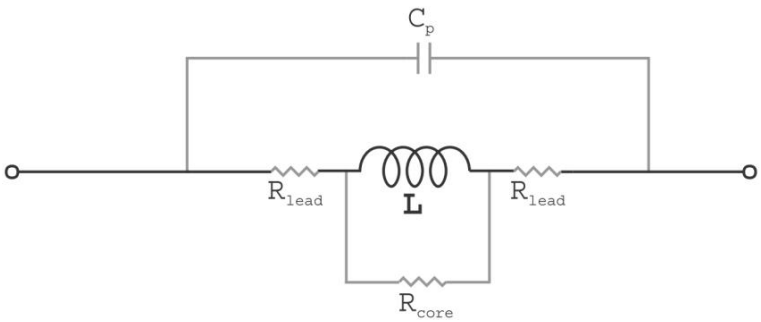

Figure 3.24. *A high-frequency equivalent circuit of an inductor* ***[16]***.

3.4.4 Capacitor's Hidden Schematic

A capacitor component's high-frequency equivalent circuit is yet one more step different from that of a conductor. Figure 3.25 shows the intentional capacitance, which normally varies significantly with frequency, charge level, temperature and the life cycle of the capacitor, emphasized in the middle. Moreover, there are parasitic resistances and inductances of the component leads and two parasitic conductances/resistances through the capacitor's dielectric; one of the conductances models an electrostatic situation and the other one an electrodynamic situation.

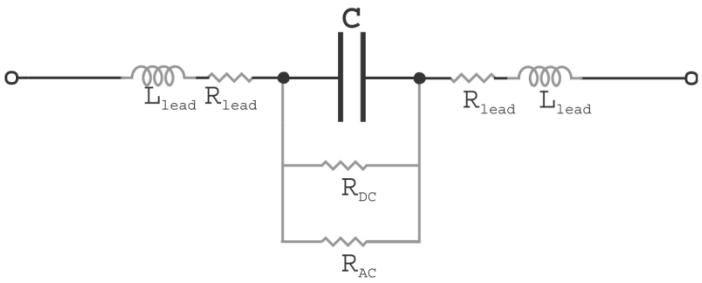

Figure 3.25. *A high-frequency equivalent circuit of a capacitor* ***[16]****.*

3.4.5 Transformer's Hidden Schematic

The transformer's high-frequency equivalent circuit is a combination of those of the above "basic" circuit elements. The more windings a transformer has, the more complex its equivalent circuit becomes. Figure 3.26 models a two-winding transformer with an equivalent circuit that includes its parasitic impedances. The equivalent circuit shows 1) the parasitic intra-winding (C_P and C_S) and inter-winding (C_{PS}) capacitances, 2) the extrinsic inductance (L_M) associated with the mutually coupled magnetic flux (ϕ_m), 3) the leakage inductances (L_{l1} and L_{l2}) associated with the self-coupled magnetic fluxes (ϕ_{l1} and ϕ_{l2}), 4) the parasitic resistive loss of the windings (R_1 and R_2), and 5) the parasitic magnetic loss of the core (R_C).

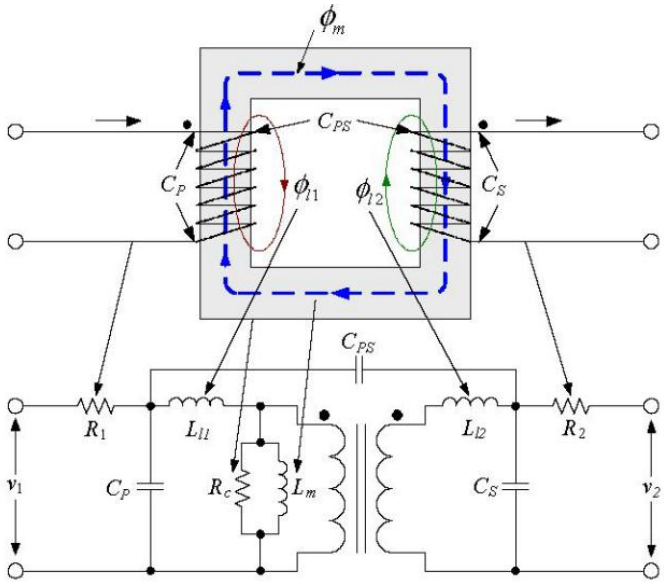

Figure 3.26. *A high-frequency equivalent circuit of a transformer* ***[26]****.*

3.4.6 Diode's Hidden Schematic

Semiconductor devices, such as diodes and transistors, have more complex physical phenomena behind their operation than the above components, and thus their high-frequency behavior cannot be explained as simply. Semiconductor devices consist of semiconductors doped with *acceptor* or *donor impurities* (*p-type* or *n-type* semiconductor, respectively), which give the device a certain behavior dependent on voltages and/or currents that it is exposed to. [**27**]

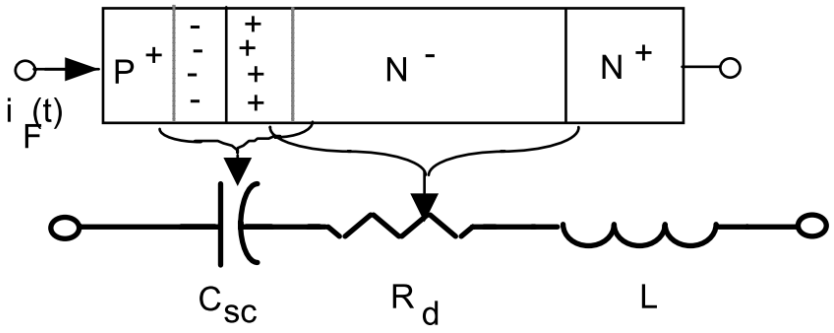

Figure 3.27. *A high-frequency equivalent circuit of a diode [**28**].*

As figure 3.27 shows, a diode's equivalent circuit has a resistance R_d, a variable accounting for the basic behavior of the diode. When the diode is *forward-biased*, R_d is small due to a large number of excess charge carriers in the *drift region* (N^-). In contrast, when the diode is *reverse-biased*, R_d is large due to a small number of excess charge carriers in N^-. However, because R_d implements the desired functionality of the diode, it is not a parasitic impedance by our earlier definition.

There are also two parasitic impedances in the equivalent circuit: the capacitance C_{SC} and the inductance L. The latter is simply caused by bonding wires that are attached to the diode's silicon wafer, but the cause of the former is more complicated. When a diode is reverse-biased, it has its *majority charge carriers* diffused across the *pn junction*, creating a *space charge layer* of opposite charge on both sides of the junction. A pair of space charge layers forms a *depletion region*, where free charge carriers are absent due to diffusion, and only ionized donor and acceptor impurities are left to constitute the space charges. Similarly with any pair of negative and positive charges, also the space charges have an electric field and a consequent capacitance, *space charge capacitance* C_{SC}, between them. Thus, a reverse-biased diode's equivalent circuit incorporates a parasitic capacitance. [**27**]

When the diode becomes forward-biased, the depletion region is removed due to an injection of excess charge carriers into the region. Consequently, the capacitance is not only discharged, but it, in fact, ceases to exist. In other words, forward-biasing "breaks" the space charge capacitance. When the diode becomes reverse-biased again, the space charge layers form again. In other words, reverse-biasing "makes" the space charge capacitance. Thus, a forward-biased diode has no parasitic capacitance in the form of space charge capacitance, but it does incorporate another form of parasitic capacitance, namely *diffusion capacitance*, located in the drift region. [**27**]

The combined effect of diode's impedances causes an overshoot at its turn-on and a *reverse recovery* at its turn-off, as illustrated in figure 3.28. The overshoot waveform is due to R_d changing, L exhibiting a voltage stipulated by the *current waveform's rate of change* (di/dt), and the capacitances smoothing out the transition. The reverse recovery is the easiest to understand merely as the negative current charging up the space charge capacitance, although also R_d changes and the voltage across L is stipulated by di/dt again, which play a part in the phenomenon as well.

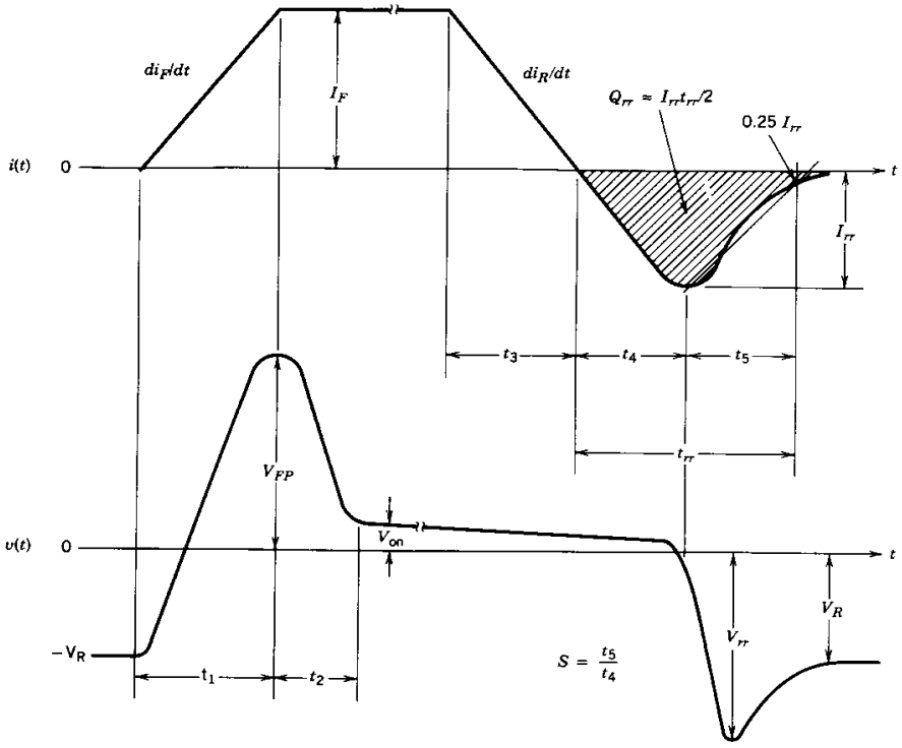

Figure 3.28. *Graphs showing diode current's and diode voltage's behavior in a forward-biasing ($t_1 – t_2$) and a reverse-biasing ($t_3 – t_5$) instance [**27**].*

3.4.7 Transistor's Hidden Schematic

Transistors consist of the same p type and n type semiconductor materials as diodes, but their structure is more complex; for example, they have several p type and/or n type regions interacting with each other. This structural difference makes the functionality of a transistor different and more complex from that of a diode. But by breaking the transistor down into its "components", an equivalent circuit can be presented all the same. Figures 3.29 and 3.30 show the physical structure, the parasitic capacitances, the parasitic *bipolar junction transistor* (BJT), and the "integral diode" of a *metal oxide semiconductor field-effect transistor* (MOSFET), which can be used to create a high-frequency equivalent circuit for a MOSFET. [**29**]

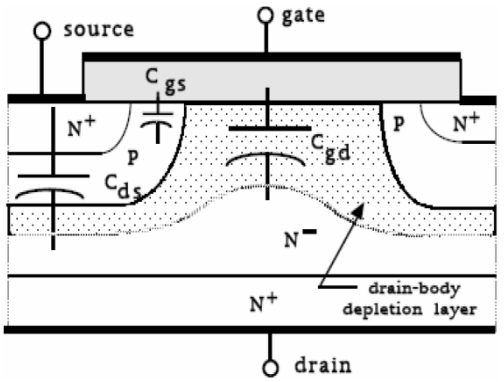

Figure 3.29. *The physical structure and the parasitic capacitances of a MOSFET [**29**].*

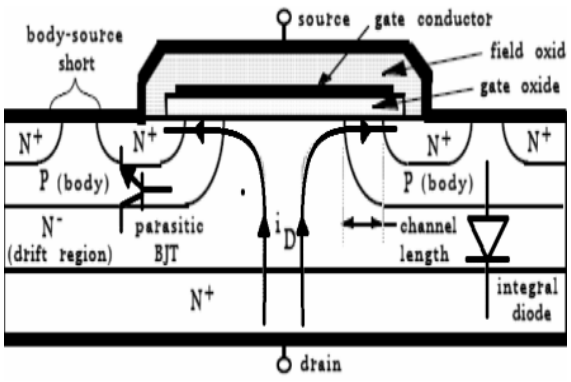

Figure 3.30. *The physical structure, the parasitic BJT and the integral diode of a MOSFET [**29**].*

4 ELECTROMAGNETIC EMISSIONS

EM emissions can be broken down into different types in several ways; an emission can be classified as *intentional* or *unintentional*, *magnetic* or *electric*, *near-field* or *far-field*, *common-mode* or *differential-mode*, *external* or *internal*, and *conducted* or *radiated* emission. Moreover, alongside all these types of emissions, there is a phenomenon called *resonance* or *standing wave*, which has a special effect on the magnitudes of the emissions.

4.1 Intentional and Unintentional Emissions

First of all, EM emissions can be intentional or unintentional. For example, the purpose of a radio transmitter is to emit intentional EM emissions, though only at specified frequencies. Devices such as induction stoves, wireless chargers and RFID scanners are intentional emitters as well, but the frequency range in which they emit EM energy is carefully limited so that the devices would only serve their intended purposes and not interfere with other devices. Most devices are not intended to emit any EM energy into their surroundings – at least at RF frequencies – and so their EM emissions are unintentional. However, unintentional EM emissions are unavoidable because all current flow, including displacement current flow and current flow of a device's normal operation, produces EM emissions into the surroundings. That is why the focus must be on how to prevent "avoidable unintentional EM emissions" from being emitted into the surroundings.

All avoidable unintentional EM emissions that a system creates can be regarded as a consequence of the inevitable existence of parasitic and stray impedances, that is, undesired inductances, capacitances, and conductances of non-ideal components in a non-ideal circuit located in a non-ideal environment. These unintentional impedances cause unintentional *near-field coupling*, which creates noise currents and voltages. These noise currents and voltages cause EM emissions either directly per se or indirectly through radiation, the latter of which is also called *far-field coupling*. We shall discuss both of the ways in this chapter.

4.2 Magnetic and Electric Emissions

The EM field consists of two components: the electric and the magnetic field, which both have three properties – *magnitude*, *flux density*, and *direction* – at every point in

space. Because vectors always have a magnitude and a direction, we use *vector fields* to present *electric field strength* (E), *electric flux density* (D), *magnetic field strength* (H), and *magnetic flux density* (B) in any given space.

An EM field is always created by charges, which are or are not moving or fluctuating. Man-made sources of EM fields are usually electric circuits, which have voltages that drive currents, or *charge gradients* that cause charge carriers to move.

Let us categorize sources of EM fields into ideal electric field sources/emitters, ideal magnetic field sources/emitters, and real-life EM field sources/emitters.

An ideal electric field source/emitter contains a voltage source that creates a high voltage between its two terminals. Despite the high voltage, the ideal electric field source/emitter has no charge carriers moving out of its terminals to the load, resulting in high voltage *U*, zero current *I*, and infinite source/emitter's characteristic impedance $Z_c = \frac{U}{I}$. Consequently, the wave impedance $Z_w = \frac{E}{H}$ in the medium around the source/emitter is also infinite because although the created E is large, H is zero. In practice, the current and thus H can be kept small when the impedance between the voltage source's terminals is large.

In contrast, an ideal magnetic field source/emitter contains a current source that drives a high current in an affiliated current loop. The ideal magnetic field source/emitter has no potential difference, or voltage drops, between the affiliated current loop's different points, resulting in zero voltage *U*, high current *I*, and zero source/emitter's characteristic impedance $Z_c = \frac{U}{I}$. Consequently, the wave impedance $Z_w = \frac{E}{H}$ in the medium around the source/emitter is also zero because although the created H is large, E is zero. In practice, the potential differences and thus E can be kept small when the impedance between the current source's terminals is small.

Real-life EM field sources/emitters have an intermediate "intrinsic nature"; they are neither ideal electric nor ideal magnetic field sources/emitters, as there is always some motion of charge carriers involved with electric field sources/emitters and some voltage drops involved with magnetic field sources/emitters. Therefore, this paper uses the designations "a good electric field source/emitter" and "a good magnetic field source/emitter" instead.

4.3 Near-Field and Far-Field Emissions

Figure 4.1 shows the change of the wave impedance of a good electric field source/emitter and that of a good magnetic field source/emitter towards the characteristic wave impedance of the medium, as section 2.2.3 explained. In the nearfield, one must know both E and H to determine the nature, or the wave impedance $Z_w = \frac{E}{H}$, of the field at a given point. In the far field, it is sufficient to know either E or H, provided the medium's characteristic impedance is also known, because the characteristic impedance gives the ratio of E and H in the far field. In vacuum this characteristic impedance has a value $120\pi\ \Omega \approx 377\ \Omega$ and is called the *free space*

characteristic wave impedance. Other mediums have their own individual characteristic wave impedance values.

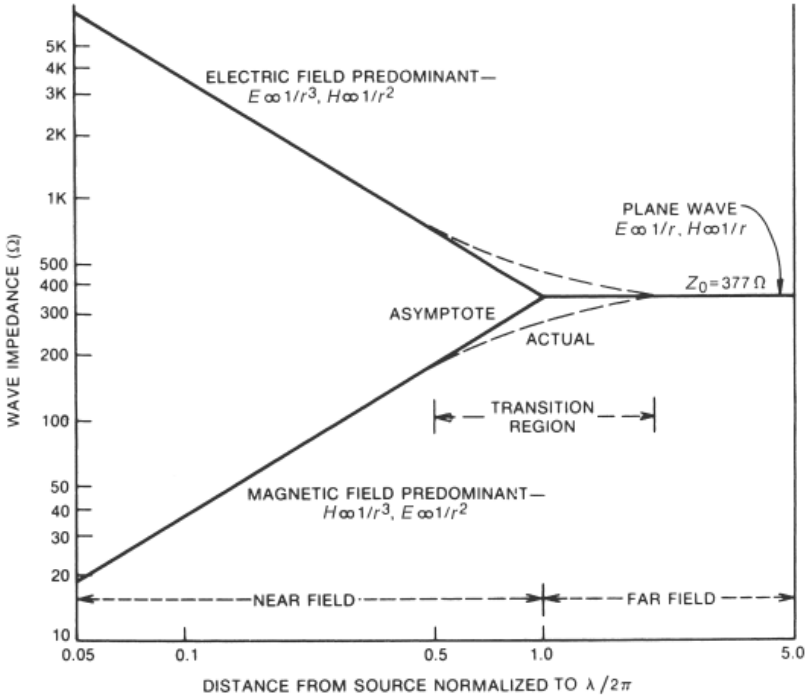

Figure 4.1. *A good electric field source/emitter's (upper) and a good magnetic field source/emitter's (lower) wave impedance as the function of distance from the source/emitter [**1**]*.

E and H components in the near field form complex patterns that can be described in terms of vector fields. The vectors in these vector fields have terms proportional to *1/r*, $1/r^2$, and $1/r^3$, where *r* is the radial distance to the source/emitter, as was mentioned in section 2.2.3. The latter two terms dominate in the near field, but at a far enough distance the *1/r* term becomes predominant. This is the boundary distance, which divides a source/emitter's EM field into a near field and a far field. The boundary distance is approximately $\lambda/2\pi$, that is, itdepends on the frequencyof the source/emitter's EM energy. In the far field, the patterns of E and H are simpler, because the *1/r* term is decisive and the ratio between E and H is stipulated by the characteristic impedance everywhere. In other words, the distribution of fields in far field follows that of a TEM wave, with the field strengths only varying as a function of *1/r* as the EM wave propagates further away from the source/emitter. [**20**]

With an electrostatic circuit, the boundary distance $\lambda/2\pi$ is in infinity, and thus the intrinsic nature of the source/emitter is reflected on the wave impedances everywhere in the surroundings, *without changing over distance*. With an electrodynamic circuit, however, the distance $\lambda/2\pi$ is finite, and so the wave impedance of the EM field of even a near-to-ideal electric or a near-to-ideal magnetic field source/emitter *changes over distance* and eventually reaches the characteristic wave impedance of the medium at a certain distance away from the source/emitter. [**20**]

4.4 Common-Mode and Differential-Mode Near-Field Emissions

An electrodynamic EM field source/emitter causes always both near-field and far-field emissions; no electrodynamic source/emitter creates only either one. Near-field emissions are always generated by near-field coupling within the EM field source/emitter or between the source/emitter and its exterior. Currents and voltages produced by near-field coupling can be either *common-mode* (CM), in which case they are usually always undesired noise or *differential-mode* (DM), in which case they can be either intentional signals of normal operation or undesired noise. Far-field emissions can also be classified as DM or CM depending on whether the "causative current", or the noise current that causes the radiation, is in DM or CM.

A *CM voltage* is a voltage between a pair of intended conductors of a current loop and the ground reference *or* a voltage between two points in the ground reference that drives current in all available ground loops, such as the ones made up by conductors of a current loop. In contrast, a *DM voltage* is a voltage between two intended conductors. Circuits' intentional voltages, that is, the intentional drivers of the circuits' functional signals or power, are DM voltages. Intentional DM voltages originate from the circuit's voltage sources and drive *DM currents* that flow 1) only along the intended send/go and return conductors or 2) partly along the intended conductors and partly along the unintended ground reference to "close" their DM current loop.

In a current loop, CM currents are equal in magnitude and in phase in the intended send/go and return conductor, whereas DM currents are equal in magnitude, but have a 180° phase shift between the send/go and the return current, that is, the DM send/go and return current flow in opposite directions. CM currents exist in current loops either due to *unbalance* of the current loop or due to external sources. Figure 4.2 illustrates CM and DM currents and voltages in a *balanced* current loop. The loop is balanced, because the DM currents in the send/go and the return conductor are equal.

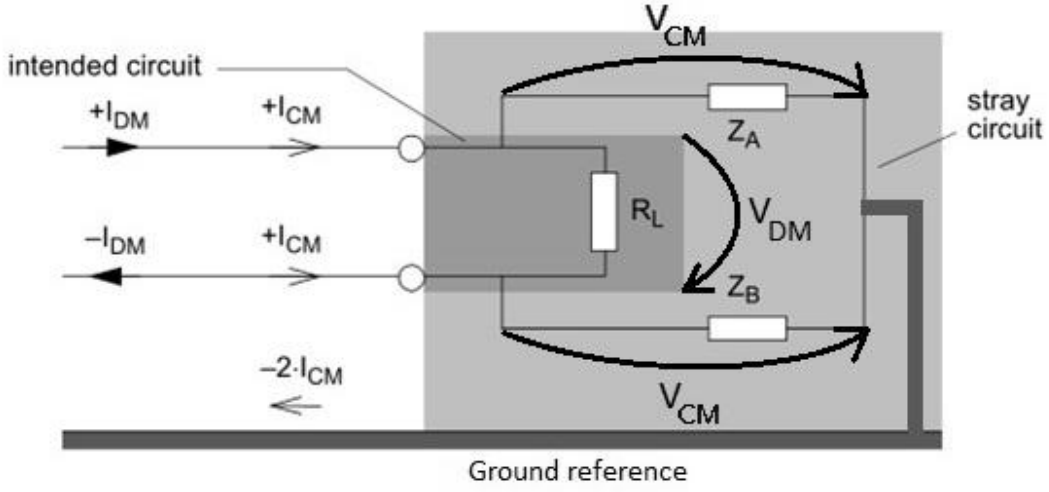

Figure 4.2. *A balanced current loop ($Z_A = Z_B$), in which DM current is equal in magnitude but opposite in direction and CM current equal in magnitude and uniform in direction in the intended send/go and return conductor* ***[21]****.*

Power and signal sources create intentional DM voltages and currents with the energy from the mains supply, and capacitors and inductors create those with the energy charging in and discharging from their electric fields and magnetic fields. But not all DM signals are intentional; part of DM voltages and currents may originate from unintentional near-field coupling through stray and parasitic impedances, causing noise and leading to impaired SI and consequent external emissions, as section 2.3.6 explained. It may be useful to model impedances as DM signal or noise sources, especially if the impedance of the given component is parasitic or variable, such as with a switching device. We shall make use of this technique in this paper.

There are a few different reasons why CM currents occur in circuits. *CM noise generation due to ground loops* is a phenomenon in which a current loop is connected to the ground reference through impedances, creating *ground loops*. A prerequisite for CM noise generation in the ground loops is a potential difference, that is, a voltage drop, between two connection points to the ground reference. One can model this voltage drop with a *noise voltage source*, which drives CM noise currents in available ground loops, which are made up of the send/go or the return conductor, the portion of ground reference between the two connection points on the ground reference, and the impedances that couple them all together into a current loop. [**22**]

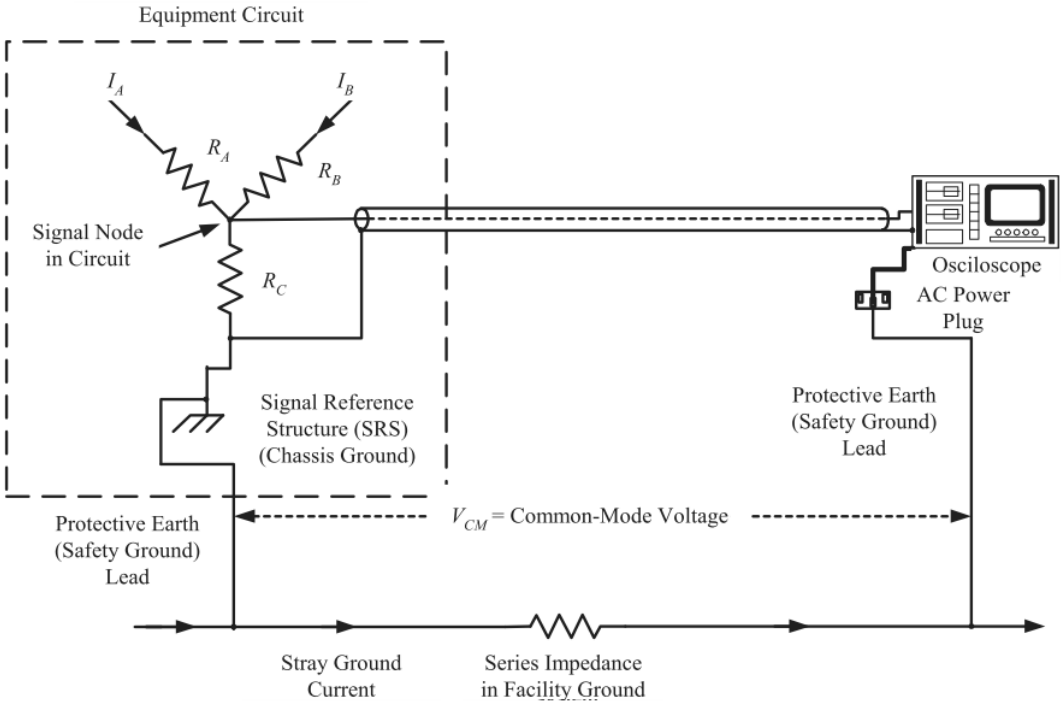

Figure 4.3. *CM noise generation due to common impedance interference coupling: an external interference source creates a voltage drop in the ground reference, which drives CM noise current in available ground loops [**22**].*

A potential difference between the two connection points on the ground reference can be created due to two reasons. One reason is *common impedance interference coupling*, in which an external interference source creates a current in the ground reference, that is, a *stray ground current*, creating a voltage drop in the ground

reference's impedance. Figure 4.3 illustrates this phenomenon. Another reason is *DM-to-CM conversion* due to an *alternative return path* for DM currents, which distributes the total return current as two return currents, a "return conductor current" and a stray ground current, the sum of which must equal the send/go current in accordance with *Kirchoff's current law*. For this reason, a voltage drop may be created in the ground reference even without any external interference sources' influence, but only if the DM current loop is *unbalanced*. Figure 4.4 illustrates this phenomenon; what essentially happens in the process is that EM energy in DM is converted into that in CM. In other words, DM-to-CM conversion can generate unintentional CM currents from intentional DM currents. [**22**]

An imbalance between the send/go current and the return conductor current is a sign that DM-to-CM conversion is taking place; when the send/go current and the return conductor current are not exactly equal in amplitude and opposite in phase, the return conductor current has lost its pairing with the send/go current. Joffe [**22**] states: "The portion of the current not flowing in the intended return path constitutes the 'common-mode' current."

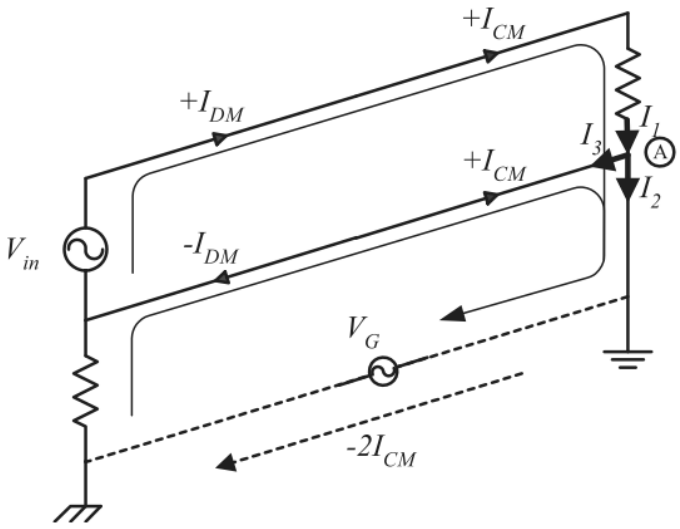

Figure 4.4. *CM noise generation by DM-to-CM conversion due to an alternative return path through the ground reference [**22**].*

Balancing a circuit prevents DM-to-CM conversion from happening in it. Ott defines: "A *balanced circuit* is a two-conductor circuit, in which both signal conductors, and all circuits connected to them, have the same nonzero impedance with respect to a reference (usually ground) and all other conductors … If the impedances of the two signal conductors to ground are unequal, then the system is unbalanced. [**1**]"

DM current that takes an alternative return path via the ground reference, that is, stray ground current, can be eliminated by balancing the current loop by making the impedances to the ground reference equal on both the send/go and the return conductor's side. We can model the load R_L in figure 4.2 with a "test voltage source" V_{DM}, which drives a "test current" opposing the current driven by the current loop's feeding electricity source. If Z_A and Z_B are equal, V_{DM} drives a net test current only in

the current loop made up of the send/go and the return conductor. This is because from V_{DM}*'s* standpoint the two possible current loops via the ground reference (one via the return conductor and Z_A, and the other one via the send/go conductor and Z_B) have equal impedances, and thus equal but opposite test currents flow in these two loops, cancelling out the net test current and thus causing no voltage drops in the ground reference. If Z_A and Z_B are unequal, however, the two possible current loops via the ground reference have unequal impedances and thus unequal test currents flow in these two loops, resulting in a net test current in the ground reference. This net test current, or stray ground current, creates a voltage drop in the ground reference, and the voltage drop drives a CM noise current in all available ground loops.

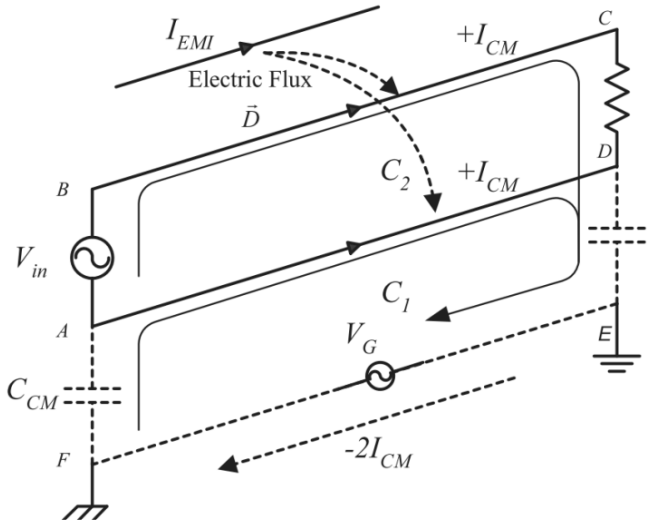

Figure 4.5. *An electric field inducing a CM current in a circuit [**22**]*.

CM currents can also be produced directly by an external source, such as an inductively or a capacitive coupling EM near field or an impinging TEM wave [**22**]. Figure 4.5 shows an electric field inducing a CM current in a current loop. CM noise currents created by these external interference sources may be unavoidably present.

Reciprocally with DM-to-CM conversion, *CM-to-DM conversion* takes place if the current loop is unbalanced and if CM currents are present in it. If the current loop in figure 4.2 is unbalanced, that is, if the impedances Z_A and Z_B are unequal, the voltages across Z_A and Z_B are also unequal. The difference of the voltages results in a DM noise voltage across the load R_L, which can be modeled with a test voltage source driving a test current, which is effectively a noise current. The resulting net voltage across the load is the superimposition of the desired DM voltage signal and the DM noise voltage, yielding a disturbed signal, a degraded SI, and DM noise currents. Thus, an unbalance in a current loop not only converts DM currents to CM currents, which may cause EMI through near-field or common impedance coupling or through radiation, but also degrades the load voltage's SI and creates DM noise currents.

But if the current loop is balanced, no DM-to-CM or CM-to-DM conversion takes place; a CM current's effect on the load is cancelled out, and no DM noise voltage is created across it, as shown in figure 4.6.

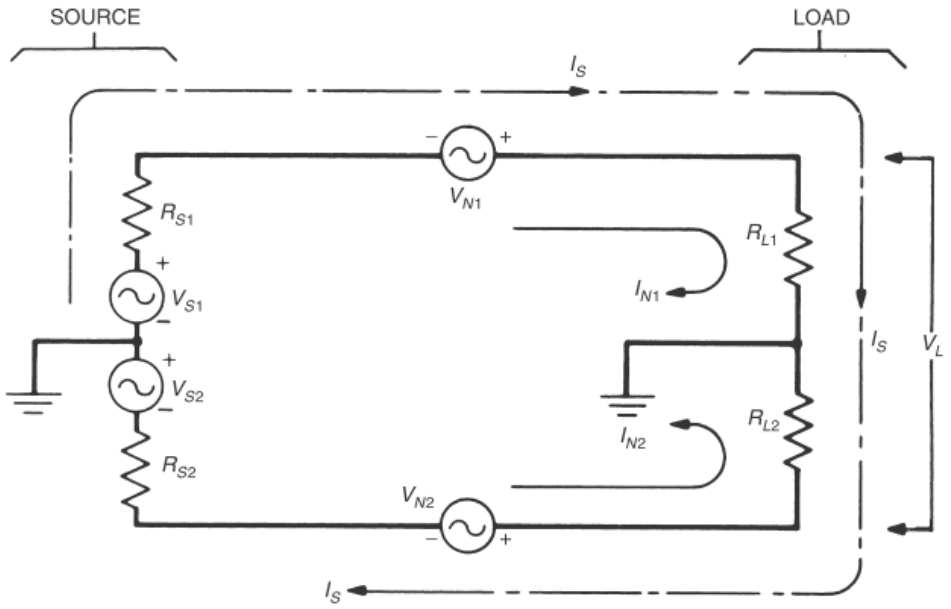

Figure 4.6. *The cancellation of CM current's effect on the load in a balanced circuit; The circuit is balanced when* $R_{S1} = R_{S2}$, $R_{L1} = R_{L2}$, $V_{N1} = V_{N2}$, *and* $I_{N1} = I_{N2}$ ***[1]***.

4.5 Conducted and Radiated Emissions

Let us call all emissions in the near field *conducted emissions*, which can be broken down into "genuinely conducted emissions" and "ostensibly conducted emissions". The former refers to EM noise propagating through conductive coupling paths, manifesting itself as movement of charge carriers along the path. Ostensibly conducted emissions refers to EM noise propagating through either capacitive or inductive coupling paths, manifesting itself as displacement currents and induced currents, respectively. With these emissions, no actual charge carriers flow through the coupling path, but the end result is the same as with genuinely conducted emissions: transfer of EM energy between the coupling points. Essentially, both genuinely and ostensibly conducted emissions are embodiments of the same phenomenon, *near-field-coupled EM energy*, and there is no need to separate the two.

Radiated emissions, in contrast, are an embodiment of *far-field-coupled EM energy*, which has a very different nature than near-field-coupled EM energy. In some literature, however, emissions through capacitive or inductive coupling paths are rather misleadingly also called radiated emissions, probably because they seem quite different from conducted currents in the traditional meaning of the word.

Far-field EM energy takes the form of a TEM wave, which travels in the space around the source/emitter until it encounters an obstacle. At the obstacle's interface, absorption, reflection and penetration of the magnetic and the electric field component of the TEM wave occur accordingly with the obstacle's EM material properties. Absorption produces currents and voltages in the obstacle in accordance with its *antenna behavior*. Also, the electric and the magnetic fields in the near field can be similarly described in terms of absorption, reflection, and penetration, which are full

wave analysis concepts, instead of capacitances, inductances, and conductances, which are circuit analysis concepts. [**1**,**16**]

The *principle of reciprocity* states that a conductor that has a certain antenna behavior as a receptor/receiver of EM waves also has an identical antenna behavior as a source/emitter of them, regardless of whether the EM waves are in the near field or in the far field. In other words, if a given EM wave absorbing into a given conductor produces a current *I* in it, current *I* driven in that conductor by a current source would cause the conductor to emit an EM wave identical with the former one. In this light, conducted EM energy and radiated EM energy are also embodiments of the same phenomenon, not different phenomena. [**13**]

In European Union's (EU) emission testing standards, conducted emissions are defined as EM emissions in the frequency range of 150 kHz to 30 MHz and radiated ones as EM emissions in the frequency range of 30 MHz to 1 GHz. In both of the tests, a connected *EMI receiver* measures current; in the *conducted emissions test* it does so at the power supply's end of the system, and in the radiated emissions test it measures the currents that EM waves generate in a receiving antenna located in the far field. Figure 4.7 shows the locations of EMI receivers in the conducted and in the radiated emissions tests.

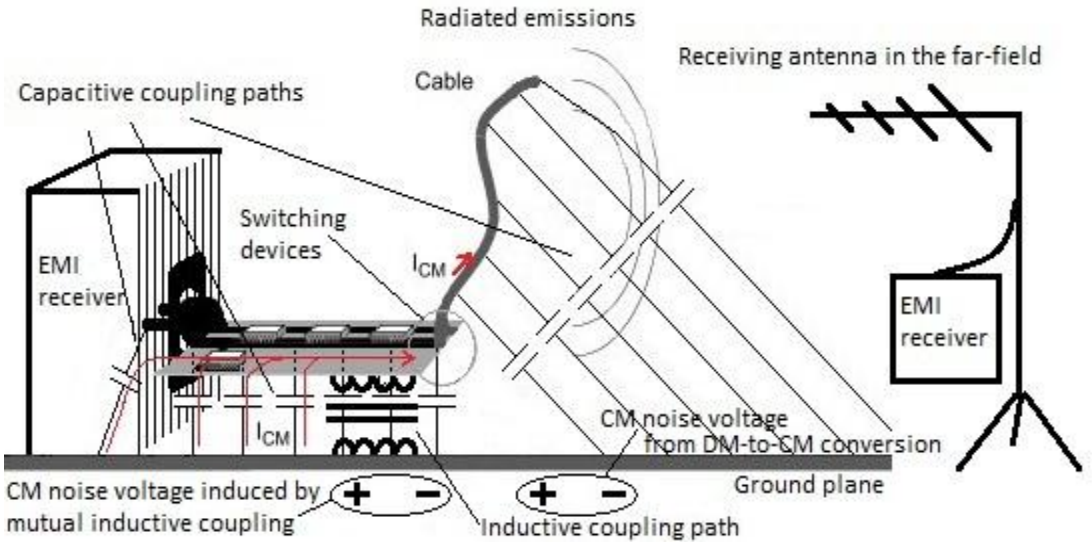

Figure 4.7. *The locations of EMI receivers in the conducted and in the radiated emissions test [**21**].*

In this paper, "conducted emissions" refers to near-field-coupled emissions that are registered by the EU standard conducted emissions test. Because the EU standard conducted emissions test only registers currents in the range of 150 kHz to 30 MHz, harmonic pollution created by rectifiers, for example, is not regarded as conducted emission because it lies at below 150 kHz. Furthermore, the measured conducted emissions are to some extent affected by capacitive and inductive coupling in the test setting because capacitive and inductive coupling can "close" numerous different loops for noise currents. The noise currents in these loops either add to the measured levels by

flowing through the EMI receiver, or do not add to them by circumventing the receiver. Because small geometrical differences can have an effect on the results, it is important that standards define the test setting in detail. Figure 4.7 illustrates various coupling paths in the emissions testing settings.

Accordingly, in this paper "radiated emissions" refers to far-field-coupled emissions that are registered by the EU standard radiated emissions test. In the test, the DUT is placed on a turntable that is rotated 360°, while two receiving antennas, one in a vertical and another one in a horizontal orientation and at varying heights during the measurements, pick up far-field-coupled emissions. However, the antennas do not register all far-field-coupled emissions; for example, the table is only rotated around the vertical axis, while for perfect registering of emissions the table would also have to be rotated around its horizontal and longitudinal axes, so that every possible direction of radiation would be covered. Moreover, the EU standard radiated emissions test only registers emissions in the range of 30 MHz to 1 GHz, so emissions outside this range are not regarded as radiated emissions.

Why is the frequency range of 150 kHz to 1 GHz not the range for both of the tests instead of there being the 30 MHz frequency division point?

As the next section will explain, the higher the frequency of a given causative current, the greater the generated radiated emissions, or the greater the EM energy in the far field. This EM energy is effectively "taken away" from the near field, as section 2.3.6 explained. The next section about far-field emissions will show that when the "causative voltage" is fixed, an increasing frequency causes conductors' intrinsic inductances to present larger impedances, decreasing current flow in the conductors and thus leading to less EM energy in the near field. In contrast, EM energy in the far field 1) remains the same for CM currents and 2) increases for DM currents, when the frequency increases.

The above can be interpreted so that the lower the frequency of an EM wave, the more likely it propagates through a near-field coupling path, and conversely, the higher the frequency of an EM wave, the more likely it propagates through a far-field coupling path. As the frequency of EM energy rises to 30 MHz, the characteristic impedance of a typical conductor wire reaches and exceeds the free space characteristic impedance, $\approx 377\ \Omega$, due to the conductor's intrinsic inductances. Thus, the free space has less impedance than the wire, and more EM energy will propagate into the free space than into the wire. The more the frequency yet rises, the bigger a proportion of EM energy takes the free space path of propagation. 30 MHz is an approximation of a typical "turnover point", above which conducted emissions and below which radiated emissions are not meaningful to measure, because they are insignificant as a cause of interference. [**12**]

The conducted emissions test is also an indirect way to measure radiated emissions. According to Ott [**1**], it has been experimentally shown that conducted emissions that flow into the AC power cable of a device and subsequently radiate into the air using the cable and the mains conductors as inadvertent transmit antennas are typically the

primary cause of interference at frequencies below 30 MHz In other words, at below 30 MHz, currents flowing in a typical device's conductors other than cables, for example PCB traces, produce such small radiated emissions that they will be thoroughly swamped by radiated emissions of currents flowing in the device's cables. Especially radiation by CM currents is dominating the radiated emissions, because cables constitute large CM current loops and consequently efficient accidental transmission antennas [**4**]. Therefore, knowing only the cables' radiated emissions, or even only the currents flowing in the cables, is sufficient for approximating the whole DUT's radiated emissions at below 30 MHz. [**1**]

According to Paul [**20**] and Ott [**1**], conducted emissions are normally too small to cause direct interference by conducting into another device via the mains supply network and the AC power cable. But according to Mammano and Carsten [**30**], the reason for the standard conducted emissions test to measure conducted noise only from the mains supply side is, because "it is here where noise currents could most readily couple to other systems through the power distribution network". Also Montrose and Nakauchi [**31**] mention the direct conduction of noise through the mains as a purpose for the conducted emissions tests. Moreover, I personally have experienced the interference of a vacuum cleaner on a CRT display monitor, although the vacuum cleaner was being used far away on a different floor – clearly an instance of conducted interference. Thus the conducted emissions test also serves a purpose as a gauge for noise that is emitted into the mains supply network.

Measuring radiated emissions at below 30 MHz with a standard radiated emissions test is impractical, because the distance $\lambda/2\pi$, that is,the boundary distance between the near field and the far field, is long for laboratory conditions; for 30 MHz the boundary distance is approximately 1.59 meters, for 10 MHz it is 4.77 meters, and for 5 MHz it is 9.54 meters [**21**]. According to the literature, attempts to measure radiated emissions closer to the DUT than the boundary distance gives errorneous results, and in practice the distance should be even longer than the boundary distance to obtain reliable results. But the space available in radiated emissions test labs isnot enough for measuring low frequencies in the farfield, and therefore the conducted emissions test is used for making an indirect conclusion of the radiated emissions. At above 30 MHz, the boundary distance is feasible for a laboratorysetting, and thus one can shift to measuring theemissions using the standard radiated emissions test instead of the conducted one. [**20**]

4.6 Common-Mode and Differential-Mode Far-Field Emissions

Common-mode radiation (CM radiation) is far-field radiation created by CM currents. When there is a sinusoidal frequency component of CM current flowing in a conductor, at a 10-meter distance it creates CM radiation equivalent to:

$$E_{10\,m} = 1.26 \cdot 10^{-4} \cdot (f \cdot L \cdot I_{CM}), \tag{4.1}$$

in which *f* is the frequency of the sinusoidal component and that of the produced CM radiation, I_{CM} the magnitude of the CM causative current, and *L* the length of the conductor in which the causative current flows. This equation is only accurate in the far field, with a vacuum as the medium, and when the wavelength of the CM current is much smaller than the quadruple of any dimension of the CM current loop. If the wavelength is not much smaller thanthe quadruple of a dimension, the equation is substituted by a set of complex equationsthat describe the *resonant behavior* for each sinusoidal frequency component of the CM current. Figure 4.8 illustrates the creation mechanism of CM radiation: V_N is a CM noise voltage that drives a CM noise current I_{CM}, which produces radiated emissions in accordance with equation 4.1. [**21**]

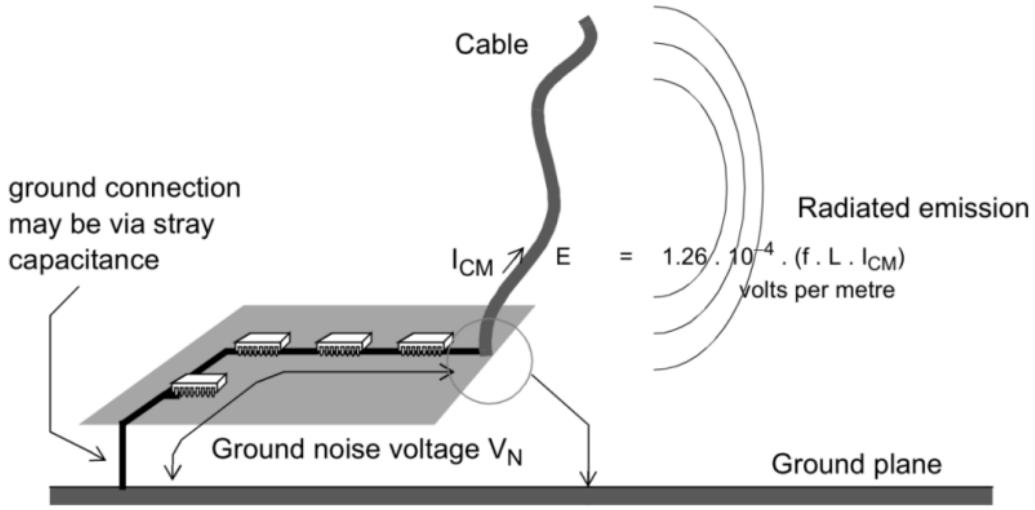

Figure 4.8*. CM noise voltages drive CM currents in ground loops"closed" by the given circuit and its coupling with the ground reference; CM currents produce CM radiation [**21**]*.

Similarly, *differential-mode radiation* (DM radiation) is far-field radiation created by DM currents. When there is a sinusoidal frequency component of DM current flowing in a conductor, at a 10-meter distance it creates DM radiation equivalent to:

$$E_{10\,m} = 263 \cdot 10^{-12}(f^2 \cdot A \cdot I_{DM})\,, \qquad (4.2)$$

in which *f* is the frequency of the sinusoidal component and that of the produced DM radiation, I_{DM} the magnitude of the DM causative current and *A* the area of the DM current loop. Also this equation is only accurate in the far field, with a vacuum as the medium, and when the wavelength of the DM current is much smaller than the quadruple of any dimension of the DM current loop. Figure 4.9 illustrates the creation mechanism of DM radiation: intentional and unintentional DM voltages drive DM currents such as I_{DM}, which produces radiated emissions in accordance with equation 4.2. [**21**]

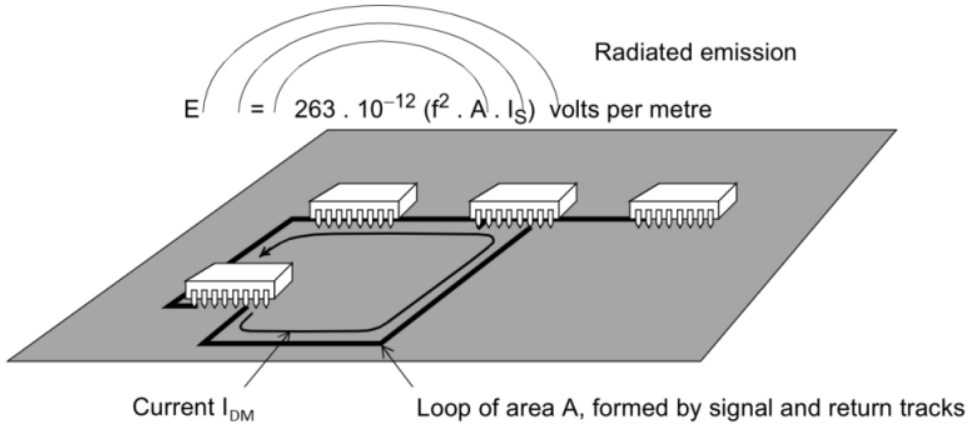

Figure 4.9. *DM currents are created by intentional and unintentional DM voltages in circuits; DM currents produce DM radiation [**21**].*

According to Mardiguian [**32**], twisting the conductors of a current loop significantly diminishes its DM radiation and even slightly its CM radiation. The DM radiation is diminished because the effective DM current loop area becomes smaller, and the CM radiation is diminished because the twisting improves the balance of the current loop, meaning less DM-to-CM conversion and thus a smaller I_{CM}.

4.7 Internal and External Emissions

Unintentional near-field coupling can yet be divided into *internal coupling* within a given system and *external coupling* between the system and objects in its surroundings. *Unintentional internal near-field coupling* causes *internal emissions*, which may interfere with the operation of the device and cause, for example, impaired SI and self-susceptibility problems. *Unintentional external near-field coupling* causes *external emissions* either directly or indirectly. Direct external emissions are CM and DM currents that arise from the system's near-field coupling with a "victim" conductor. Indirect external emissions are CM and DM radiation that arise from CM and DM currents created by near-field coupling, as described in the previous section.

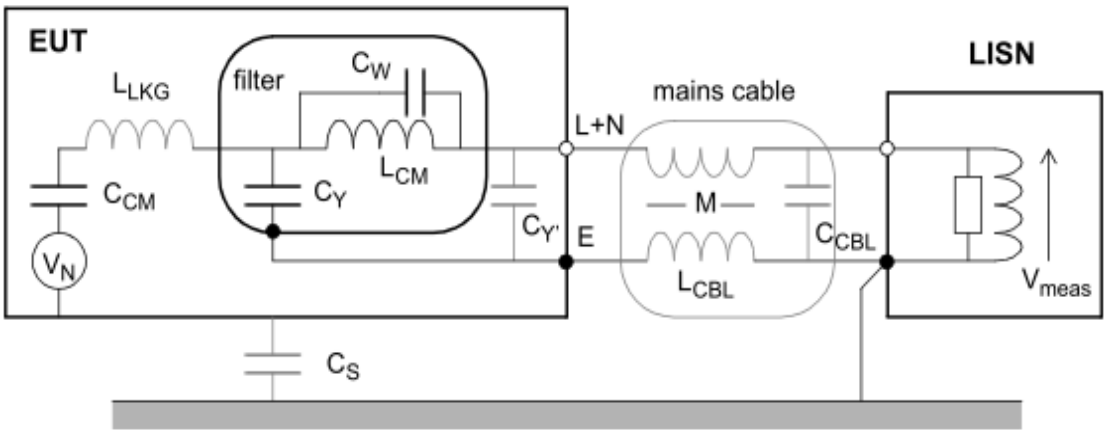

Figure 4.10. *Internal and external near-field coupling of a flyback converter under conducted emissions test [**21**].*

Figure 4.10 shows an equivalent circuit of a flyback charger with its associated stray and parasitic impedances in a conducted emissions test setting. External capacitive coupling paths (C_S) can create CM noise currents in the system's ground loops by hindering the system's balance and by providing a low-impedance ground loop for CM noise driven by a voltage drop in the ground reference. External inductive coupling paths (not depicted) can create DM noise currents in external current loops, CM currents in the system's own or external ground loops, and eddy currents in external conductors. Internal capacitive coupling paths (for example C_{CM}) can create CM noise currents by hindering the system's balance or by providing a low-impedance ground loop for CM noise or can create DM noise currents by providing a low-impedance DM loop for DM noise originating from, for example, crosstalk capacitance C_{CBL} or junction capacitances of semiconductor devices. Internal inductive coupling paths (for example L_{CBL}) create DM noise currents in current loops within the system, which may further be converted into CM noise currents through DM-to-CM conversion.

4.8 Resonances

All circuits have resonance frequencies at which their currents or voltages experience a *resonant gain*, called their *Q factor*. Q factors of ten or more, that is, gains of 20 dB or more, are common in ordinary electrical and electronics circuits. Q factors of 100, that is, 40 dB, are not unusual, and even gains of 1000, that is, 60 dB, do exist. A low resistance is favorable for high Q factors, because the losses by resistances mitigate the Q factor. [**13**]

A resonance occurs when an EM wave with a "fitting" wavelength reflects between impedance discontinuities along a transmission line. When an EM wave is injected into a stretch of transmission line with impedance discontinuities at both ends, there will be theoretically an infinite number of reflected EM waves. What ultimately determines whether a resonance results from this or not, is the wavelength of the EM wave and the type of the impedance discontinuities.

As an afterthought, the reason why the desired signal in figure 2.7 exhibited degraded SI in the form of ringing was due to the resonance behavior of the 120-mm-long PCB trace; the ringing frequency was the trace's resonance frequency.

4.8.1 Impedance Discontinuities and Reflections

When an EM wave is propagating along a transmission line with impedance changes, part of the EM wave will reflect at the *impedance discontinuity* points, that is, *impedance interfaces*. If the EM wave encounters an impedance higher than the characteristic impedance of the transmission line it is propagating along, the reflected wave will be in phase with the *incident wave* at the reflection point. In contrast, if the EM wave encounters an impedance lower than the characteristic impedance of the transmission line it is propagating along, the reflected wave will be opposite in phase with regard to the incident wave at the reflection point. After the first reflection, there

are two EM *traveling waves*, the incident wave and the reflected wave, moving in opposite directions and meeting each other, if we assume that the source is constantly injecting new EM waves into the transmission line. Such EM waves add up together, amplifying each other where their signs are the same and attenuating each other where their signs are the opposite. The Poynting vector gives the magnitude and the sign of an EM wave at each point. Also the electric and the magnetic field component individually behave in the same manner, so the same scrutiny can be used with them separately. [**13**]

Let us further explain how EM energy is reflected at impedance interfaces. The proportion of reflected EM energy from a load depends on the transmission line's characteristic impedance Z_0 and the load's characteristic impedance Z_L. The *reflection coefficient* is:

$$\Gamma_E = \frac{E_i}{E_r} = \frac{Z_L - Z_0^*}{Z_L + Z_0}, \tag{4.3}$$

which gives the ratio between the incident and the reflected E after a reflection from the load Z_L. Any other *field quantity* or *circuit quantity*, such as H, current, or voltage can be used in place of E in the equation, and the reflection coefficient will be the same for the given impedance interface, unless the incident quantity at the interface is zero. The reflection coefficient gets a negative value when Z_L is smaller than Z_0, meaning, as mentioned earlier, that the reflected electric field strength experiences a 180-degree phase shift. The reflection coefficient at the source's end is similarly:

$$\Gamma_E = \frac{E_i}{E_r} = \frac{Z_S - Z_0^*}{Z_S + Z_0}, \tag{4.4}$$

which gives the ratio between the incident and the reflected E after a reflection from source the Z_S. In real life, the reflection coefficients can never reach unity due to no load's or source's characteristic impedance ever being zero or infinite.

The power reflection coefficient at the load's end is:

$$\Gamma_P = |\Gamma|^2 = \left|\frac{Z_L - Z_0^*}{Z_L + Z_0}\right|^2, \tag{4.5}$$

which gives the ratio of the reflected and the incident EM power, or EM energy per time unit, at the impedance interface after a reflection from the load Z_L. The power reflection coefficient at the source's end is similarly:

$$\Gamma_P = |\Gamma|^2 = \left|\frac{Z_S - Z_0^*}{Z_S + Z_0}\right|^2, \tag{4.6}$$

which gives the ratio of the reflected and the incident EM power at the impedance interface after a reflection from the source Z_S. [**33**]

Usually, an EM wave propagating along a transmission line will eventually encounter impedance discontinuities at both of its ends, leading to a number of reflected EM waves ricocheting back and forth along the stretch of transmission line between the impedance interfaces. The incident and the reflected waves amplify and/or attenuate each other at each point along the stretch, leading to a superimposed net EM wave, called the *resultant wave*. When the source is disconnected, the resultant wave will eventually decay away unless the reflections are perfect, which only happens in the

theoretical situation that the load and the source are zero-impedance and/or infinite impedance. [**13**,**16**]

However, impedance discontinuities do not have much of an effect on reflections, if they only occur over distances less than *λ/6*. By dividing the length of the transmission line into sections of *λ/6* and determining the impedance of each, we can determine what the effects on SI, PI, and the emissions will be when an EM wave travels from the source to the load. If all the *λ/6* sections in a transmission line, including the driver and the load, have the same characteristic impedance, the EM energy of an EM wave will be fully transmitted from the source to the load, except for losses associated with resistances. We then talk about a *matched transmission line*. With a matched transmission line the integrity of an EM wave's waveform is retained and, as a consequence, the transmission line functions as a very inefficient accidental antenna, so the emissions remain low and the immunity high. [**13**]

4.8.2 Standing Waves

Resonance is a special situation in which the electrical length of a stretch of transmission line is some multiple of quarter-wavelengths of the EM wave traveling along it. In such a case, the resultant wave forms a standing wave instead of a *non-standing resultant wave*.

What is special about a standing wave compared with a traveling wave in any wave phenomenon in nature is that the amplitude of a standing wave is a function of location. A traveling wave's oscillation yields a given point along the wave's propagation path with a value $f(t,x) = A \cdot \sin(\omega t + x)$, where t is time and x is the location of the point in radials, and therefore every point x gets values $-A \ldots +A$ over one oscillation period. In other words, the amplitude is the same for every point. In contrast, a standing wave's oscillation yields a given point a value $f(t,x) = A(x) \cdot \sin(\omega t + x)$, in which $A(x) = A \cdot \sin(x)$, and therefore every point x gets values $-A(x) \ldots +A(x)$ over one oscillation period. In other words, the amplitude at each point along one wave's length varies. Figure 4.11 illustrates a standing wave as a resultant wave ("combined wave") superimposed from two traveling waves moving in opposite directions at five consecutive points in time, $t_0 \ldots t_4$.

Equivalently, for *EM standing waves* the electric field quantities with their associated voltages and the magnetic field quantities with their associated currents are all functions of location. In an EM standing wave, the electric field and the magnetic field component have the same wavelength, but a *λ/4* phase difference, as figure 4.12 illustrates. Furthermore, in an EM standing wave both components have 1) fixed-location *node points*, at which the electric field or the magnetic field amplitude is at zero and 2) fixed-location *crest points*, at which the electric field or the magnetic field amplitude is at maximum. It follows that, if the electric field has a node at a given point, then the magnetic field has a crest at the same point, and if the magnetic field has a node at a given point, then the electric field has a crest at the same point. [**16**]

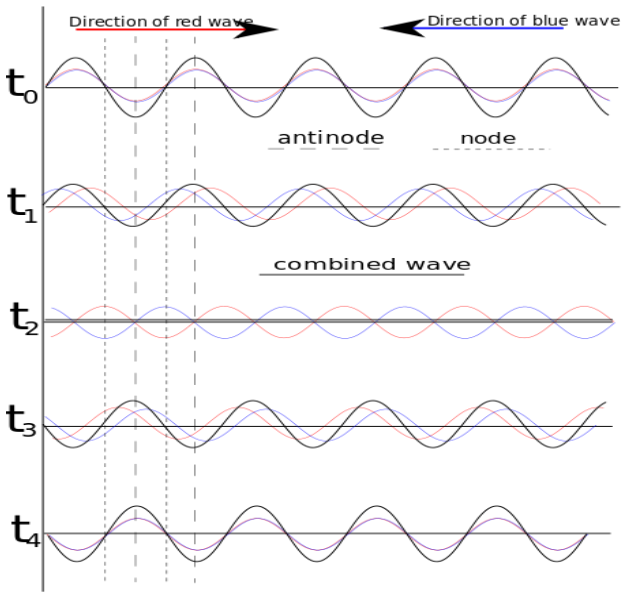

Figure 4.11. *Two opposing traveling waves of an equal and "fitting" wavelength superimpose to form a special resultant wave, a standing wave [**34**].*

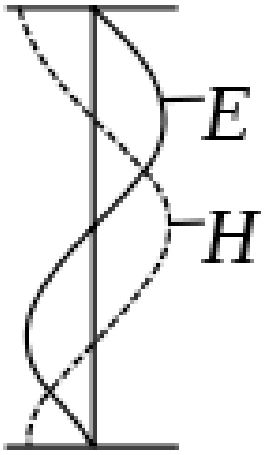

Figure 4.12. *An EM wave's electric and magnetic field component [**35**].*

It is peculiar that if one determines the wave impedance $Z = \frac{V}{I} = \frac{E}{H}$ of an EM wave using its *instantaneous* E and H at each point along a transmission line, the wave impedance appears to be changing 1) by time with regular EM traveling waves, 2) by location with standing waves, and 3) by both time and location with non-standing resultant waves, even if the transmission line has a uniform characteristic impedance. In other words, the "instantaneous wave impedance" generally seems not to be matching with the transmission line's characteristic impedance.

However, if one uses peak or *root mean square* (RMS) values of E and H over time instead of the instantaneous values, the wave impedance *does* match with the transmission line's characteristic impedance for a traveling wave. But if one uses peak or RMS values of E and Hof a standing wave, the wave impedance still varies by location and therefore does not generally match with the characteristic impedance. This is clear when considering that at every node of E, or crest of H, the impedance is at zero, and at every node of H, or crest of E, the impedance is at infinity. Between the crests and the nodes the impedance gets some intermediate value, only one of which matches with the characteristic impedance.

One may interpret standing wave's location-dependent wave impedance so that a standing wave can render the impedance of a given point along a transmission line different from its characteristic impedance. How the phenomenon appears on the transmission line's load end and source end is described in terms of *input impedance* and *output impedance*. Input impedance determines how the transmission line and its load appear to the source at a given frequency and is dictated by the transmission line's characteristic impedance, the load impedance, and the wavelength of the EM wave. Output impedance determines how the transmission line and its source appear to the

load at a given frequency and is dictated by the transmission line's characteristic impedance, the source impedance, and the wavelength of the EM wave. [**16**,**22**]

Not only standing waves exhibit wave impedances that change by location, and thus not only standing waves exhibit input and output impedances that differ from the transmission line's characteristic impedance. The phenomenon is the easiest to understand with standing waves, but it occurs with all resultant waves, that is, superimpositions of incident and reflected EM waves. The difference is that the instantaneous wave impedance of a non-standing resultant wave is not only a function of location or time, but both of them [**16**]. At the impedance interface between a transmission line and its 1) source and 2) load, a resultant wave's wave impedance dictates 1) the input and 2) the output impedance of the transmission line. Moreover, the input impedance of the transmission line also equals the output impedance of the source, the *source impedance*, and the output impedance of the transmission line equals the input impedance of the load, the *load impedance*.

Table 4.1 shows how the input impedance Z_i of transmission line, that is, the source impedance, and the load impedance Z_L depend on each other, the transmission line's physical length l, and the wavelength λ of the EM wave. When a source is injecting EM waves into a transmission line, the source impedance equals the input impedance of the transmission line. Thus, the source impedance is subject to variation and dictated by the load impedance, the wavelength, and the transmission line's characteristic impedance and length. [**22**]

Table 4.1. *The input impedance of transmission line Z_i and the load impedance Z_L with various values of physical length l [**22**].*

Case	$\mathbf{Z_i}$	$\mathbf{Z_L}$	$\mathbf{Z_C}$	***l* (physical)**
1	$= Z_C = Z_L$	$= Z_C = Z_i$	$0 < Z_C < \infty$	$0 < l < \infty$
2	$= jZ_C\tan(2\pi l/\lambda)$	$= 0$	$0 < Z_C < \infty$	$\neq \lambda/4 \cdot (2k - 1)$
3	$= jZ_C\cot(2\pi l/\lambda)$	$= \infty$	$0 < Z_C < \infty$	$\neq \lambda/4 \cdot (2k - 1)$
4	$= Z_C^2 / Z_L$	$0 < Z_L < \infty$	$0 < Z_C < \infty$	$= \lambda/4 \cdot (2k - 1)$
5	$= \infty$	$= 0$	$0 < Z_C < \infty$	$= \lambda/4 \cdot (2k - 1)$
6	$= 0$	$= \infty$	$0 < Z_C < \infty$	$= \lambda/4 \cdot (2k - 1)$
7	$= Z_L$	$0 < Z_L < \infty$	$0 < Z_C < \infty$	$= \lambda/2 \cdot k$
8	$= 0$	$= 0$	$0 < Z_C < \infty$	$= \lambda/2 \cdot k$
9	$= \infty$	$= \infty$	$0 < Z_C < \infty$	$= \lambda/2 \cdot k$

Table 4.1 can be broken down as follows:

1) The load is matched with the transmission line ($Z_L = Z_C$) and thus $Z_i = Z_C$.
2) The load is zero-impedance, and thus Z_i is only dependent on Z_C, λ, and l.
3) The load is infinite-impedance, and thus Z_i is only dependent on Z_C, λ, and l.
4) The transmission line's physical length is an odd multiple of quarter-wavelengths, and thus Z_i is only dependent on Z_C and Z_L.
5) A special case of 4: when Z_L is zero-impedance, Z_i is infinite-impedance.

6) A special case of 4: when Z_L is infinite-impedance, Z_i is zero-impedance.
7) The transmission line's physical length is a multiple of half-wavelengths, and thus Z_i is only dependent on Z_L.
8) A special case of 7: when Z_L is zero-impedance, Z_i is zero-impedance.
9) A special case of 7: when Z_L is infinite-impedance, Z_i is infinite-impedance. [**22**]

Let us observe a standing wave in a transmission line. From figure 4.13 one can see that a quarter-wavelength long transmission line has an infinite input impedance when the load is zero-impedance. This is because at the load's end the voltage waveform must be at zero while the current waveform is at its maximum, and at the source's end, conversely, the voltage waveform must be at its maximum while the current waveform is at zero. This is due to the length of exactly quarter of a wavelength. In contrast, a half-wavelength long transmission line has a zero input impedance when the load impedance is zero, as can also be seen from the figure.

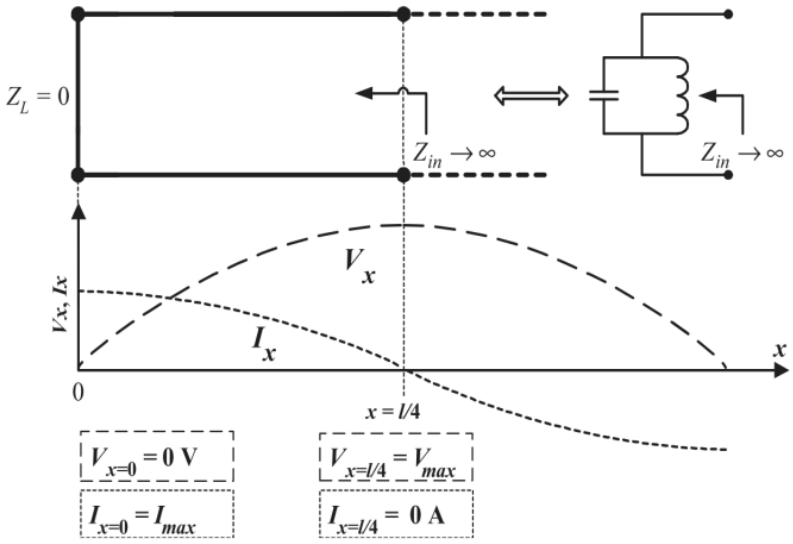

***Figure 4.13**. A short-circuited load appears as an open circuit for the source when the transmission line is a quarter-wavelength long. This effect can be modeled with a parallel resonance at that frequency [**22**]*.

Figures 4.14 and 4.15 show a transmission line's input impedance as a function of wavelength normalized to the transmission line's length for 1) a short-circuit load and 2) an open-circuit load, respectively.

The resonance and the *anti-resonace* frequencies in figures 4.14 and 4.15 are those at which the input impedance changes its sign due to the current changing its direction, as was seen in figure 4.13. At resonance frequencies the input impedance is zero, allowing an immense flow of EM energy into the transmission line. A quarter-wavelength "further", there is an anti-resonance, at which the input impedance is infinite, blocking all flow of EM energy into the transmission line. Yet a quarter-wavelength "further" there is the second resonance, another quarter-wavelength "further" the second anti-resonance, and so on. [**22**]

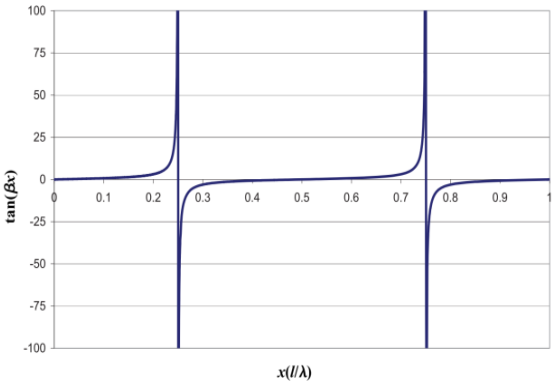

***Figure 4.14**. A transmission line's input impedance when the load is short-circuited [**22**].*

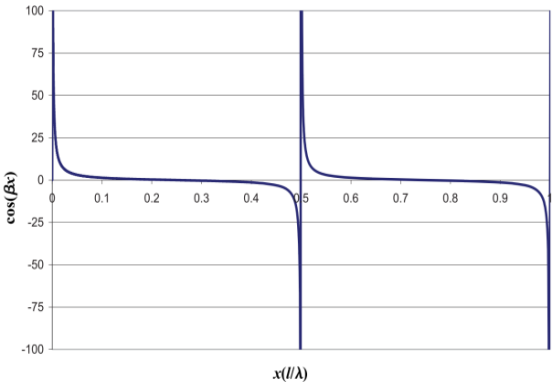

***Figure 4.15.** A transmission line's input impedance when the load is an open circuit [**22**].*

One can use an ideal parallel resonant circuit, consisting of a capacitor and an inductor in parallel, as figure 4.13 depicts, as an equivalent circuit to model the resonance and the anti-resonance of a transmission line. From figures 4.14 and 4.15, it becomes obvious why a parallel resonant circuit is used for this purpose instead of a series resonant circuit;the shape and the behavior ofinput impedance's frequency responsematches expressly with that of aparallel resonant circuit. The capacitance value of the capacitor and the inductance value of the inductor must be chosenso that the parallel resonance occurs at a frequency that is the anti-resonance frequency desired for the model. Any givennumber of resonance and anti-resonance frequencies can then be modeled usingacorresponding number of parallel resonant circuitsconnected in series and resonant at the accordant frequencies.

Figure 4.16 illustrates standing waves in short-circuit and open-circuit loading conditions, while the source is zero-impedance. The figure illustrates how, at the impedance interfaces with the source and the load, the wave impedance inevitably matches with the transmission line's input and output impedance, respectively. Both the upper and the lower picture depict a resonance, and not an anti-resonance, because the input impedance in both cases is zero. If the frequency of the wave is changed so that the wavelength becomes slightly longer, the input impedance of the transmission line, that is, the source impedance, adopts some value other than zero because the electrical length of the transmission line is not a multiple of half-wavelengths anymore. This is depicted in the upper picture of figure 4.17. In the process, the standing wave "gets broken" and becomes a non-standing resultant wave, the wave impedance of which is dependent on both location and time.

With the new, longer wavelength, a standing wave can be obtained again by extending the electrical length of the transmission line through changing the load impedance. Figure 4.18 shows how capacitance or inductance added to the load extends a cable's electrical length, making it match with a longer standing wave. Figure 4.17's lower picture illustrates how a suitable "compensating addition", in this case an inductive one due to the short-circuited load, into the load impedance aligns the

resultant wave so that the input impedance is again zero at the source's interface. Consequently, the non-standing resultant wave is turned into a standing wave. Similarly, adjusting the load impedance and thus the electrical length of a transmission line using a variable capacitor is the usual way to tune analogue radios' reception circuits for radio stations at various frequencies.

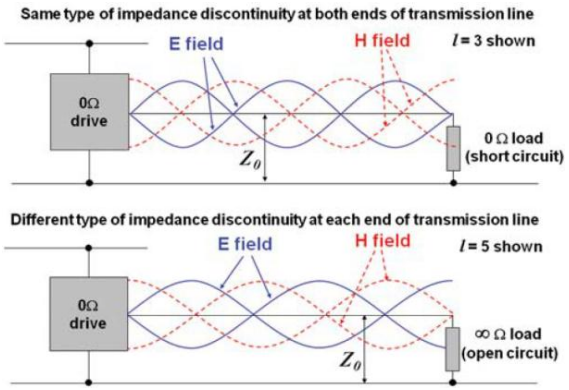

Figure 4.16. *A transmission line with a zero input impedance and 1) a short-circuit load and a three half-wavelengths' length and 2) an open circuit load and a five quarter-wavelengths' length [**13**].*

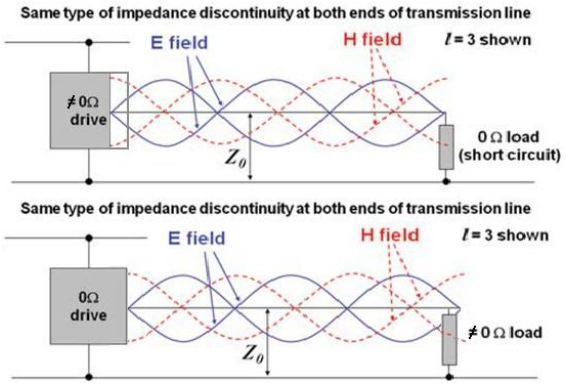

Figure 4.17. *A transmission line with a short-circuit load and 1) a less than three half-wavelengths' electrical length and 2) a three half-wavelengths' electrical length and an inductive compensation [**13**].*

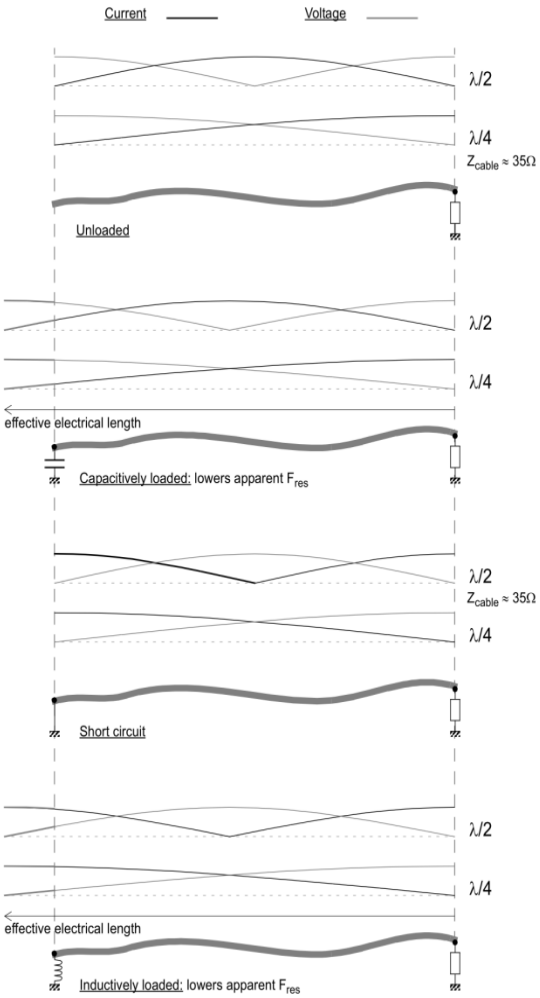

Figure 4.18. *The lengthening effect of a capacitive and an inductive load on the electrical length of a transmission line [**21**].*

4.8.2 Antenna Efficiency

We now know that standing waves have an ability to "boost" or "mitigate" the current at the impedance interface between the source and the transmission line, manifesting itself as a zero or an infinite input impedance, respectively. Therefore, if we have a signal generator driving a sinusoidal wave with a set amplitude and at an adjustable frequency, and we gradually increase the frequency, we would measure a higher-than the set amplitude when the frequency is nearing a resonant frequency. Similarly, we

would measure lower-than the set amplitude when the frequency is near an anti-resonant frequency.

The way standing waves affect a current's magnitude is similar to how they affect the near-field and the far-field coupling efficiency of the EM fields associated with the current. Only before reaching the frequency spectrum's *resonant region*, in which the wavelength is short enough for standing waves to occur, the current's magnitude is not correlating well with the near-field and the far-field coupling efficiency. In this *non-resonant region*, far-field and near-field coupling get less efficient more abruptly than current's magnitude gets smaller as the wavelength increases. At DC, far-field and near-field coupling are non-existent due to no EM waves existing, whereas the current has the magnitude determined by the driver and the circuit's resistances.

Near-field coupling efficiency can be analyzed by breaking it down into electric and magnetic coupling. From the definitions of capacitive and inductive reactive impedance we know that both capacitively-coupled current and inductively-coupled voltage are directly proportional to frequency. The fundamental near-field coupling efficiency depends on the geometries, distances, and materials of and between the "culprit" and the "victims".

It is not useful to break far-field coupling down into electric and magnetic field components, because far-field radiation's wave impedance has settled to the characteristic wave impedance of the medium. But there are two kinds of far-field radiation, CM radiation and DM radiation, which have a distinct behavior in the non-resonant region, as section 4.6 explained.

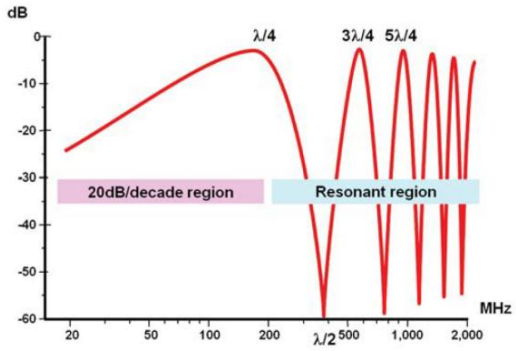

Figure 4.19. *CM radiation antenna efficiency of a 200-mm-long PCB trace [**13**].*

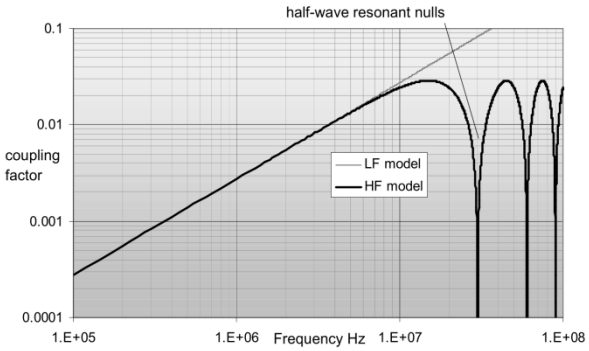

Figure 4.20. *Efficiency of CM near-field coupling [**21**].*

Figure 4.19 illustrates a CM current loop's far-field coupling efficiency spectrum in both the non-resonant (20 dB/decade) and the resonant region. The Y-axis shows the proportion of available EM energy radiated into the far field, where 0 dB means all the available EM energy is radiated. A CM current loop is effectively an *electric monopole* type antenna, which has its tip connected to the ground reference through a high impedance (the output impedance). Therefore, the first resonance wavelength is four times the antenna's electrical length, that is, the first resonance is a *λ/4* resonance. The corresponding coupling efficiency spectrum for a DM current loop, that is, effectively

for a *magnetic loop* type antenna, would be similar in shape. However, there would be two differences: 1) the lower end of the spectrum would be a "40 dB/decade region" due to DM radiation being proportional to *f* squared instead of just *f*, as section 4.6 showed us, and 2) the first resonance would occur when the DM current loop's electrical length is *λ/2* and the following resonances at multiples of *λ/2*, which is due to the output impedance of a magnetic loop antenna being low.

In contrast, figure 4.20 illustrates a CM current loop's near-field coupling efficiency spectrum in both the non-resonant and the resonant region. The Y-axis in the figure shows the proportion of available EM energy coupled through the near field, where *1* means all the available EM energy is coupled through it.

4.9 Electromagnetic Emissions Tests and Measurements

Different regulatory authorities define different EMC standards, which further define a myriad of EM emissions tests. Some of the most significant EMC regulatory authorities are the *International Electrotechnical Commission* (IEC), *Comité International Special des Perturbations Radioélectriques* (CISPR), *European Community* (EC), *European Normalization Commission* (CENELEC), and the earlier-mentioned Federal Communications Commission (FCC).

IEC is the global coordinator and standardizer of all electrotechnical aspects and activities, including EMC. IEC has about two hundred technical committees. Their work's outcome is technical reports, international standards and recommendations, which can be recognized from the prefix *IEC* in their title. CISPR is one of the most EMC-focused technical committees of IEC. CISPR's purpose is to draft measuring methods and limits for conducted and radiated EM emissions in the frequency range from 9 kHz to 300 GHz and also those for immunity measurements of communication equipment. In short, CISPR issues product standards. Many national laws regarding EMC are based on CISPR documents [**32**]. [**3**]

A country or a group of countries may include IEC standards or recommendations partly or wholly in their legislation and also add their national extensions and riders in it, usually to make the requirements stricter. The EC, or the EU, is an example of such a group of countries. Before IEC standards can be adopted by the EC as *European norms*, they have to go through a *harmonization* process, the organization in charge of which is CENELEC. Harmonization often requires revising the IEC standards until the majority of CENELEC members vote in the favor of the revised edition. European norms can be recognized from the prefix *EN* in their title. [**3**]

The EC has enforced a law, that is, a *directive*, concerning EMC aspects. This *EMC directive* stipulates that all electronic and electrical equipment in the European market must be sufficiently EM compatible. European norms form the foundation of the EMC directive, defining the emission limits and measurement methods for assessing the EM compatibility. The *CE mark* in a product is an indication that the manufacturer of the

product pledges that the product meets the requirements of all EC directives relevant to it, including the EMC directive [**21**]. [**3**]

FCC is the American regulatory authority in EMC aspects. FCC standards are stipulated in the *Code of Federal Regulations* (CFR). These regulations can be recognized from the prefix *CFR* or *FCC* in their title. Similarly with the CE mark, the *FCC mark* is an indication of a pledge from the manufacturer that the product complies with the FCC standards. [**1**,**3**,**31**]

Two universal tests in the standards of most authorities are 1) the conducted emissions test and 2) the radiated emissions test. Moreover, in most standards these two tests are defined quite similarly. Their purpose is generally to be the gauge that dictates whether a given product is electromagnetically compatible to be released on the regulated market. Thus, let us call these two tests the "qualifying tests".

Pre-compliance EMC tests may be defined in a standard as well. Their purpose is usually to provide, during the product design and the prototyping phase, an educated guess on the results of the future qualifying tests. This can save costs, because the qualifying tests are expensive to perform. However, pre-compliance EMC measurements are not applicable for qualifying purposes, because 1) their results have typically a poor repeatability and reproducibility, and 2) their results correlate with those of the qualifying tests only to some extent. In other words, the result of a pre-compliance test may have a poor correlation with the levels of emissions the DUT causes into the surroundings.

4.9.1 Conducted Emissions Tests

In the conducted emissions test, the standards stipulate that an *artificial mains network* (AMN), that is, a *line impedance stabilization network* (LISN), must be used. AMN/LISN is a device between the DUT and the mains that fixes the impedance of the hot/live/phase conductor and that of the cold/neutral/zero conductor at a specified impedance value with regard to the ground. The specified impedance also follows a specified frequency response in the measurement frequency range. One component forming the AMN/LISN's specified impedance is the *measurement impedance*, across which the conducted emissions are measured with an EMI receiver. [**3**]

When an AMN/LISN is used, the DUT "sees" the specified impedance as the mains' impedance, because the AMN/LISN also incorporates a low-pass filter that presents such a high impedance at the EM emissions' measurement frequencies that the impedance at the mains side is solely determined by the AMN/LISN. This is necessary because the impedances of mains networks vary between testing locations and DUT's, affecting the EMI receiver's measurement readouts and thus making the reproducibility of the tests poor [**1**]. Another purpose of the AMN/LISN's low-pass filter is to prevent noise flowing into the measurement circuit to be falsely registered as conducted emissions from the DUT. [**3**]

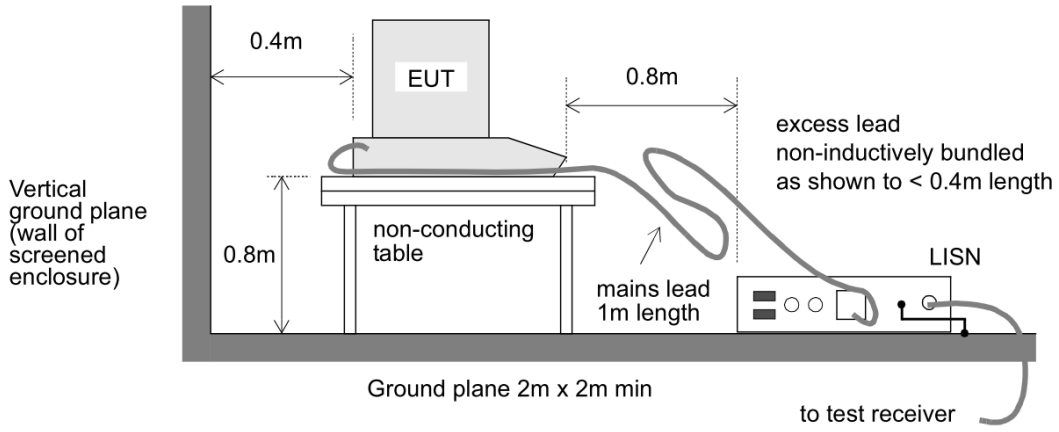

Figure 4.21. *An illustration of conducted emissions test set-up [**21**].*

Figure 4.21 shows a usual set-up for a standard conducted emissions test. Equipment under test (EUT) is another word for DUT, and the ground plane predominantly constitutes the ground reference in the setting. The placement of the EUT and its cables with respect to the ground plane and the LISN is carefully defined in the standards. [**21**]

4.9.2 Radiated Emissions Tests

Usually, the only radiated emissions test that is part of the qualifying tests in EMC standards is a measurement of the electric field strength at frequencies higher than 30 MHz, instead of a measurement of the magnetic field strength at frequencies lower than 30 MHz, which is also defined in CISPR standards. The magnetic field strength measurement is stipulated as the measurement-of-choice for radiated emissions at below 30 MHz, most likely because 1) low-frequency magnetic field is more harmful than low-frequency electric field due to the fact that a magnetic field's reflection from conductor surfaces is much weaker than that of an electric field and 2) because the measurement is meant to be a gauge of the mostly magnetic-field radiation originating from the cables, which are deemed the major radiator in devices at below 30 MHz.

This "radiated magnetic-field emissions test" may be inevitable to be performed, at least at the lowest frequencies, within the near field of the DUT, because the long wavelengths at the lowest frequencies make the near field reach too far for measuring in the far field when performing the measurements in any built measurement premises. This is problematic from the test's repeatability and reproducibility standpoint, but may still yield trustworthy results, if the disposition of the DUT's cables is accurately defined and thus their radiation patterns more or less fixed. In contrast, the "radiated electric-field emissions test" is stipulated to be always performed in the far field. Thus, it is rather insignificant whether the radiated electric-field emissions test is a measurement of the electric or the magnetic field strength, because in the far field the wave impedance has adopted the value of the medium's characteristic wave impedance. However, this is the way the two tests are defined. [**3**]

The conducted emissions test is normally used as the qualifying test for radiation originating from the cables, that is, at frequencies below 30 MHz, instead of the radiated

magnetic-field emissions test. Because the radiated electric-field emissions test is usually the sole qualifying test for direct radiated emissions, let us refer to it as *the* radiated emissions test.

The radiated emissions test must take place in an *open area test site* (OATS) or an equivalent test setting. In practice, the test setting is usually an anechoic chamber, which provides a reflection-free and EM environment-wise isolated space for the test. In the test, the DUT is located on a turntable at a prescribed distance away (usually 3 m, 10 m, or 30 m) from the measurement antenna and at a height of 1 meter. The whole test set-up is located on a conductive ground plane, which predominantly constitutes the ground reference, similarly with the conducted emissions test. [**3**]

The DUT is rotated between 0° and 360° so that the radiation maximum can be found. Next, the antenna is moved vertically between 1-4 meters (at a 10-m measuring distance) so that the radiation maximum dictated by the antenna's vertical position can be found. This method is called a *cylindrical scan*, which undeniably misses plenty of radiation directions with possible radiation maximums. Figure 4.22 shows a usual set-up for a standard radiated emissions test. At a radiation maximum, the direct radiation from the DUT to the measurement antenna and the indirect radiation from the DUT reflected via the ground plane to the measurement antenna are in phase and thus add up. Moreover, one must measure both the horizontally and the vertically polarized field components of the electric field strength. [**3**]

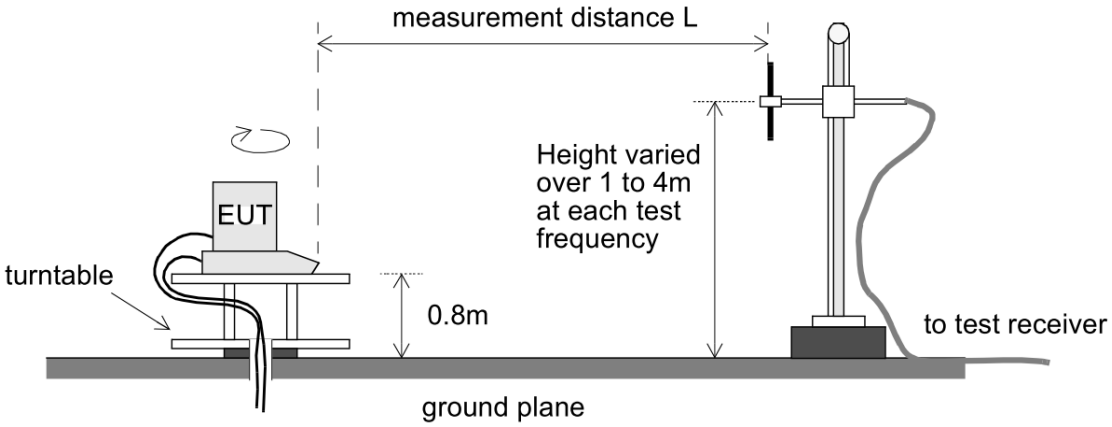

Figure 4.22. *An illustration of radiated emissions test setup [**21**].*

4.9.3 Pre-Compliance EMC Measurements

The di/dt and the *voltage waveform's rate of change* (dv/dt) are decisive characteristics in terms of EM emissions. They are also called current waveform's and voltage waveform's *slew rate*. The larger the dv/dt between two given points in a circuit, the more effective the available parasitic and stray capacitive coupling paths are in coupling noise displacement currents through them. Similarly, the larger the di/dt in a given a current loop in a circuit, the more effective the available parasitic and stray inductive coupling paths are in inducing voltages in conductors within the near field and further in

driving noise currents in them. The larger the noise currents caused by the parasitic and stray coupling paths, the larger the "avoidable unintentional emissions" are.

One can get a clue of a circuit's radiated emissions just by measuring the dv/dt and the di/dt at different points in it, especially by paying attention at the magnitude of non-idealities in the waveforms. This does not provide much insight of the distribution of noise at different frequencies, however, unless one breaks the measured waveforms into their frequency components and then scrutinize each frequency component's amplitude on a spectrum. But even with an accurate knowledge of the amplitudes of any given waveform's frequency components, we could not predict the circuit's conducted or radiated emissions' spectrum accurately. The matter is more complicated, because the resulting spectrum is the outcome of all available current loops, formed by intended, parasitic, and stray impedances, emitting EM energy into the surroundings and having their contributions superimposed. Also, additional factors that affect the resulting spectrum are the current loops' geometries and orientations, other objects and materials that are present, the objects' and materials' geometries, the current loops' resonances, and the effect of the measurement instrument and its probe. In short, measuring the current and voltage waveforms of a circuit can give only a rough guess of its actual EM emissions. [**1**,**21**]

One can conceive measurements with *near-field probes*, which are sensitive to electric field and/or magnetic field, as a means to measure waveforms and magnitudes of currents and voltages without a need to have a direct contact with the DUT. Near-field probe measurements are also a classic example of pre-compliance measurements as they can 1) pinpoint problem areas and frequencies of the DUT and 2) provide an approximation of the actual EM emissions. Therefore, they may be very useful in the design and in the prototype stage of a product development project. Figure 4.23 shows the structure of a simple near-field probe sensitive to electric field and that of a simple near-field probe sensitive to magnetic field.

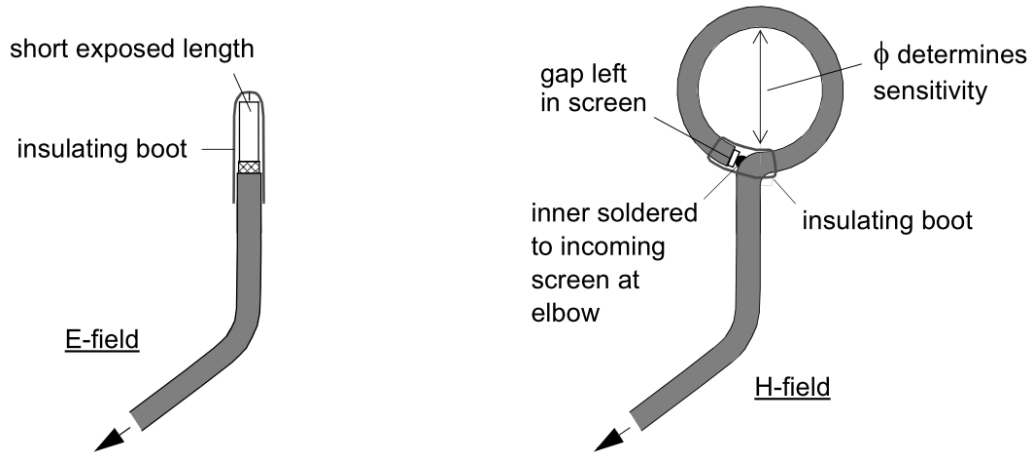

Figure 4.23. *An illustration of an electric near-field probe and a magnetic near-field probe [**21**].*

5 FLYBACK CHARGER

The experiments in this paper concern a *flyback type switching converter*: a certain cell phone charger model designed and manufactured by *Salcomp Group*. This chapter describes the *flyback topology* in general, the particular charger model, and the transformer used in it. The motive for this chapter is to answer the question: *why is the charger prone to produce significant radiated EM emissions and what is its transformer's part in it?*

5.1 Flyback Topology

Cell phone chargers typically function as constant current sources that have a voltage restriction. Charging is controlled by *switching mode operation*, that is, by controlling a semiconductor device between its on and off stages. In this operation, the charger creates pulse-like currents and pulse-like voltages. The switching frequencies are typically from tens of kilohertz up to several hundreds of kilohertz. In this chapter, when we talk about *switching devices* of flyback, we refer to both the *flyback transistor* and the *flyback diode*, which are essential elements of the flyback topology and its switching action. [**36**]

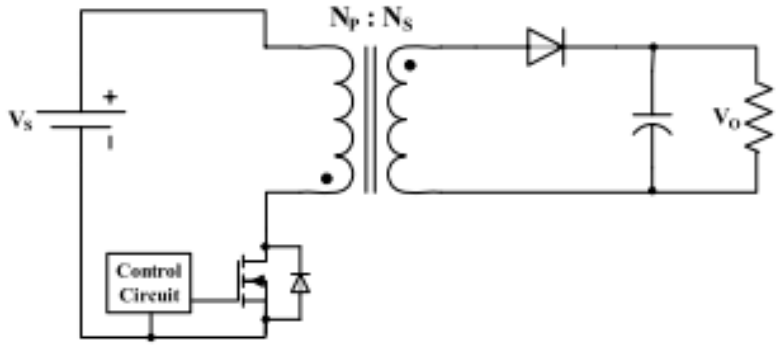

Figure 5.1*. A simplified model of a flyback converter [**37**].*

A flyback is best suited for applications of below 200 watts, with the advantages of a simple design and a small quantity of components [**36**]. Figure 5.1 depicts a simple and stripped-down model of a flyback converter. Basically, a flyback consists of a switching device and its control circuit on the primary side and a rectifier and a filter capacitor on the secondary side. The primary and the secondary circuit are *galvanically separated* but magnetically connected by a high-frequency transformer.

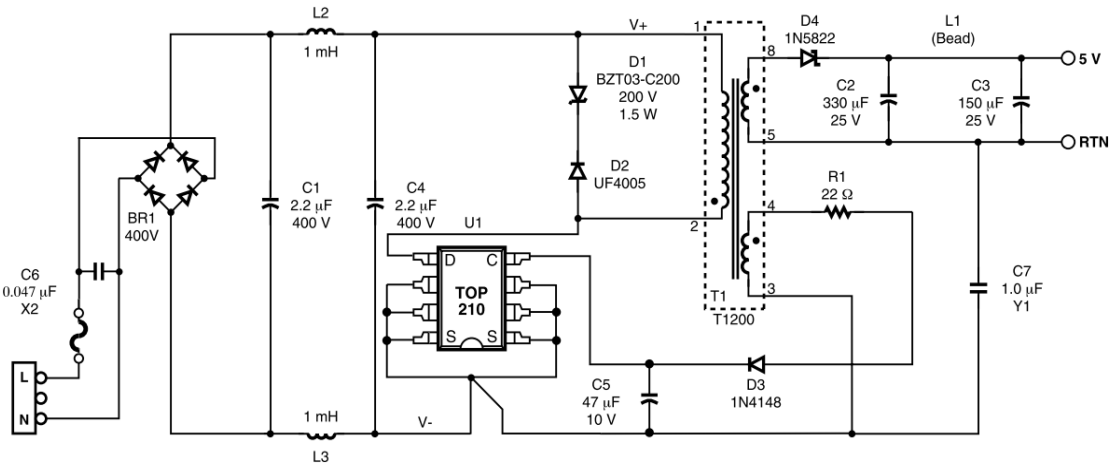

Figure 5.2 *A schematic for a low-power flyback-based charger [**38**].*

A commercial flyback-based charger has a more complex circuit than the one in figure 5.1; a commercial flyback charger contains additional components for, for example, rectifying and measuring current, mitigating voltage overshoot, and filtering noise. Moreover, the simplified model only contains two transformer windings, the *primary* and the *secondary*. Usually flyback chargers incorporate more windings, such as an *auxiliary winding*, which functions as part of the control system, and a *compensation winding*, which mitigates conducted EMI. Figure 5.2 presents a practical schematic for a low-power flyback charger, such as a cell phone charger. [**36**]

5.2 Flyback Transformer

Flyback uses a transformer for setting the *conversion ratio* of the voltage from the primary side to the secondary side and, at the same time, for creating a galvanic isolation between the mains and the output side, which is a requirement in charger applications. The conversion ratio, that is, the ratio of the number of turns in the primary (N_1) and in the secondary winding (N_2), stipulates the magnitude of voltage on the secondary side together with the *pulse ratio* (D). The pulse ratio is defined as the ratio of time the switch is on (t_{ON}) and the total time of one *switching period* (T_S):

$$D = \frac{t_{ON}}{T_S}. \tag{5.1}$$

The ratio of the secondary side and the primary side voltage and its dependence on N_1, N_2, and D is given by

$$\frac{U_{SEC}}{U_{PRI}} = \frac{N_2}{N_1}\frac{D}{1-D}. \quad [\mathbf{36}] \tag{5.2}$$

In addition to voltage conversion and isolation, flyback transformer also functions as a "memory element" for current, that is, as a magnetic energy storage. The primary side current begins to increase after the switch is turned on, storing EM energy in the primary winding's intrinsic inductance, whereas the current on the secondary side is or closes to zero. When the primary side current reaches a set maximum value, the control circuit turns the switch off, forcing the primary side current towards zero.

Simultaneously, the primary-secondary extrinsic inductance starts to disgorge its stored magnetic energy into the secondary circuit as a secondary side current. [**36**]

Figure 5.3 depicts an equivalent circuit of a high-frequency transformer. The resistances R_1, R_2 and R_C are the primary, the secondary, and the core loss resistance, which represent the resistive and the magnetic power loss in the transformer. The capacitance C_P lumps together the capacitances from the primary and the capacitance C_S those from the secondary winding. The capacitance C_{PS} is the primary-secondary inter-winding capacitances lumped into one capacitance. The inductances L_{l1} and L_{l2} are the primary and the secondary side leakage inductances, which cause voltage stress on the circuit of their respective side when the current rapidly changes due to switching action. L_M is the extrinsic inductance, or the transformer's *magnetizing inductance*, but the actual transformer functionality is represented by the ideal transformer circuit element between the primary and the secondary side. [**26**,**37**,**36**]

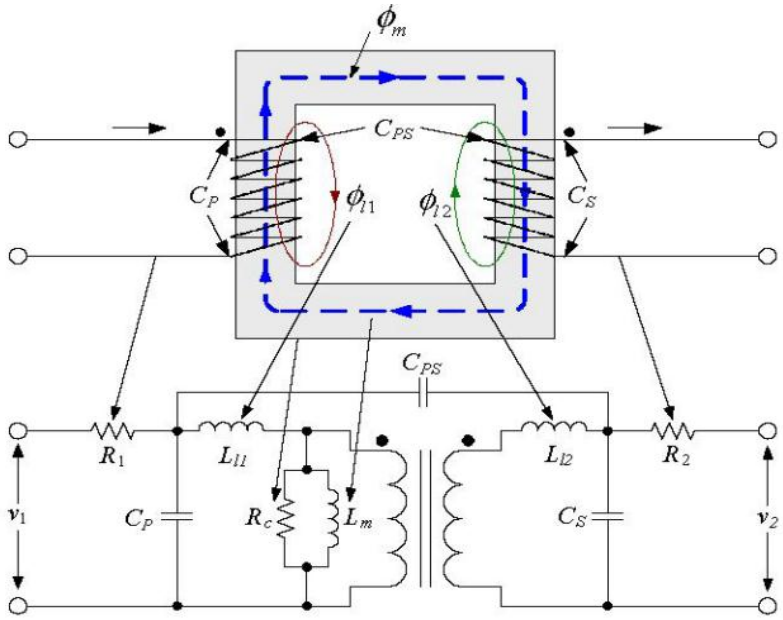

Figure 5.3 *An equivalent circuit of a high-frequency transformer [**26**].*

Flyback transformer's magnetizing inductance is a characteristic that affects the current's waveform and the switching frequency. The designer can adjust the magnetizing inductance with N_1, the size of the core, and the size of the *air gap*. If the air gap is too small, the transformer becomes easily *saturated*, which increases its magnetic emissions, core losses, and heat generation, in other words, degrades the coupling between the transformer windings [**39**]. If the air gap is too large, the core losses become easily very large due to the magnetic circuit's poor overall permeability. The magnetizing inductance is given by

$$L_m = \frac{\mu_0 \mu_r N_1^2 A_g}{l_g}, \tag{5.3}$$

in which μ_0 is the permeability of free space, μ_r the core material's permeability normalized to μ_0, N_1 the number of winding turns in the primary winding, A_g the surface area of the air gap, and l_g the length of the air gap. [**36**]

5.3 Flyback as a Source of Emissions

Radiated emissions of a flyback originate from five major sources/emitters:

1) High-frequency DM currents in the primary loop that consists of the transformer's primary winding, the switching transistor, and the primary capacitor. The DM currents are created especially by the transistor and the primary winding.
2) High-frequency DM currents in the secondary loop that consists of the transformer's secondary winding, the rectifier diode, and the filter capacitors. The DM currents are created especially by the diode and the secondary winding.
3) High-frequency CM currents in ground loops, which are formed by parasitic and stray capacitances within the flyback and between the ground reference and the flyback. The CM currents are created especially by the transistor, the diode, and all the transformer windings through DM-to-CM current conversion.
4) The transformer's leakage inductances, especially during current peaks that saturate the core, because the leakage inductances increase and consequently cause more radiated emissions.
5) The EMI filter inductors, which ironically also increase the radiated emissions, because an inductor adds inductance the magnetic flux of which that cannot be made to cancel out. [**32**]

Other possible, but likely only minor sources/emitters are the transformer control loop's high-frequency DM currents, which are created by the microcontroller and its clock and the high-frequency DM currents in the auxiliary and the compensation winding's current loop, created by the windings.

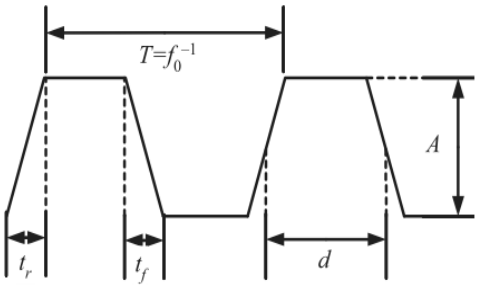

Figure 5.4. *A trapezoidal wave without non-idealities [**22**].*

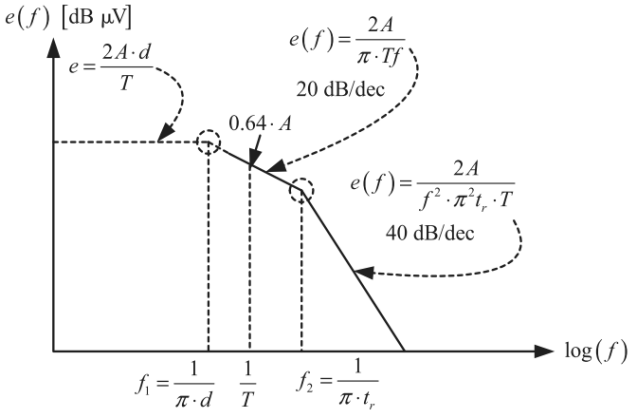

Figure 5.5*. The spectrum envelope of the adjacent trapezoidal wave [**22**].*

Flybacks have a natural tendency to create strong EM emissions into their surroundings. This stems from the intrinsic nature of switched mode operation, in which pulsating current and voltage waveforms at the frequency of the switching action play a central part. Flybacks use switching devices to "chop" currents, consequently creating *rectangular*, or *pulse train*, waveforms of current and voltage. To be precise, because rectangular waveforms in real flybacks have finite rise and fall times – t_r and t_f, respectively – they are, in fact, *trapezoidal waveforms*.

The frequency of the trapezoidal waves, or the switching frequency of the flyback, has a positive correlation with the emission levels produced. Figure 5.5 illustrates the *spectrum envelope* for the trapezoidal wave of figure 5.4. The amplitude at the fundamental frequency, that is, at the switching frequency f_S, and at the low end of the spectrum until f_1 is dictated by the trapezoidal wave's amplitude and pulse ratio, $2A \cdot t_{ON}/T_S$. In a trapezoidal wave's spectrum envelope, the fundamental frequency stipulates the location of the "corner frequency" f_1, and the rise and the fall time of the rectangular wave's edges stipulate the location of the corner frequency f_2. The higher the fundamental frequency, the higher on the frequency axis f_1 is located and the shorter the rise and the fall time, the higher on the frequency axis f_2 is located. The higher f_1 and f_2 are located, the higher the high-frequency harmonic content is. [**22**,**36**]

Flybacks typically have relatively high switching frequencies, from tens of kilohertz up to several hundreds of kilohertz, because high switching frequency minimizes the size of the transformer and consequently that of the whole flyback. Also, the rise and fall times of the pulses are typically designed short to minimize the switching device's power dissipation, that is, the *switching losses*. Incidentally, the harmonic content of flybacks' waveforms is rich in high-order harmonics, that is, their high-frequency sinusoidal components have significant amplitudes until very high frequencies. Moreover, a flyback's parasitic and stray impedances together with the circuit's numerous inductors, capacitors, and impedance interfaces form complicated resonance circuits, which enhance emissions at a number of resonance frequencies.

5.3.1 Switching Operation and Switching Devices

A switching device creates intentional DM voltage and DM current transients by switching the impedance across itself from low to high and vice versa, that is, from conductive (turned-on) to non-conductive (turned-off) state and vice versa [**30**]. The current transients cause high di/dt's to occur in the entire DM loop incorporating the switching device. Loops with high di/dt can induce a DM voltage through intrinsic and extrinsic inductances. The voltage transients cause large dv/dt's to occur across components, which can then be modeled using "test voltage sources" that drive "test currents", as was already explained in section 4.4, or by using "test current sources".

A test current models partly the intentional current flow of the switching converter's operation and partly the unintentional current flow that is effectively DM noise. One can interpret the DC and the low-frequency components of the test current to emulate intentional and its high-frequency components to emulate unintentional currents. A DM current by a high di/dt or dv/dt can also result in CM noise voltages and CM noise currents through DM-to-CM conversion.

Flyback's switching causes the largest dv/dt to occur 1) across switching devices, because their impedance changes rapidly from low to high and vice versa and 2) across transformer windings, a) because the flux that stipulates their voltage switches rapidly from a winding's own flux to the mutually coupled flux originating from its winding

counterpart and vice versa and b) because their leakage inductance "tries" to satisfy Lenz's law by self-inducing a voltage that cancels out the flux change.

An ideal switch in a flyback can be modeled with a rectangular wave voltage source (on/off fashion) and a more realistic one with a trapezoidal wave voltage source (finite fall and rise times of edges). However, a real flyback's primary and secondary circuits have parasitic capacitances and inductances, which change the voltage waveform into a yet more non-ideal shape that exhibits, for example, positive and negative overshoots and ringing. Compared with a trapezoidal waveform, the voltage waveform with these non-idealities has more high-order harmonic content, which couples noise currents more readily through capacitive coupling paths and is thus more likely to create more EM noise. [**7**]

A large dv/dt across the transistor, depicted in figure 5.6's V_{DRAIN} waveform, occurs across its *drain* and *source*, depicted in figure 5.7. Parasitic capacitances of the transistor, the primary winding, and the diode and the leakage inductance of the secondary winding cause overshoot in the primary current and ringing in the secondary circuit's voltages and consequently in the primary winding voltage, typically at frequencies between 3-12 MHz as denoted in figure 5.6 with f_3. A large dv/dt across the rectifier diode, depicted in figure 5.6's V_{DIODE} waveform, occurs across its *anode* and *catode*, depicted in figure 5.7. Parasitic capacitances of the transistor, the diode, and the secondary winding and the leakage inductance of the primary winding cause overshoot and ringing in the primary circuit's voltages and consequently in the secondary winding voltage and the secondary side current, typically at frequencies between 20-30 MHz as denoted in figure 5.6 with f_4. [**36**,**38**]

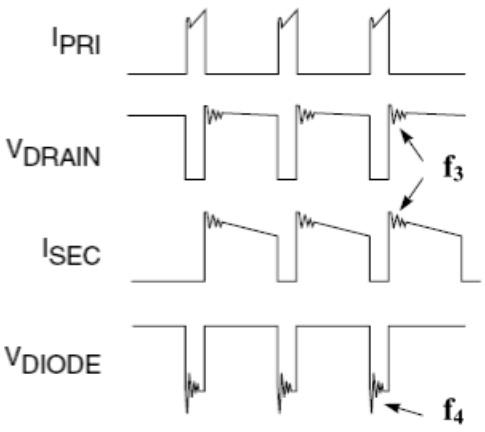

Figure 5.6. *The waveforms of the primary current, the transistor voltage, the secondary current, and the diode voltage in a flyback [**38**].*

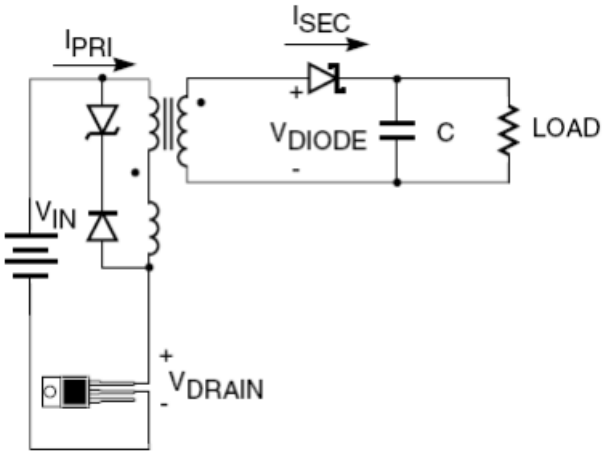

Figure 5.7. *A simplified flyback circuit diagram showing where the waveforms of figure 5.6 were measured [**38**].*

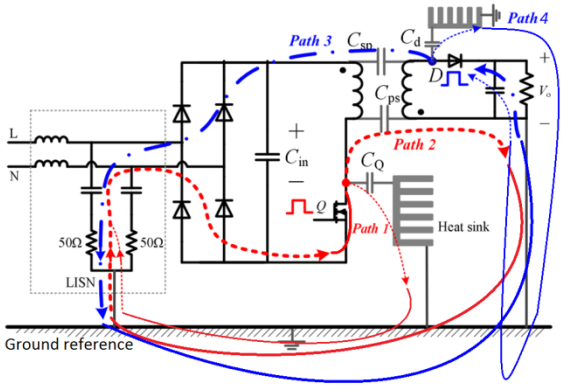

Figure 5.8. *The unbalanced DM noise currents by switching devices create stray ground currents and CM noise, as in this flyback charger connected to a LISN [**8**].*

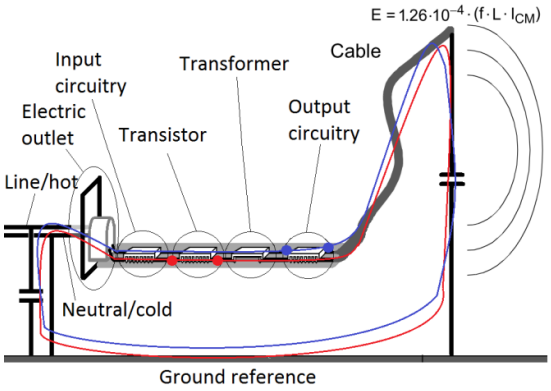

Figure 5.9. *A flyback charger's CM noise currents via the output cable caused by switching devices' unbalanced DM noise [**21**].*

Figure 5.8 depicts the major resulting DM noise currents when the switching devices are modeled with test voltage sources that createwaveforms with high-frequency content, as those in figure 5.6. In the figure, the switching devices' heat sinks, and possibly the flyback's metal enclosing, provide major capacitive coupling paths to the ground reference, as often in flybacks that are equipped with such.

When a switching device creates DM noise, a lot of DM-to-CM conversion occurs, because the circuit is greatly unbalanced from the switching devices' standpoint. The unbalance of the DM noise creates stray ground currents, which cause CM noise voltages in the ground reference. The CM noise voltages, in turn, drive CM noise currents in available ground loops, as figure 5.9 illustrates (only ground loops via the output cable are depicted). Because the DM and the CM noise currents by switching devices have very high-frequency contents, conductive coupling paths with high inductance, such as transformer windings, provide poor (high-impedance) propagation paths, whereas capacitive coupling paths provide good (low-impedance) coupling paths for them. This explains the depicted paths for the major noise currents.

5.3.2 Switching Operation and Transformer

When one measures a transformer winding voltage, he measures either 1) the voltage associated with the "residual magnetic flux" or 2) the voltage associated with the "mutually-coupled but not-cancelled-out flux" originating from the mutually-coupled winding counterpart. Which one he measures depends on whether he measures the winding that is more "dominant", that is, has a larger magnetic flux due to current that is driven in it by a driver/source than its winding counterpart, the "submissive" winding. The voltage measurement yields the voltage associated with the residual magnetic flux when one measures the dominant winding and the voltage associated with the mutually-coupled but not-cancelled-out flux originating from the mutually-coupled winding counterpart (the dominant winding) when one measures the submissive winding.

The voltage associated with the dominant winding's residual flux enforces a di/dt in the winding. This voltage is the difference between the voltage associated with the dominant winding's total magnetic flux and the voltage associated with the "mutually-coupled and cancelled-out flux". Moreover, the voltage associated with the mutually-coupled and cancelled-out flux enforces a di/dt in the submissive winding.

The di/dt enforced by the voltage associated with the dominant winding's residual magnetic flux can be modeled with a test current source in the place of the winding. When the primary winding is the dominant one, the test current source must drive a current waveform that satisfies:

$$v_{L1}(t) - v_{N1}(t) = L_{res}\frac{di_1(t)}{dt} \tag{5.4}$$

$$\Leftrightarrow \frac{di_1(t)}{dt} = \frac{v_{L1}(t) - v_{N1}(t)}{L_{res}}, \tag{5.5}$$

in which $v_{L1}(t) - v_{N1}(t)$ is the voltage associated with the primary winding's residual magnetic flux, L_{res} the "residual intrinsic inductance" which is associated with the residual magnetic flux, and $\frac{di_1(t)}{dt}$ the current's rate of change in the primary winding (see figure 5.10 for reference). Therefore, to model di_1/dt, one must determine the voltage across the primary winding, $v_{L1}(t) - v_{N1}(t)$, and the value of the residual intrinsic inductance, L_{res}. The residual intrinsic inductance's value is dependent on the secondary side current, not solely on the geometry of the setting. Thus, such an inductance is not a real inductance, as per our earlier definition for inductances, but let us have it in this context because it allows more generally applicable equations 5.4 and 5.5 than when using leakage inductance instead of it.

In contrast, the di/dt enforced by the voltage associated with the mutually-coupled and cancelled-out flux can be modeled with a test current source in the place of the submissive winding. When the primary winding is the dominant one, the test current source must drive a current waveform that satisfies:

$$v_{N1}(\mathrm{t}) = -M_{co}\frac{di_2(t)}{dt} \tag{5.6}$$

$$\Leftrightarrow \frac{di_2(t)}{dt} = -\frac{v_{N1}(t)}{M_{co}}, \tag{5.7}$$

in which $v_{N1}(t)$ is the voltage associated with the mutually-coupled and cancelled-out flux, M_{co} the "cancelled-out extrinsic inductance" which is associated with the mutually-coupled and cancelled-out flux, and $\frac{di_2(t)}{dt}$ the current's rate of change in the secondary winding (see figure 5.10 for reference). Thus, to model di_2/dt, one must determine the voltage associated with the mutually-coupled and cancelled-out flux, $v_{N1}(t)$, and the value of the cancelled-out extrinsic inductance, M_{co}. The cancelled-out extrinsic inductance's value is dependent on the secondary side current, and thus also this inductance is not a real one, as per our earlier definition for inductances, but let us have it in this context because it allows more generally applicable equations 5.6 and 5.7 than when using primary-secondary extrinsic inductance instead of it.

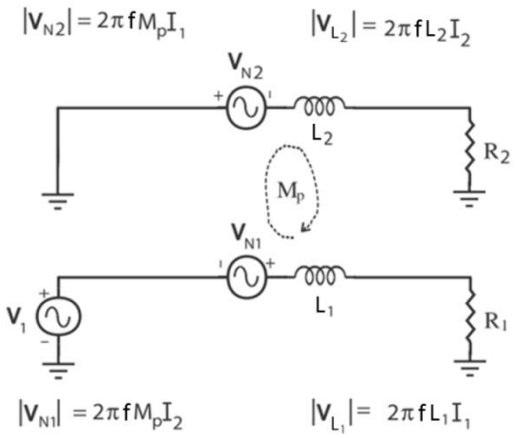

Figure 5.10. *An equivalent circuit of inductive mutual coupling through extrinsic inductance [**16**].*

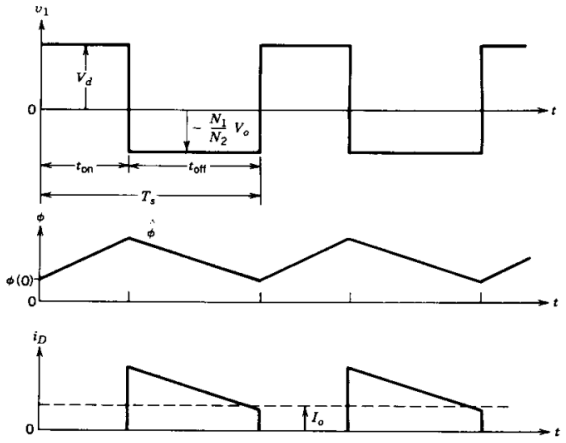

Figure 5.11. *The ideal waveform of 1) primary winding voltage, 2) transformer core's magnetic flux and 3) secondary side current of a flyback [**27**].*

The voltage associated with the mutually-coupled but not-cancelled-out flux originating from the dominant winding does not enforce any di/dt; it merely "reflects" the voltage of the dominant winding across the submissive one, taking into account the winding turn ratio of the windings. A flyback's primary winding voltage with the transistor off is an example of this, as figure 5.11 illustrates. This is because in flybacks only either the primary loop or the secondary loop is conducting at once; when the primary loop is not conducting, the submissive primary winding voltage only "reflects" the dominant secondary winding voltage. Although the current flow in the primary and in the secondary winding is thus discontinuous, the magnetic flux in the transformer core is continuous, as figure 5.11 shows.

When a flyback's transistor is on and diode reverse-biased, the primary winding is the dominant winding and the secondary winding the submissive one and consequently:

1) The voltage across the primary winding is associated with its residual magnetic flux. Thus, the primary winding voltage enforces a di/dt in itself. Because there is no secondary side current, there is no mutually-coupled and cancelled-out flux nor an associated voltage that would enforce a di/dt in the secondary winding.
2) The voltage across the secondary winding is associated with the mutually-coupled but not-cancelled-out flux originating from the primary winding. Thus, the voltage across the secondary winding does not enforce any di/dt; it only "reflects" the primary winding voltage in itself.

Contrarily, when the transistor is off and the diode forward-biased, the secondary winding is the dominant winding and the primary winding the submissive one and consequently:

1) The voltage across the secondary winding is associated with its residual magnetic flux. Thus, the secondary winding voltage enforces a di/dt in itself. Because there is no primary side current, there is no mutually-coupled and cancelled-out flux nor an associated voltage that would enforce a di/dt in the primary winding.

2) The voltage across the primary winding is associated with the mutually-coupled but not-cancelled-out flux originating from the secondary winding. Thus, the voltage across the primary winding does not enforce any di/dt; it only "reflects" the secondary winding voltage in itself.

Figure 5.11 shows ideal waveforms over two switching cycles for 1) the primary winding voltage, 2) the transformer core's magnetic flux, and 3) the secondary side current in a flyback. But a real winding has parasitic intra-winding capacitances, which together with a real switching device's parasitic capacitances "round up" the edges of voltage pulses and consequently affect the shape of the core's magnetic flux waveform and its associated currents. Furthermore, the parasitic capacitances together with the windings' inductances introduce resonances, which manifest themselves as ringing. Thus, in reality the waveforms of figure 5.11 would show such non-idealities.

In a real flyback, for a while right after the transistor turn-off, during the "transition time", some current still flows in the primary winding due to the transistor's space charge capacitance charging up with current from the winding's leakage inductance and due to intra-winding capacitances discharging via the winding. At the beginning of the transition time the voltage across the primary winding is associated with its own residual magnetic flux and by the end of it with the mutually-coupled but not-cancelled-out flux originating from the secondary winding. Similarly, during the transition time after the transistor turn-on some current still flows in the secondary winding due to the diode's space charge capacitance charging up with current from the winding's leakage inductance and due to intra-winding capacitances discharging via the winding. At the beginning of the transition time the voltage across the secondary winding is associated with its own residual magnetic flux and by the end of it with the mutually-coupled but not-cancelled-out flux originating from the primary winding.

In conclusion, modeling a transformer winding during the transition time is difficult, because one must know how the voltage transient across the winding behaves, that is, what its wave shape is like and at what point it goes to zero meaning the voltage changes from being associated with the residual flux to being associated with the mutually-coupled but no-cancelled-out flux. An easy solution is to disregard the effect of the parasitic impedances that allow concurrent current flow on both the primary and the secondary side, but this naturally lowers the accuracy of the modeling.

5.3.3 Transformer's Parasitic and Stray Impedances

From earlier discussion, it became evident that the root cause of EM noise in a flyback is its switching action, which renders switching devices and transformer windings into EM noise sources. These EM noise sources ideally only produce DM noise currents, which can be effectively filtered, that is, directed into small DM current loops by input and output filters, minimizing their radiation. But a flyback's unbalance from these EM noise sources' standpoint causes DM-to-CM conversion.

The unbalance is great from the switching devices' standpoint because the transformer's inductances and parasitic inter-winding capacitances as well as the output

cable's send/go and return conductors with their stray capacitances to the ground reference are unsymmetrically located in relation to the switching devices. From transformer windings' standpoint a flyback circuit is more symmetrical, but parasitic and stray impedances, such as stray capacitance from switching devices' heat sinks, may cause major unbalance from the windings' standpoint too.

Also, the number of transformer windings, their location, and the distribution of their winding turns in relation to each other, that is, the "coherence" of the windings, affects the balance because these factors are reflected in at least the values of the transformer's parasitic intra-winding and inter-winding capacitances as well as in its parasitic leakage inductances. Thus, an educated guess is that measuring a transformer's intentional and parasitic impedances, and perhaps other properties, functions as a gauge for the degree of unbalance from the switching devices' and from the transformer windings' standpoint. Figure 5.12 depicts a flyback transformer's parasitic capacitances and stray capacitances with the ground reference and with the rest of the flyback circuit.

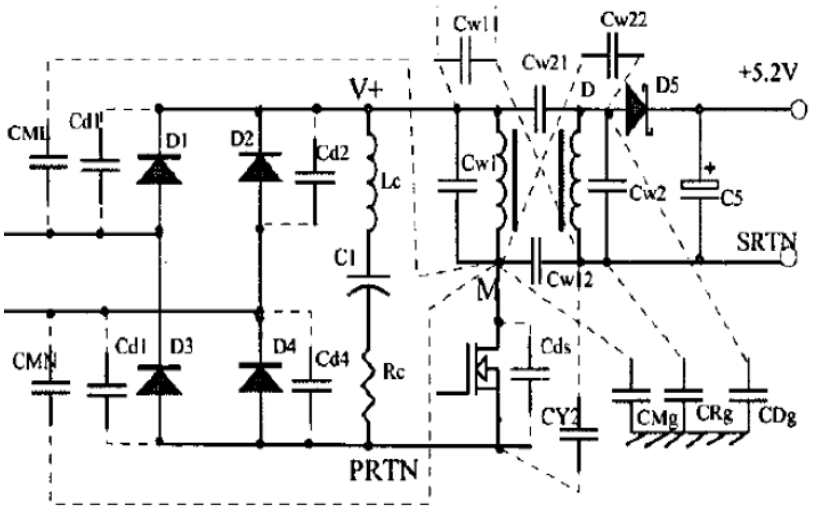

Figure 5.12. *Various parasitic and stray capacitances of a flyback transformer [**41**].*

Flyback's parasitic and stray capacitances along ground loops, such as inter-winding capacitances, are also a possible significant source of CM noise [**40**]. One may model an inter-winding capacitance's noise source properties with a trapezoidal wave test voltage source that is capacitively connected in between the windings. One may then interpret the test currents it drives as noise current spikes produced by the charging and the discharging of the capacitance. But the capacitance will not be charged unless some source drives high-frequency current through it, and it will not be discharged unless it drives current into a current loop formed between its two coupling points. In a flyback, the switching devices' and the transformer windings' high-frequency noise currents are largely responsible of charging parasitic and stray capacitances. Thus, let us simplify things by considering inter-winding capacitances and other parasitic or stray capacitances along ground loops merely to affect the magnitude of CM currents created by switching devices and transformer windings with the given unbalance. In other

words, let us disregard modeling the capacitances with test voltage sources and just think of them as impedances along ground loops.

Parasitic and stray capacitances affect CM currents' magnitudes by contributing substantial impedances to the ground loops. Particularly parasitic primary-secondary winding capacitances are pivotal impedances in ground loops via the secondary side, which in turn are substantial in flyback chargers because the output cable has strong capacitive coupling with the ground reference. Thus, an educated guess is that measuring a transformer's parasitic capacitances, especially the primary-secondary winding capacitance, functions as a gauge for the magnitude of CM currents.

According to the literature [**36**], a transformer's EMI-wise most significant impedances are its primary winding intrinsic inductance, resistive losses, leakage inductances, and parasitic capacitances, implicating the above educated guesses may be accurate.

5.4 Four Theoretical Speculations as the Premise for Experiments

In summary, based on the theory presented in these first five chapters, the following speculations are the premise for the experiments conducted in this research:

1) Measuring a flyback transformer's impedances, and perhaps other properties, functions as an indirect way of measuring the flyback circuit's degree of unbalance from the switching devices' and the transformer windings' standpoint. Further, the circuit's unbalance is a gauge for the degree of DM-to-CM conversion taking place in it.
2) Measuring a flyback transformer's parasitic capacitances is an indirect way of measuring the magnitude of CM currents in the flyback circuit with the given unbalance.
3) Measuring a flyback circuit's CM currents is an indirect way of measuring its CM radiated emissions.
4) Measuring a flyback circuit's DM currents is an indirect way of measuring its DM radiated emissions.

6 MEASUREMENTS

As mentioned, the charger under scrutiny, or the DUT in this paper's experiments, represents the flyback topology, albeit a Salcomp proprietary version which contains a much more complex circuit with a number of "additional" components compared with a generic flyback circuit. Details of the charger's design and operational characteristics are company confidential, but some details about the transformer will be disclosed in this chapter.

Three different kinds of measurements were implemented to test the theoretical speculations of section 5.4. Each measurement was repeated with a number of transformer samples; if the flyback charger was used in the measurement, the rest of the flyback circuit was maintained the same when the transformer was changed. In the measurements, a 7.5 Ω resistive "dummy load" was used to provide the loading to the charger. Because the maximum output when charging a cell phone is 5 V and 1 A, such a load was deemed appropriate in assessing the charger's emissions. Moreover, the magnetic dipole characteristics of the charger are predominant with such a relatively small load, which was beneficial for the near-field probe measurements. [**42**]

The first kind of measurements was a simple measurement of electrical and physical properties of the given transformer. These measurements yielded one measurement value for each measured transformer, and the measurements could be done with the transformer detached from the charger and thus without the transformer carrying any currents or voltages, that is, while being "offline".

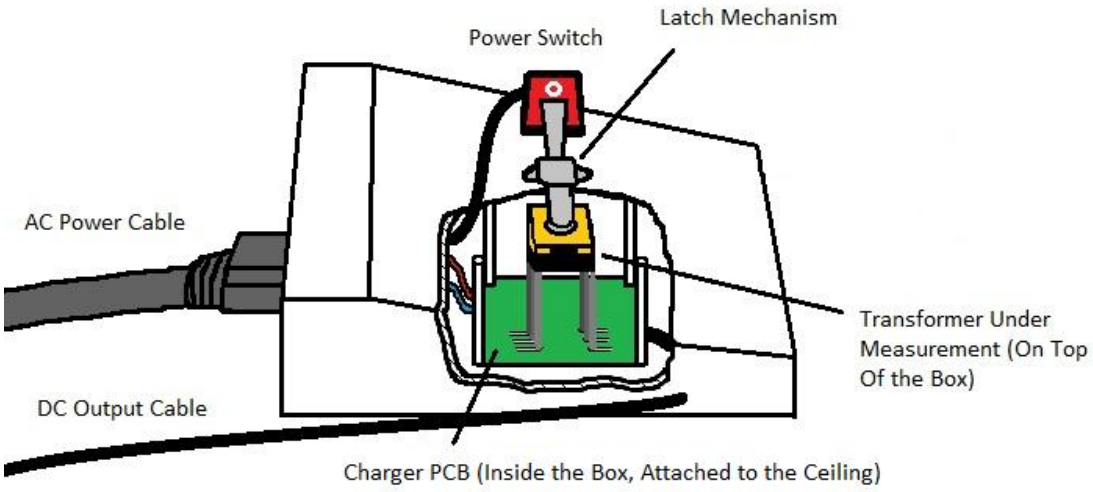

Figure 6.1. *The measurement box used in the radiated emissions and the near-field probe measurements.*

The second kind of measurements made use of near-field probes that are sensitive to the magnetic near field of the charger and that of the transformer. In contrast to the first kind of measurements a powered-on, or "online", charger with a transformer was measured in the near-field probe measurements. The procedure was to measure the magnetic near field of the charger equipped a given transformer sample and then change the transformer, while keeping the rest of the charger unchanged. The change in the measurement readout would thus show the effect of the transformer on the charger's magnetic near field.

The third kind of measurements was the radiated emissions test following the *EN 55022/CISPR 22* directions. Similarly, the measurement box was used also in this set-up to determine the effect of the transformer on the variations in the whole charger's radiated emissions.

A tailor-made "measurement box", depicted in figure 6.1, was used for the second and the third kind of measurements. It contained a charger PCB fixed to the ceiling of the box and six upright "contact rods" with one end soldered on the transformer pads on the PCB and the other end at the ceiling of the box. The ceiling had six holes exactly where the contact rods reached it, so that the transformer's pins could be placed into the holes. A latch mechanism, when closed, applied force on the transformer, pushing the transformer pins firmly against the contact rods. The rods contained a spring mechanism, which applied a counter force against the transformer pins, ensuring a good electrical contact between the two without a need for soldering.

The first kind of measurements pertained to speculations 1 and 2 and the second kind to speculations 3 and 4 in section 5.4. The third kind of measurements, the radiated emissions test, provided the data whereby the speculations could be verified.

6.1 Measurements of Transformer Properties

The DUT's transformer had six windings: a primary, a secondary, an auxiliary, and three compensation windings. These windings were wound between eight pins. Figure 6.2 shows the location of each winding in relation to the eight pins and figure 6.3 the physical location of the pins on the transformer bobbin. The figures are from Salcomp's internal documentation. Table 6.1 shows the winding configuration, that is, the starting and the finishing pins of and the number of turns in each winding.

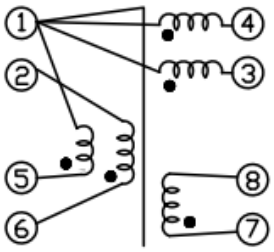

Figure 6.2. *The windings of the transformer.*

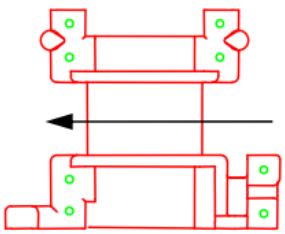

Figure 6.3. *The pins of the transformer.*

A variety of electrical properties, which can be divided into 1) inductances, 2) capacitances, and 3) other electrical properties, were measured from the transformers. The only physical property measured was the transformer's weight. Hereafter, "transformer properties" refers to the electrical properties and the weight together.

Table 6.1. *The winding configuration of the transformer.*

Winding type	**Starting pin**	**Finishing pin**	**Turns**	**Designation**
Compensation winding	5	1	37	W1
Primary winding	2	6	164	W2
Auxiliary winding	1	4	25	W3
Compensation winding	1	Turn pin	15	W4
Secondary winding	7	8	12	W5
Compensation winding	3	1	8	W6

The electrical properties were measured at two different points along the transformer manufacturing process: 1) before the installation of the transformer core, when the transformer only had the windings wound on the bobbin and no varnish and 2) when the transformer was fully completed, that is, with the transformer core installed and the whole transformer varnished and dried. The purpose for the two measurement points was to see whether already the earlier point would give away the same information on correlation with the radiated emissions as the later one. If so, sub-standard transformers could be spotted and screened out earlier, which saves costs.

The inductance measurements covered the measurements of 1) the leakage inductances of the transformer's windings, 2) the primary winding intrinsic inductance, and 3) the primary-secondary extrinsic inductance. The capacitance measurements covered the measurements of 1) the primary self-capacitance (intra-winding capacitance), 2) the primary-secondary capacitance (inter-winding capacitance), and 3) the capacitance between compensation windings *W4* and *W6*. The other electrical measurements covered 1) the measurement of the transformer's *Q value* and 2) the "EMC box measurement", a measurement done with Salcomp's proprietary measurement equipment, the operational logic of which is company confidential.

The weight of the transformer was measured both before and after the varnishing work phase in the transformer manufacturing process. The weight of the varnish was calculated as the difference between the weight after and the weight before varnishing.

6.1.1 Measurement Set-Up

The electrical properties were measured using *Hewlett-Packard/Agilent 4284A Precision LCM Meter* and Salcomp's proprietary EMC box, and the transformer's weight was measured using an electronic scale. The measured properties with associated measurement instructions are tabulated in table 6.2. The instructions describe which pins are to be short-circuited and which ones connected to the LCM meter's input when

measuring a given property. The information in table 6.2 is from the transformer supplier's specification sheet and Salcomp's internal documentation.

Table 6.2. *The measured transformer properties and their measurement instructions.*

Transformer property	**Measurement instruction**
Leakage 1 (secondary)	Connect pins 2 and 6, short pins 7 and 8
Leakage 2 (compensation)	Connect pins 2 and 6, short pins 1 and 5
Leakage 3 (auxiliary)	Connect pins 2 and 6, short pins 1 and 4
Leakage 4 (compensation)	Connect pins 2 and 6, short pins 1 and 3
Leakage 5 (all)	Connect pins 2 and 6, short all other pins
Primary self-inductance	Connect pins 2 and 6
Primary-secondary inductance	Connect pins 2 and 7
Primary self-capacitance	Connect pins 2 and 6
Primary-secondary capacitance	Connect pins 2 and 7
Capacitance between W4-W6	Connect pins 1 and 3
Q value	Connect pins 2 and 6
EMC box	Use proprietary Salcomp measurement device
Weight before varnish	Before the dip varnishing work phase
Weight after varnish	After the dip varnishing work phase and drying
Varnish weight	The difference between the two above

6.2 Near-Field Probe Measurements

Two different kinds of near-field probes were used for measuring the near field of the DUT. Because EM field theory states that moving charges generate a magnetic field, near-field probe measurements of the magnetic field is an indirect way to measure the amount of moving charges that caused it, that is, an indirect way to measure current. One type of near-field probes used was *clamp-on current probe*, which is a magnetic-field-sensing probe that is clamped around a wire or a cable and which measures the currents flowing in it. The second type used was *magnetic near-field probe*, which is a magnetic-field-sensing probe with a loop-shaped tip that one must place near the conductor whose currents are to be measured. Two probes of both types, a large one and a small one, were used. Besides their physical size difference, which affected where and how they could be placed, the large and the small probes had differences in, for example, their sensitivity and their frequency range.

Figures 6.4-6.7 show the large magnetic near-field probe, the small magnetic near-field probe, the large clamp-on current probe, and the small clamp-on current probe and how they were placed in relation to the measurement box and the transformer under measurement. The locations and the positions of the probes in relation to the transformer and the cables were decided, within the limitations of the probes' physical sizes, based on test runs with each measurement set-up; the position and/or location that

seemed to yield the largest output for a given probe was chosen as the final one. Section 6.2.1 describes how the "constancy" of the measurement set-ups was secured.

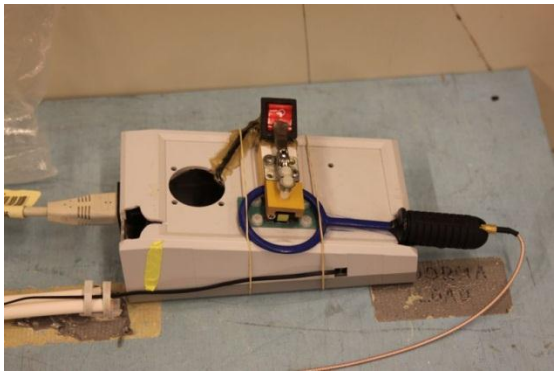

Figure 6.4. *The large magnetic near-field probe in use in the accordant measurement set-up.*

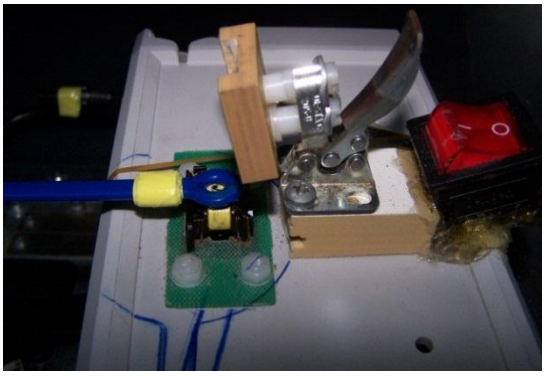

Figure 6.5. *A close-up of the small magnetic near-field probe, the transformer under measurement, and the measurement box.*

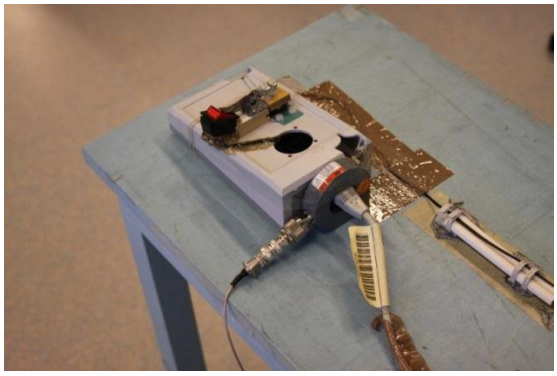

Figure 6.6. *The large clamp-on current probe in use in the accordant measurement set-up.*

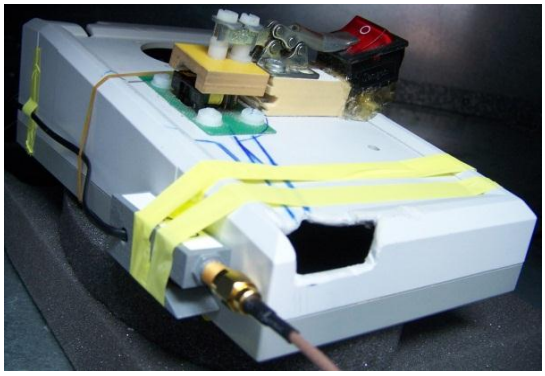

Figure 6.7. *A close-up of the small clamp-on current probe, the transformer under measurement, and the measurement box.*

The clamp-on current probes should quite accurately measure CM currents flowing in the cable around which they are clamped, because the current paths that can affect the measurement readouts are simply just the send/go and the return wire inside the cable. Clamp-on current probes make use of the same principal in their operation as transformers; the wire or the cable under measurement functions as the primary and the probe as the secondary side. If the probe is clamped around only a single wire, the probe measures any currents flowing along it. If the probe is clamped around a cable with both a send/go and a return wire, the magnetic fields associated with DM currents flowing in the wires cancel each other out, and the probe registers only CM currents. This suits us well because in chargers CM currents are undesired noise currents and thus interesting to measure, whereas DM currents in the input and the output wires are largely intentional. Magnetic fields from the surroundings or other parts of the DUT than the cable cause only minor disturbance in the clamp-on current probe measurement

readouts, except for some FM radio stations' broadcasts, which are readily picked up by the cables, as can clearly be seen in the spectrums of appendix B.

In contrast, it is not explicit as to which currents the magnetic near-field probes were exactly measuring. Because the magnetic near-field probes were positioned in the proximity of the transformer windings, they were predominantly measuring the magnetic fields associated with currents in the windings. But there were six different windings, some of which had differing directions of current flow in relation to each other, and all in all over 200 turns of winding tightly packed together, making it futile to try to measure the magnetic field associated with any particular current. Thus, the magnetic near-field probes measured some kind of an aggregate magnetic field of all the windings, but mainly that of the primary and the secondary due to their stronger magnetic fields compared with the compensation and the auxiliary windings.

6.2.1 Measurement Set-Up

Each of the four near-field probe measurements had a unique measurement set-up that had to be fixed so that:

1) The *repeatability* of the measurement was sufficient to obtain reliable results.
2) The measured fields were large enough to give a good *signal-to-noise ratio*.

A "sufficient" repeatability and a "good" signal-to-noise ratio were obviously subjective opinions. However, varying the measurement set-ups and seeing the effect on the measurement readouts provided a rather good insight as to what degree of repeatability and signal-to-noise ratio are achievable and what factors, such as probe and cable positions, locations and orientations, have an effect on them.

The measurements were carried out on a wooden table, which was located near a grounded metal wall, as shown in figures 6.8 and 6.9. The EMI receiver, the computer it was connected to, and the power supply for the DUT were located on another table about 1½ meters away. In the power supply end, a LISN was used for filtering possible noise coming in from the building's local mains distribution network and for providing a balanced and specified-impedance input circuit for the charger. With the magnetic near-field probe measurements, also ferrite ring filters were used at the LISN's output to filter out CM noise, that is, to render the impedance of ground loops through the LISN higher and thus the CM-to-DM conversion for the given unbalance smaller. This way, CM noise's effect on what was meant to be a "DM-noise-only measurement" was minimized.

A *Rohde & Schwarz EMI Test Receptor/receiver ESPC* connected to a PC was used as the measuring instrument in the near-field probe measurements. As each measurement's output the instrument gave a spectrum graph and a file with a tabulated measurement readout for each frequency point. The frequency range in which the measurements were done was 30-100 MHz. A *peak detector* was used with a 120-kHz *resolution bandwidth* and a 20-millisecond *step time*.

Several factors were suspected to affect the repeatability and the signal-to-noise ratio of the measurements. With the magnetic near-field probes, the ability to keep the

probes' positions around the transformer unchanged when changing the transformer in the measurement box was deemed the most important. With the clamp-on current probes, the location and the position of the DC output cable and the AC power cable in relation to the grounded metal wall, which was effectively the ground reference in this case, was deemed the most important. Also, fixing the location and the position of the measurement box and those of the *pre-amplifier* with its signal and power cables on the table was deemed reasonable. Thus, the positions and locations were fixed using aids such as rubber bands, tape, polystyrene, cable ties, and alignment markings. After many test runs with variations of the measurement set-ups in terms of locations and positions of the table, the measurement box, the probes, and the cables, a final set-up was ultimately fixed for each measurement.

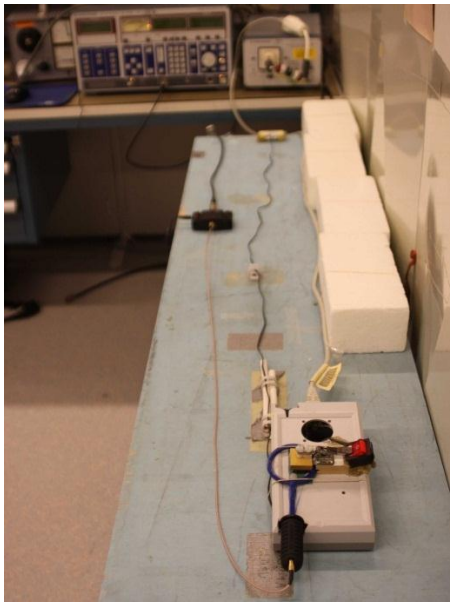

Figure 6.8. *The measurement set-up for the large magnetic near-field probe measurement.*

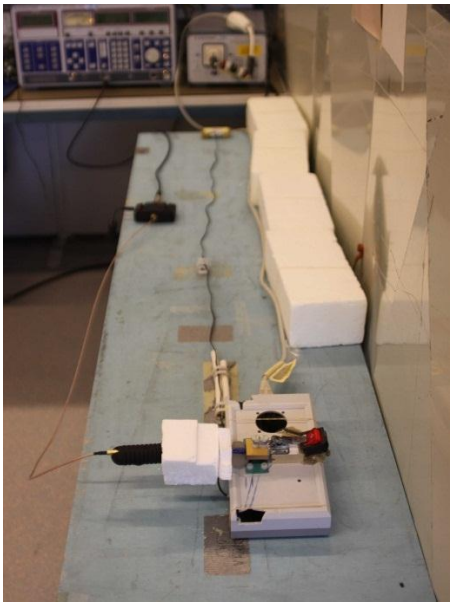

Figure 6.9. *The measurement set-up for the small magnetic near-field probe measurement.*

With the magnetic near-field probes, the table's long side was chosen to be placed facing the grounded metal wall, as shown in figures 6.8 and 6.9. Because varying the positions of the cables in relation to the metal wall was found to have no effect on the measurement readouts, other positions of the table were not deemed necessary to experiment with. But, as suspected, the positions of the magnetic near-field probes had a significant effect on the readouts. This is because the near field of the transformer has a very complex shape, and even a slight transition of a measurement probe to any direction may greatly change the measurement readouts. Thus, the probe positions were fixed as well as possible.

With the clamp-on current probes, the table's short side was chosen to be placed facing the grounded metal wall, keeping the measurement box and the cables far away from the metal wall, as shown in figure 6.10; this particular disposition of the cables was found to yield the highest readouts and thus likely the best sensitivity and signal-to-

noise ratio. As suspected, the location and the position of the cables in relation to the metal wall had a significant effect on the measurement readouts. This is because the cables' positions and locations in relation to the metal wall determine the strength and the distribution of capacitive coupling paths between them, or in other words, the total amount of CM current and its share that flows so that a clamp-on current probe can register it.

Figure 6.10. *The measurement set-up for the clamp-on current probe measurements.*

Intuitively, one might assume that the closer a cable is to the metal wall, the more efficient the capacitive coupling, the smaller the ground loops' impedances, and the larger the CM currents that the clamp-on current probe registers. Higher measurable CM currents, in turn, mean a higher sensitivity and a higher signal-to-noise ratio of the measurements. However, during pretesting the measurement readouts were found to be higher when the table's short side was facing the metal wall, keeping only the ends of the cables close to the wall and thus allowing only the cable's end to have efficient capacitive coupling with the wall. This could be explained by the way how capacitive coupling between the cables and the metal wall is formed. In graphical illustrations, an output cable's capacitive coupling is conventionally depicted as one lumped capacitance at the end of the cable and the CM current loop as one single loop formed by the "longest ground loop", as in figure 6.11. In actuality, however, there are innumerable capacitive coupling paths between the circuit and the ground reference and thus innumerable CM current loops along the circuit.

In the case of the table's long side next to the metal wall, the situation is like that of figure 6.12, because the capacitive coupling paths to the ground reference are significant along the entire cable's length. In contrast, in the case of the table's short side next to the metal wall, the situation is like that of figure 6.11, because the capacitive coupling paths at the ends of the DC output cable and the AC power input are predominant. Thus, in the latter case almost all CM current takes the "longest ground loop", making it an easy task to place the current clamp-on probe so that it can register nearly all the CM currents. To the contrary, in the former case a significant share of CM current has already shunted to the metal wall through capacitive coupling at the point where the

clamp-on current probe is located. On the other hand, the impedance of a ground loop dictates its CM current's magnitude with the given unbalance, and when the table's short side is next to the metal wall, the ground loops' combined impedance may be higher and thus the totality of CM currents' magnitudes lower than in the case of the table's long side placed next to the metal wall.

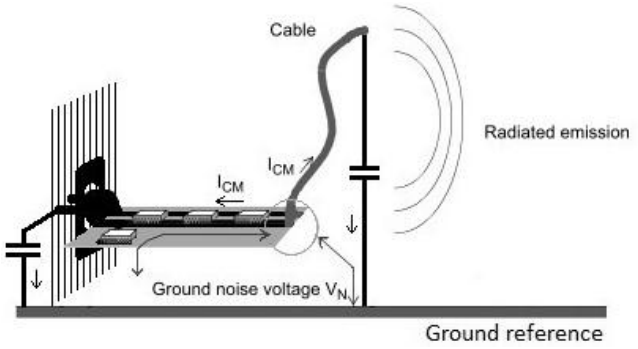

Figure 6.11. *A conventional presentation of CM current loops in a circuit with a cable, in this case a charger circuit [**21**].*

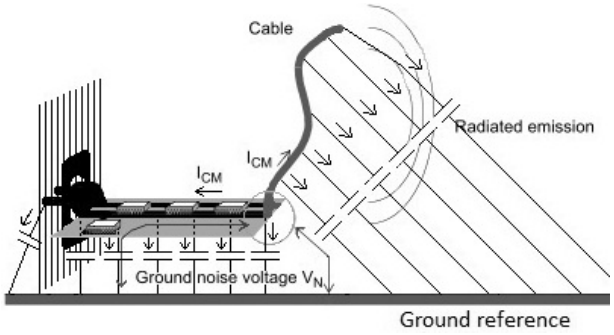

Figure 6.12. *A more realistic presentation of CM current loops in the circuit [**21**].*

6.3 Radiated Emissions Test

The performed radiated emissions test followed the directions of *EN 55022/CISPR 22*, but the frequency range was, against the standard, chosen to be only 30-100 MHz to speed up the measurements of the vast number of transformer samples. As was mentioned, the radiated emissions test also used the measurement box to enable the easy changing of the transformer samples while keeping the charger PCB and the rest of the set-up constant.

6.3.1 Measurement Set-Up

Figure 6.13 shows an illustration of the measurement set-up. The distance from the measurement box to the measurement antenna was 3 meters and the measurement was performed in an anechoic room.

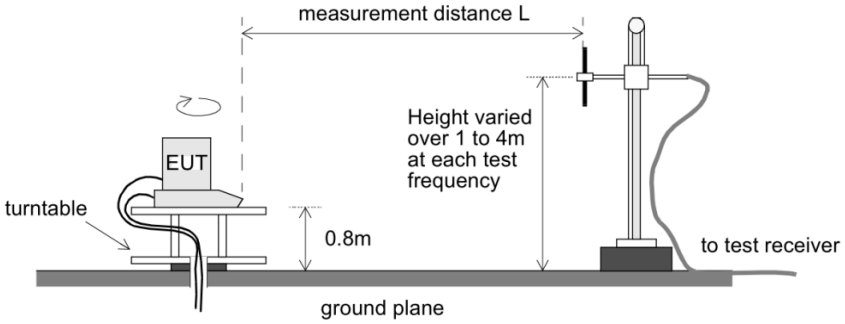

Figure 6.13. *An illustration of the radiated emissions test [**21**].*

6.4 Repeatability and Reproducibility Considerations

The measurement set-ups used for the transformer property or the near-field probe measurements were not analyzed using a *Measure System Analysis* (MSA), such as *Gauge Repeatability and Reproducibility* (Gauge R&R). The purpose of MSA is to verify the validity of the measurement data obtained from a measurement system. A measurement system consists of several components, such as operations, procedures, gauges, equipment, software, materials, facilities, and personnel. All these components contribute to the measurement system's *stability*, *bias*, and *variability*. Stability refers to the measurement system's ability to remain constant over time. Bias refers to the difference between a given measurement's average readout and the reference value that represents the "absolute" value for the property being measured. Variability refers to the variation in the readouts of a given measurement. [**43**]

Variability can be broken down into *process variability* and *measurement system variability*. The measure of measurement system variability is *precision*, which can be further broken down into *repeatability* and *reproducibility*. Repeatability is the variability of the gauge; it is the variability that occurs when the same person conducts the measurement with the same equipment, in the same facilities, and in the same conditions. Reproducibility is the variability that occurs when a different person (for example a third party) is trying to reproduce the measurements with similar equipment but different specimens, in different facilities, and under different conditions, but following precise instructions on how to reproduce them. [**43**]

As said, no quantitative analysis on the repeatability and reproducibility of the transformer property and the near-field probe measurements was performed. However, qualitative information regarding the repeatability of the measurements was gathered during the pretesting to fix the measurement set-ups for the final measurements.

With some samples the transformer property measurements gave exceptionally low or high readouts for certain properties compared with the average. When re-measured, the new readout was most of the time no more exceptional than with any other sample. This "correction" of the readout at the second measurement time was especially noticeable with the leakage inductance and the Q value measurements. The differences of the "corrected" values compared with the first measured value were in the range of 2-

24 %; with leakage inductances and Q values the differences ranged 7-24 %. The final data analysis was carried out using the re-measured values.

The repeatability of the near-field probe measurements was assessed by measuring four arbitrarily chosen transformer samples, each three times. After the first measurement with these four "repeatability assessment transformers", the second measurement was done, that is, after about 10-15 minutes. The third and the last measurement with these four transformers was done after measuring all the other transformer samples, that is, after about 3-4 hours, to check if the measurement set-up had remained constant during the measurements. The outcome of each repeatability assessment measurement was a spectrum image, same as in the actual measurements. If the spectrum images of the first two repeatability assessment measurements were significantly different, the measurement set-up was adjusted and the repeatability assessment then started over again to check if the repeatability had improved. Only after the repeatability was satisfactory, the actual measurement of all the transformer samples was followed through. The repeatability check spectrums are shown in appendix B for each near-field probe.

In the repeatability tests, it was noticed that the charge status of the charger's capacitors affected the measurement readouts of the near-field probe measurements. This is because the capacitance of a real capacitor is a function of its charge. The varying capacitances on the flyback, in turn, have an effect on the noise generated. This had to be taken into account in the measurements.

The charge status of the flyback's capacitors starts to change once the power of the measurement box is turned off or on. It had to be turned off, because changing the transformer would have otherwise been impossible without causing damage to the circuit. If the flyback had been powered off a long time so that its capacitors were fully discharged, after powering it on again it took about one minute for the capacitors to reach a charge status after which charging the capacitors further had no effect on the measurement readouts. If the flyback's capacitors were fully charged, it took about one minute after powering it off for the capacitors to reach a charge status after which discharging the capacitors further had no effect on the measurement readouts.

The effect of the capacitors' charge status was taken into account by ensuring that the capacitors were fully charged before each measurement. Before starting a measurement session, the measurement box was powered on for at least one minute. Changing the transformer was done routinely in 5-10 seconds, which thus was the time needed to have the measurement box powered off and to allow the capacitors to discharge. With a new transformer just mounted onto the measurement box, the box was powered on before a new measurement for about 30 seconds, which is approximately the time it took to save the measurement readouts of the previous transformer into a file. It was deemed that the 5-10 seconds' discharge of the capacitors is fully compensated by charging them for the 30 seconds before a new measurement. Therefore, this process was considered to ensure that the flyback's capacitors were always fully charged before any measurement.

7 DATA, PROCESSING AND ANALYSIS

In the data analysis, the aim was to find a correlation between 1) the measured far-field radiated emission levels and 2) the transformer property measurement readouts *or* the near-field probe measurements readouts. In other words, the radiated emission measurement data acted as the *response variable* and the transformer property and the near-field probe measurement data as the *predictor variables*.

7.1 How the Data were Filtered

Measurements were carried out on 98 transformers of supplier A and 45 transformers of supplier D, altogether 143 transformers. Each transformer was measured in a standard radiated emissions test set-up and, as a result, given a measurement readout at each frequency point between 30.0 MHz and 100 MHz at intervals of 0.1 MHz, meaning 701 individual measurement values. In fact, each transformer was given $2 \cdot 701$ individual measurement values because the standard radiated emissions test records one value for horizontally and one for vertically polarized radiation at each frequency point. Another 701 individual measurement values for each transformer were given by each of the four near-field probe measurements. In addition, 13 different transformer properties were measured from each transformer at two different points along their manufacturing process, as explained before. Therefore, the outcome was $143 \cdot (701 \cdot 2 + 701 \cdot 4 + 13 \cdot 2) = 605{,}176$ values of measurement data.

There were a number of different sets of response variable-predictor variable pairs that could be used in the analysis. Table 7.1 illustrates this variety of ways in which the measurement data could be structured and analyzed.

Firstly, the transformers included in the analysis could be all the 143 units from both suppliers, only the 98 units from supplier A or only the 45 units from supplier D.

Secondly, the response variable could be chosen to be only the horizontal or only the vertical polarization of radiated emissions, or a combination in which each frequency point was given the value of whichever polarization's readout was greater. Henceforward, we denote the vertical polarization with "blue" and the horizontal polarization with "green", as corresponding with the colors used in the EMI receiver equipment's measurement spectrums. Examples of the measurement spectrums can be seen in appendix C.

Table 7.1. *Different combinations of measurement data in the data analysis.*

A								**A & D**								**D**							
Blue			**Green**			**Blue & Green**		**Blue**			**Green**			**Blue & Green**		**Blue**			**Green**			**Blue & Green**	
4 NF Probes	13 T-former properties		4 NF Probes	13 T-former properties		4 NF Probes	13 T-former properties	4 NF Probes	13 T-former properties		4 NF Probes	13 T-former properties		4 NF Probes	13 T-former properties	4 NF Probes	13 T-former properties		4 NF Probes	13 T-former properties		4 NF Probes	13 T-former properties	
	1st	2nd		1st	2nd		1st		1st	2nd		1st	2nd		1st		1st	2nd		1st	2nd		1st	2nd

Thirdly, the predictor variable could be chosen to be the measurement readout of any of the four near-field probe measurements or that of any of the transformer property measurements. Moreover, the transformer property measurement readout could be one measured before the core was installed (“first measurement”) or one measured with a fully completed transformer (“second measurement”).

7.2 Data Analysis Methods

Simple data *pre-processing* and *data filtering* methods were used in an attempt to uncover underlying signs of correlation from the raw measurement data.

The motive for data pre-processing was a speculation that due to variation in the physical structure of the transformers the resonance frequency points may “drift”. For example, let us say that one transformer sample has a resonance caused by the primary winding at 70.1 MHz. The resonance caused by the primary winding in another transformer may be different, because the transformer manufacturing process has variation which causes the physical dimensions of primary winding to vary from transformer to transformer. Thus, the resonance peaks that can be seen in the radiated emissions spectrum of a given transformer cannot be assumed to appear at the same frequency points with other transformers. Instead, the resonance may have drifted either to a higher or a lower frequency point.

A data pre-processing algorithm was designed to take the drifting resonance frequencies into account. The algorithm goes through all the 701 frequency points from 30.0 MHz to 100.0 MHz and compares together the radiated emission readouts of a pre-defined number (“*n*”) of adjacent frequency points around each frequency point. Thus, *n* readouts above and below a given frequency point make up a comparison range, the greatest value of which the algorithm sets as the “radiated emission resonance value” for the given frequency point. Similarly, the corresponding near-field probe readouts at the frequency that had the greatest radiated emissions are set by the algorithm as the

"near-field probe resonance value" for the given frequency point. By picking the greatest values within the comparison range, the algorithm tries to identify resonance peaks, the locations of which vary along the frequency scale.

C1-T	C2	C3	C4	C5	C6	C7	C8	C9	C10	C11	C12	C13	C14	C15	C16
ID	Freq	Rad	Mag Lar	Mag Sma	Cur Lar	Cur Sma	Rad Reson	Mag Lar Reson	Mag Sma Reson	Cur Lar Reson	Cur Sma Reson	Rad 3 min	Count	11 avg	Rad Reson - 11 avg
A1	30.0	29.01	72.26	70.82	56.23	65.09	29.01	72.26	70.82	56.23	65.09	28.49	2	29.4717	-0.4617
A1	30.1	28.49	72.79	70.98	54.75	63.48	29.01	72.26	70.82	56.23	65.09	28.25	3	29.7486	-0.7386
A1	30.2	28.25	72.63	72.06	55.93	66.51	28.84	72.83	72.75	55.61	66.17	28.25	3	29.7450	-0.9050
A1	30.3	28.84	72.83	72.75	55.61	66.17	30.42	73.10	72.53	55.91	66.94	28.25	3	29.5722	0.8478
A1	30.4	30.42	73.10	72.53	55.91	66.94	31.82	73.40	71.96	56.54	67.62	28.84	3	29.5570	2.2630
A1	30.5	31.82	73.40	71.96	56.54	67.62	31.82	73.40	71.96	56.54	67.62	30.42	3	29.6618	2.1582
A1	30.6	31.41	73.42	72.26	56.09	64.36	31.82	73.40	71.96	56.54	67.62	29.72	3	29.8645	1.9555
A1	30.7	29.72	73.15	71.87	54.27	64.74	31.41	73.42	72.26	56.09	64.36	28.19	3	30.1355	1.2745
A1	30.8	28.19	73.39	70.59	56.81	66.93	29.72	73.15	71.87	54.27	64.74	28.19	3	30.4918	-0.7718
A1	30.9	29.42	72.83	70.27	54.80	64.59	30.71	72.79	68.94	52.89	62.49	28.19	3	30.6191	0.0909
A1	31.0	30.71	72.79	68.94	52.89	62.49	31.24	72.28	67.92	51.97	63.17	29.42	3	30.4118	0.8282
A1	31.1	31.24	72.28	67.92	51.97	63.17	31.47	72.10	68.46	52.67	64.48	30.71	3	30.0345	1.4355
A1	31.2	31.47	72.10	68.46	52.67	64.48	32.17	71.27	67.63	51.95	64.32	31.24	3	29.8382	2.3318
A1	31.3	32.17	71.27	67.63	51.95	64.32	32.17	71.27	67.63	51.95	64.32	30.24	3	29.7582	2.4118
A1	31.4	30.24	69.63	65.80	50.64	63.50	32.17	71.27	67.63	51.95	64.32	28.14	3	29.7373	2.4327
A1	31.5	28.14	70.50	65.86	53.90	63.11	30.24	69.63	65.80	50.64	63.50	27.67	3	29.5936	0.6464
A1	31.6	27.67	70.41	65.86	52.17	64.18	29.25	71.35	67.23	52.31	63.88	27.67	3	29.2745	-0.0245

Figure 7.1. *An illustration of the data pre-processing and the data filtering methods.*

Figure 7.1 illustrates the function of the data pre-processing algorithm. The shown data are radiated emission and near-field probe measurement data for a transformer sample labeled *A1*. The data are sorted by frequency points in an ascending order beginning from 30.0 MHz. The column "Rad" has the readout of the radiated emissions measurement, the column "Mag Lar" the readout of the large magnetic near-field probe measurement, the column "Mag Sma" the readout of the small magnetic near-field probe measurement, the column "Cur Lar" the readout of the large clamp-on current probe measurement, and the column "Cur Sma" the readout of the small clamp-on current probe measurement. The following five columns are the above-mentioned "radiated emissions resonance value", and the corresponding "near-field probe resonance value" of the large magnetic near-field, the small magnetic near-field, the large clamp-on current, and the small clamp-on current probe, respectively. If frequency point 31.0 MHz (framed in bold black) is the frequency point under scrutiny and *n* is one, the comparison range covers one adjacent frequency point above and below 31.0 MHz, that is, points 30.9 and 31.1 MHz. The comparison yields 31.1 MHz as the frequency with the greatest value of Rad, and therefore the algorithm sets the Rad, Mag Lar, Mag Sma, Cur Lar, and Cur Sma from 31.1 MHz (framed in blue) as the 31.0 MHz's resonance values (framed in red).

Two kinds of correlation analysis were used. One does not use the pre-processed data; it calculates the correlation between the values in Rad and the values in Mag Lar, Mag Sma, Cur Lar, or Cur Sma at each given frequency point. This one we shall call "exact frequency point analysis". The other kind of analysis makes use of the pre-processed data that attempted to identify resonance peaks. That analysis calculates the correlation between the values in "Rad Reson" and those in "Mag Lar Reson", "Mag Sma Reson", "Cur Lar Reson", and "Cur Sma Reson". This one we shall call "resonance frequency point analysis".

Data filtering was speculated to remove “noise” in the measurement data and thus reveal the underlying correlations more clearly. The basis for filtering was either a column named “Rad - 11 avg” or a column named “Rad Reson - 11 avg” (framed in green in figure 7.1), depending on whether the analysis was exact frequency point or resonance frequency point type. Let us call that column the “filter column”. In the filter column, a moving average of 11 frequency points (5 adjacent frequency points above and below the frequency point under scrutiny) was subtracted from either Rad or Rad Reson, again depending on the type of analysis. The data was then sorted by Rad - 11 avg or Rad Reson - 11 avg in descending order.

The data analysis was started first with all the data included: all chosen transformer samples’ data on all frequency points between 30.0-100.0 MHz. The filtering was done by removing data that had the smallest values in the filter column, removing 10,000 rows of data at a time. As the filtering screened rows out, only those frequency points remained in the analysis that had a large Rad value compared with their adjacent ten frequency points’ average Rad. The hoped effect of this was to screen out radiation measurement readouts which were dictated by radiation sources other than the currents that the near-field probes were measuring, and which therefore obscured the underlying linear correlation between the near-field probe and the radiation measurement readouts. Radiation measurement readouts were speculated to be dictated by unknown radiation sources when the given frequency point was not a resonance point, that is, when the radiation measurement readout at that point was not a peak compared with its adjacent frequency points.

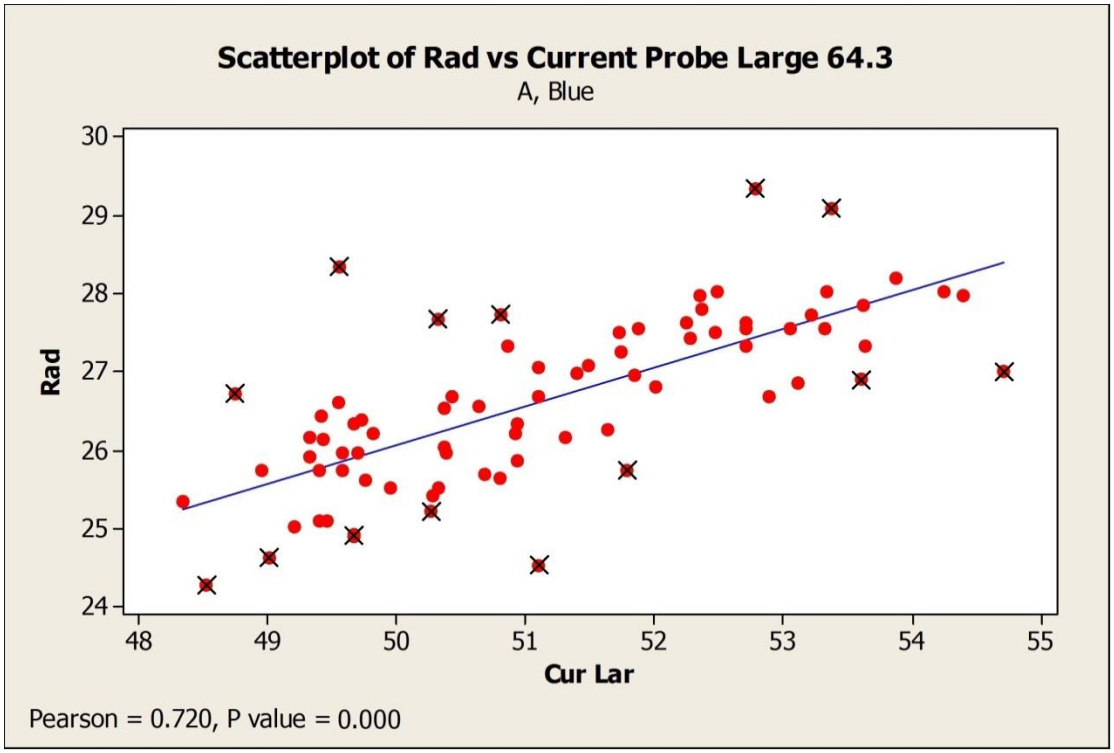

Figure 7.2. *A scatterplot showing each transformer sample’s radiation and large current probe measurement readouts at the 64.3 MHz frequency point. The crossed-out dots demonstrate the desired removal of stray data by the data filtering algorithm.*

There are two reasons why the data filtering approach was deemed appropriate:
1) There is no resonance at a given frequency point, and thus the radiation by currents that the near-field probe measures is so low that it may get swamped by the "noise floor" created by unknown sources of radiation. Therefore, the unknown sources may dictate the radiation readout at that frequency, in which case an underlying correlation between the radiation and the near-field probe measurement readout is obscured.
2) There is such a high noise floor created by unknown sources of radiation that it may exceed and swamp the radiation resonance peaks created by currents that the near-field probe measures. Again, there is no correlation between the two measurements' readouts.

Figure 7.2 shows the data points measured from supplier A's transformers at the frequency of 64.3 MHz situated in a coordinate system which has radiated emissions measurement readouts on the Y axis and large clamp-on current probe measurement readouts on the X axis. As an educated guess, the above point 1) is the reason why there are stray data points below the linear regression fit and point 2) the reason why there are stray data points above it. The crossed-out stray data points demonstrate the desired effect of filtering; the filtering algorithm is intended to screen out data points whose radiated emission readouts are dictated by some radiation sources other than what the near-field probe is measuring.

8 RESULTS

The results of the data analysis gave an insight of 1) the repeatability of the measurements, 2) the effects of applying pre-processing and filtering, and 3) the correlations between different response variable and predictor variable data sets with different combinations of data included.

8.1 Repeatability

From appendix B, it is clear that repeatability is better with the clamp-on current probes than with the magnetic near-field probes. Of the two magnetic near-field probes, the repeatability with the large one is better than that with the small one.

8.2 The Effects of Pre-Processing and Filtering

Appendix D shows *Pearson correlations* with radiated emissions at each frequency point for all four near-field probe measurements using all four pre-processing methods and with filtering at steps of 10,000 rows of filtered-out data.

From the figures in appendix D, no clear conclusion can be drawn as to whether pre-processing had the desired effect, that is, detection of resonances at adjacent frequencies, and thus whether it provided generally better Pearson correlations or not. No clear conclusion of the benefits of filtering can be drawn either, although at first sight it may appear as if filtering disclosed higher Pearson correlations in the data. However, it is no surprise that larger Pearson correlations are obtained as more and more data is filtered away, because a smaller amount of data has a greater tendency to exhibit false correlations, which are in actuality only results of a pure chance.

Because of the lack of clear indication of benefits, pre-processing and filtering were omitted from the analysis described in appendices F and G, which contain only results without pre-processing and filtering.

8.3 General Observations on Correlations

For the clamp-on current probes, the correlations in the “Pearson correlation spectrums” depicted in appendix F are positive over the most of the 30-100 MHz frequency range, but the spectrums’ upper ends, above approximately 70-80 MHz, exhibit mixed Pearson correlations. If a *P value* condition $P<0.005$ is included for the data displayed in the spectrums, misleading and outright false correlation values which are due to too few

data points included in the correlation computations are screened out. With the P value condition, the Pearson correlation spectrums for the clamp-on current probes showed slightly negative or mixed correlations at above 90 MHz and strongly positive ones everywhere else. Another observation for the clamp-on current probes from the Pearson correlation spectrums is that horizontal (green) orientation of the radiation as the response variable data set or the supplier D's transformers as the predictor variable data set give somewhat weaker and less consistent correlations in overall compared with other data sets.

From the Pearson correlation spectrums of appendices D and F, it is interesting to notice that the magnetic near-field probes have distinct "frequency sub-ranges" which exhibit consistent negative, consistent positive, or mixed correlation. The number, the locations, the range, and the nature of these sub-ranges vary somewhat depending on the data sets that are included, and whether the P condition is in place. With the magnetic near-field probes, the horizontal orientation of the radiation as the response variable data set or the supplier D's transformers as the predictor variable data set give a lot weaker and less consistent correlations compared with other data sets.

A factor that hinders the correlations with the horizontal-oriented radiation is the format of the results from the standard radiated emissions test. The EMI receiver equipment recorded, by default, an image of the measured spectrum and numerical values only at its highest peaks, as one can see in appendix C. These spectrum images had to be digitized into numerical values by using a plot digitizing software. When comparing the digitized values of the spectrum's highest peaks with the values recorded automatically by the equipment, the digitizing was assessed to be so precise that its inaccuracy would only cause an occasional rounding error. However, a greater detriment of the digitizing stemmed from the fact that in the spectrum image the blue spectrum was overlaid on top of the green spectrum, and thus the digitizer was unable to capture the values of every frequency point for the green spectrum, possibly explaining the poorer correlation spectrums for horizontal-oriented radiation.

8.4 Strong Correlation

The clamp-on current probes' readouts have a strong correlation with the radiated emissions in the 30-70 MHz range. At some frequency points the correlation is stronger than at others, but it is difficult to point out any individual frequency points and generalize that the correlation is strong at that frequency, because the correlations vary depending on the data sets used as the response and the predictor variables. However, some "generally linearly behaving" frequencies with the analyzed response-predictor variable pairs could be pinpointed, as appendix H shows.

Of the transformer properties, the ones showing the strongest correlation with the radiated emissions are leakage 2, leakage 3, leakage 5, and Q value, especially in the second measurement stage, as can be seen from appendix G. Note that every "count" in the graphs refers to one frequency point that exhibits the Pearson correlation value

denoted by the X axis under the count. Here it can also clearly be seen that the *P<0.005* condition makes genuine correlations easier to be detected by removing misleading, non-existing correlations from the graphs. Interestingly, leakage 2 has a strong correlation with the radiated emissions already at the first measurement stage, while Q value's correlation is efficiently non-existent. Other properties than leakage 2 do not exhibit a correlation that could be considered strong in the first measurement.

8.5 Weak Correlation

The clear-cut division of the frequency scale into sub-ranges of negative and positive correlations implies that a connection between the magnetic near-field probes' readouts and the radiated emissions test readouts was discovered in this research, although the Pearson correlations are not very large. If there was no correlation between the two, the positive and the negative correlations would not be clustered into distinct frequency sub-ranges, but instead be scattered haphazardly in the entire 30-100 MHz range. However, the discovered correlation is not very strong at even the best selected frequency points when using the most favorable filters, as appendix H shows, and thus the reliability of any single magnetic near-field probe measurement in predicting radiated emissions is rather questionable.

The primary inductance seemed to consistently have a negative correlation with the radiated emissions in the second measurement stage, but no correlation whatsoever in the first one, whereas the primary-secondary inductance and the primary self-capacitance seemed to consistently exhibit a negative correlation with the radiated emissions in the first measurement stage. However, in the second measurement the primary-secondary inductance had a weaker correlation than in the first one, and the primary self-capacitance had changed its correlation from negative to positive. Despite the rather absurd behavior, I am confident that a weak correlation does exist between these two and the radiated emissions.

8.6 No Correlation

As said, all the near-field probe measurement readouts were deemed to correlate with the radiated emissions at least to some extent. Thus, the only measurements that were found to have absolutely no correlation with the radiated emissions were those of transformer properties: the capacitance between W4 and W6, EMC box, leakage 1, leakage 4, and the primary-secondary capacitance, as well as the transformer and the varnish weights. The biggest surprise was that the primary-secondary capacitance was found to have no correlation with the radiated emissions, contrary to the theoretical speculations presented. It shall remain a mystery whether this was due to something being done wrong during the measurements or the data handling and analysis, or if the theory for some reason was not directly applicable to this particular case and setting.

9 CONCLUSIONS

The motive for making this research was to find a quick and inexpensive method to detect a flyback charger's sub-standard transformers in terms of radiated emissions. Based on the results, near-field probe measurements and measurements of some of the transformer's electrical properties are feasible methods for detecting such sub-standard transformers.

The research discovered statistically significant correlations between 1) the charger's radiated emission levels and its near-field probe measurement readouts and 2) between the charger's radiated emission levels and its transformer property measurement readouts. The radiated emissions test and the near-field probe measurements were conducted so that the transformer was changed between each instance of the given measurement, keeping the rest of the charger unchanged to eliminate all variables unrelated to the transformer. This way, the effect of only the transformer on the radiated emissions and on the near field could be captured. The transformer properties were measured directly from the transformer, while it was not attached to the charger circuit. Of the four near-field probe measurements, two were conducted with magnetic near-field and two with clamp-on current probes. The transformer property measurements covered the measurement of a selection of electrical and physical properties of the transformer.

However, this paper is unable to give explicit answers as to how to use the output of these measurements to screen out sub-standard transformers. It is only clear that, based on the results, there is no single measurement to which a simple rule, for example a fixed tolerance limit, could be applied for reliable screening of the transformers. This becomes evident from the graphs in appendix H: the inaccuracy of the measurements is high, causing much variance even at selected, best-correlating frequency points. And if using only selected, well-correlating frequency points for screening out transformers, the radiated emission limits might as well be exceeded at the remaining, poorly-correlating frequency points.

Several factors hampered the accuracy of the measurements and thus, for example, increased the deviation from the linear fit in the graphs of appendix H. With magnetic near-field probes, even slight changes in the position of the probe around the transformer affected the readout. Moreover, when changing the transformer, the magnetic near-field probes had to unavoidably be removed and then placed back to the same position – with a limited accuracy. The effect of these inaccuracies can be seen in

the repeatability tests' results in appendix B. In contrast, with clamp-on current probes the location and the position of the probe had a very minimal effect on the measurement readouts, and the probes did not need to be touched when changing the transformer. Thus, the clamp-on current probe measurements had a better repeatability, and their readouts had higher Pearson correlations with the radiated emissions than those of the magnetic near-field probes.

A more complex rule for screening purposes that combines several of the measurements at all the well-correlating frequencies could be studied and developed. In other words, one could pick only those frequency points that reliably, that is, with various transformer sample sets, exhibit a strong correlation in a near-field probe or a transformer property measurement and compose a set of rules for rejection based on tolerance limits. Such a follow-up research could focus on repeating the measurements that this research found to be the most potential ones for radiated emission prediction with improved measurement accuracy. One must note that a repetition of the measurement process and the data analysis must be done every time this method is intended to be applied on a new DUT to determine the well-correlating frequency points and suitable tolerance limits.

In any case, the development of a production line-ready solution for screening out sub-standard transformers would be likely to face a number of new challenges. One justified questions is whether a transformer that the measurements identify as sub-standard would invariably be sub-standard also if mounted on a different specimen of the fly back charger than the one used in the measurements. After all, EMC is a system-wise matter, not a sum of its parts, so the charger's circuit certainly also has an effect on the behavior of the transformer in terms of emissions.

REFERENCES

[1] Henry W Ott, *Electromagnetic Compatibility Engineering*, 1st ed. New Jersey, USA: Wiley, 2009.

[2] Keith Armstrong, "The EMC Design of SMP (Switch-Mode Power Supplies) and PWM (Pulse Width Modulated) Power Converters," *EMC Journal*, no. 93, pp. 26-33, March 2011.

[3] Mart Coenen and Jasper J Goedbloed, *Electromagnetic Compatibility*, 1st ed., Michiel den Dulk, Ed. Netherlands: MYbusinessmedia BV, 2010.

[4] Clayton R Paul, "A Comparison of the Contributions of Common-Mode and Differential-Mode Currents in Radiated Emissions," *IEEE Transactions on Electromagnetic Compatibility*, vol. 31, no. 2, pp. 189-193, May 1989.

[5] A Orlandi and R Scheich, "EMC in Power Electronic Devices: Radiated Emissions from a Silicon Controlled Rectifier," in *Electromagnetic Compatibility, 1994. Symposium Record. Compatibility in the Loop., IEEE International Symposium on Electromagnetic Compatibility*, Chicago, 1994, pp. 303-307.

[6] Mohammad R Yazdani, Hosein Farzanehfard, and Javad Faiz, "Conducted EMI Modeling and Reduction in a Flyback Switched Mode Power Supply," , 2011, pp. 620-624.

[7] Xiao-jie Zang and Xiang-peng Liu, "Study of Conducted EMI Prediction in Switch Mode Power Supplies," *Electric Drive*, vol. 41, no. 6, pp. 27-30, 2011.

[8] Peipei Meng, Junming Zhang, Henglin Chen, Zhaoming Qian, and Yuwen Shen, "Characterizing Noise Source and Coupling Path in Flyback Converter for Common-mode Noise Prediction," in *Applied Power Electronics Conference and Exposition (APEC), 2011 Twenty-Sixth Annual IEEE*, Fort Worth, 2011, pp. 1704-1709.

[9] D Lee, J Lee, S Min, B Cho, and B Lee, "Exact Simulation of Conducted EMI in Switched Mode Power Supplies," in *34th Intersociety Energy Conversion Engineering Conference Proceedings*, Vancouver, 1998.

[10] Babak Abdi, Mohammad H Joukar, and Amir H Ranjbar, "Effect of Leakage Inductance on High Frequency Transformer Harmonics," in *Compatibility and Power Electronics CPE2009 6th International Conference-Workshop*, 2009, pp. 359-362.

[11] Vladimir Kraz, "Near-Field Methods of Locating EMI sources," *Compliance Engineering Magazine*, May/June 1995.

[12] David Mawdsley, "Why not use near field probes to measure my emissions," *The EMC Journal*, no. 86, pp. 27-29, 2010.

[13] Keith Armstrong, "The Physical Basis of EMC," *The EMC Journal*, no. 85, pp. 26-34, November 2009.

[14] Piet Van der Laan, *Electromagnetic Fields in Electrical Engineering– Understanding Basic Concepts*, 2010th ed. Eindhoven, The Netherlands: Shaker Publishing, 2005.

[15] Keith Armstrong, "The Physical Basis of EMC," *The EMC Journal*, no. 86, pp. 30-42, January 2010.

[16] Ron Schmitt, *Electromagnetics Explained*. Amsterdam: Newnes, 2002.

[17] Mark I Montrose, *Printed Circuit Board Design Techniques for EMC Compliance*.

New York: Wiley, 2000.

[18] FCC. (2011, October) GPO – U.S. Government Printing Office. [Online]. http://www.gpo.gov/fdsys/pkg/CFR-2011-title47-vol1/pdf/CFR-2011-title47-vol1-sec2-801.pdf

[19] FCC. (2012, October) GPO – U.S. Government Printing Office. [Online]. http://www.gpo.gov/fdsys/pkg/CFR-2012-title47-vol1/pdf/CFR-2012-title47-vol1-sec15-3.pdf

[20] Clayton R Paul, *Introduction to Electromagnetic Compatibility*, 2nd ed. New Jersey, USA: Wiley, 2006.

[21] Tim Williams, *EMC for Product Designers*, 4th ed. Oxford, UK: Elsevier, 2007.

[22] Elya B Joffe and Kai-Sang Lock, *Grounds for Grounding*. New Jersey: Wiley, 2010.

[23] Jeff Barrow, "Reducing Ground Bounce in DC-to-DC Converters – Some Grounding Essentials," *Analog Dialogue*, 2007.

[24] Keith Armstrong, "Design Techniques for EMC part 2 – Cables and Connectors (second half of part 2)," *the EMC Journal*, no. 64, May 2006.

[25] David J Griffiths, *Introduction to Electrodynamics*. New Jersey: Prentice Hall, 1999.

[26] Tarateeraseth V, Maneenopphon T, and Khan-ngern W, "The Comparison of EMI and Electrical Performances of High Frequency Transformer Windings for SMPS Applications," in *Power Conversion Conference – PCC '07 –* , Nagoya, 2007, pp. 435-440.

[27] Ned Mohan, Tore M Undeland, and William P Robbins, *Power Electronics – Converters, Applications, and Design*, 3rd ed. New Jersey: Wiley, 2003.

[28] Teuvo Suntio, Lecture Notes, "Diodes for Power Electronic Applications", 2010, Tampere University of Technology – Power Electronics Components (Course).

[29] Teuvo Suntio, Lecture Notes, "Part 2: MOSFET", 2004, Tampere University of Technology – Power Electronics Components (Course).

[30] Bob Mammano and Bruce Carsten, "Understanding and Optimizing Electromagnetic Compatibility in Switchmode Power Supplies," Texas Instruments, Dallas, Technical report 2003.

[31] Mark I Montrose and Edward M Nakauchi, *Testing for EMC Compliance – Approaches and Techniques*. Piscataway, USA: Wiley, 2004.

[32] Michel Mardiguian, *Controlling Radiated Emissions by Design*. Boston: Kluwer Academic Publishers, 2001.

[33] Pavel V Nikitin et al., "Power Reflection Coefficient Analysis for Complex Impedances in RFID Tag Design," *IEEE Transactions for Microwave Theory and Techniques*, vol. 53, no. 9, pp. 2721-2725, September 2005.

[34] Wjh31. (2013, June) Wikipedia. [Online]. http://en.wikipedia.org/wiki/File:Standingwaves.svg

[35] ZooFari. (2013, June) Wikipedia. [Online]. http://en.wikipedia.org/wiki/File:Standing_wave.svg

[36] Jani Ingman, *The influence of transformer in flyback converter's EMI properties*. Tampere: Tampere University of Technology, Master's thesis 2007.

[37] Tanathep Maneenopphon, Vuttipon Tarateeraseth, and Werachet Khan-ngern, "The

Comparison of Conducted Electromagnetic Interference Effect on High Frequency Transformer Winding Techniques," in *Power Conversion Conference PCC '07*, Nagoya, 2007, pp. 435 - 440.

[38] Power Integrations, "TOPSwitch Power Supply Design Techniques for EMI and Safety (AN-15)," Application Note 2005.

[39] Maxim Integrated Products. (2002, August) Application Note 716 – Proper Layout and Component Selection Controls EMI. [Online]. www.maxim-ic.com/an716

[40] Krishna Mainali and Ramesh Oruganti, "Conducted EMI Mitigation Techniques for Switch-Mode Power Converters: A Survey," *IEEE Transactions on Power Electronics*, vol. 25, no. 9, pp. 2344-2356, September 2010.

[41] P Chen, H Zhong, Z Qian, and Z Lu, "The Passive EMI Cancellation Effects of Y Capacitor and CM Model of Transformers Used in Switching Mode Power Supplies (SMPS)," in *35th Annual IEEE Power Electronics Specialists Conference*, 2004, pp. 1076-1079.

[42] S Cristina, Antonini F, and Orlandi A, "Switched Mode Power Supplies EMC Analysis: Near Field Modeling and Experimental Validation," in *Electromagnetic Compatibility, 1995. Symposium Record., 1995 IEEE International Symposium on Electromagnetic Compatibility*, Atlanta, 1995, pp. 453-458.

[43] Thomas McCarty, Michael Bremer, Lorraine Daniels, and Praveen Gupta, *The Six Sigma Black Belt Handbook*.: McGraw-Hill, 2004.

APPENDIX A – Transformers' Structural Variance in X-Ray Photos

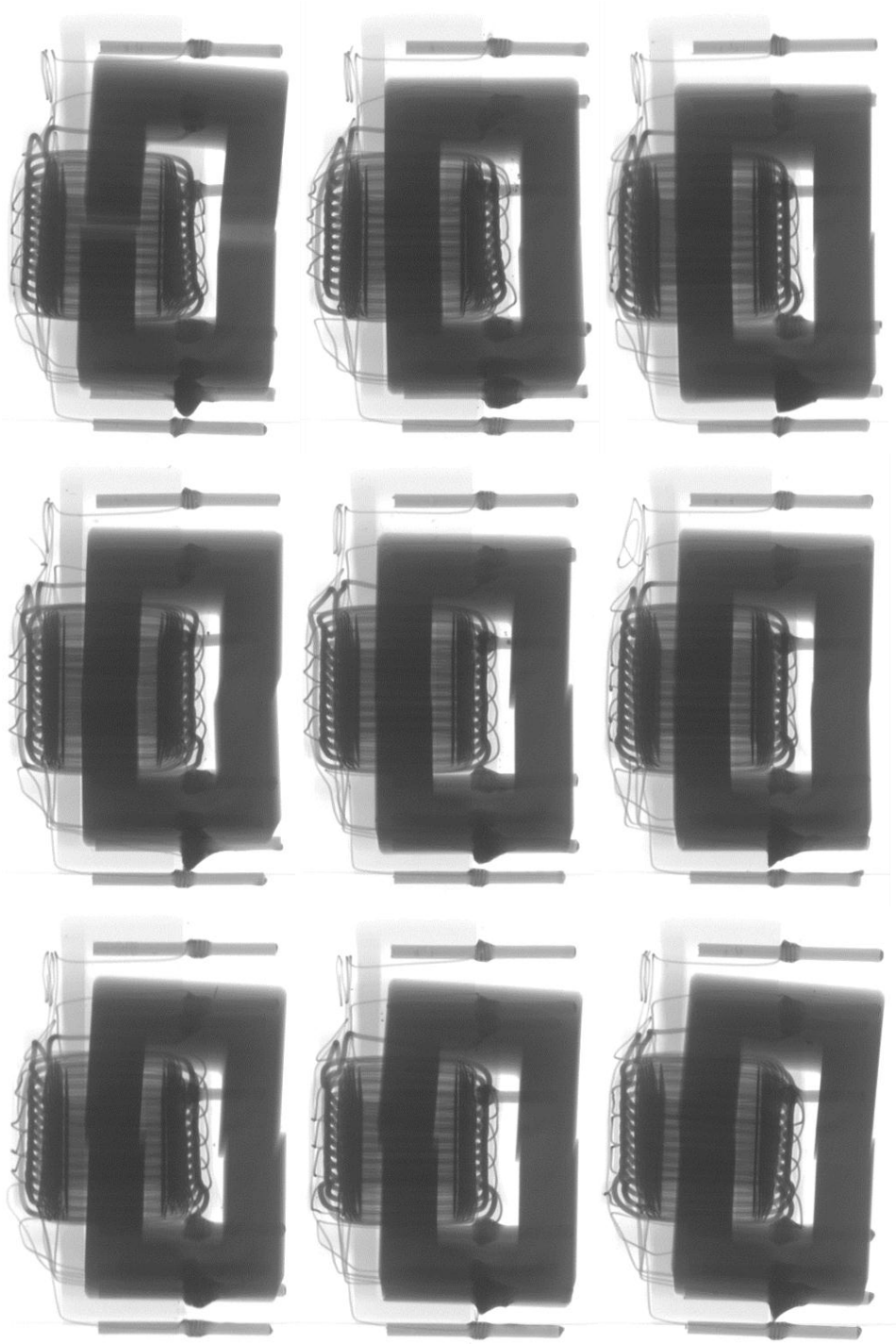

Figure A.1. *The X-ray photos of nine of the transformer samples shows the structural variance between different individuals.*

APPENDIX B – Repeatability with Near-Field Probes

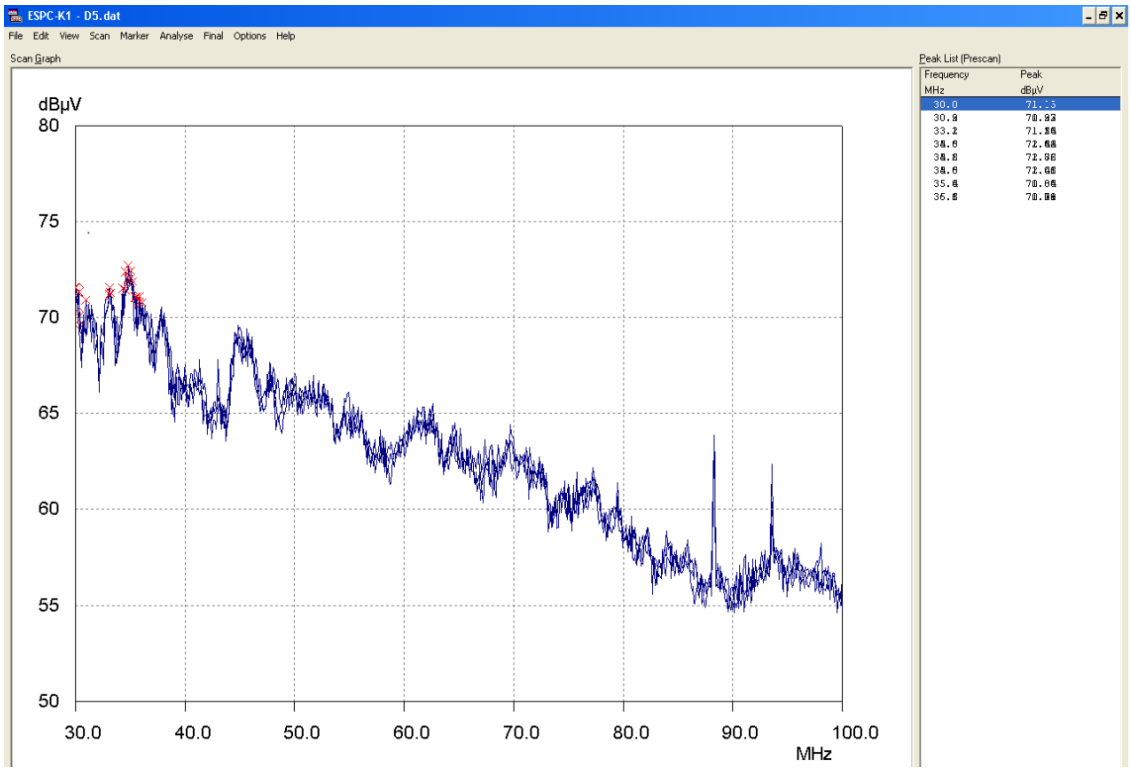

Figure B.2. *The overlaid spectrums of three repeatability tests done to transformer D5 using the large magnetic field probe.*

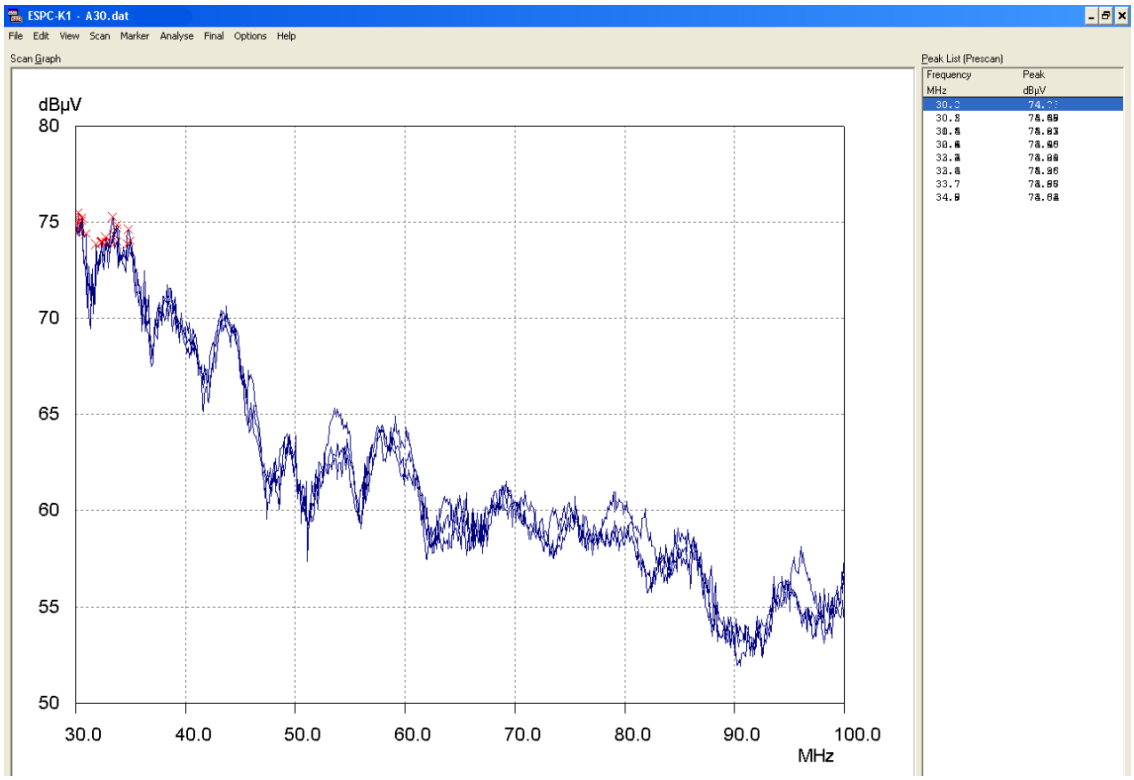

Figure B.2. *The overlaid spectrums of three repeatability tests done to transformer A30 using the small magnetic field probe.*

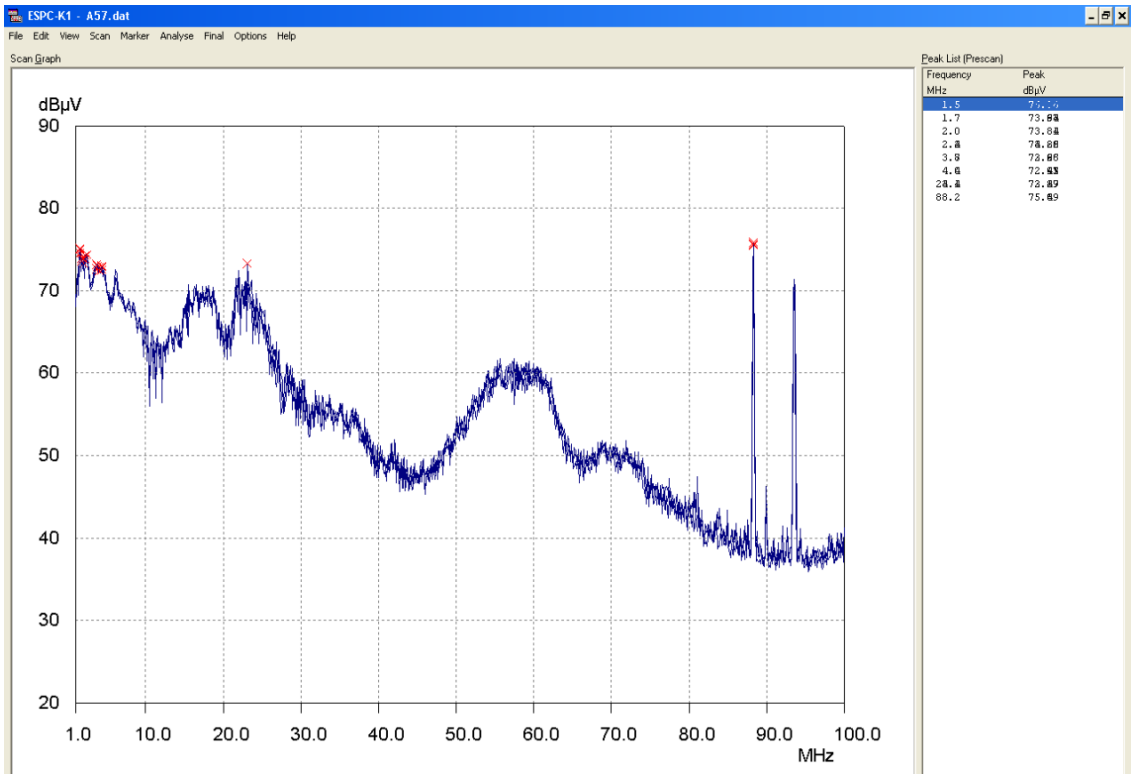

Figure B.3. *The overlaid spectrums of three repeatability tests done to transformer A57 using the large current probe.*

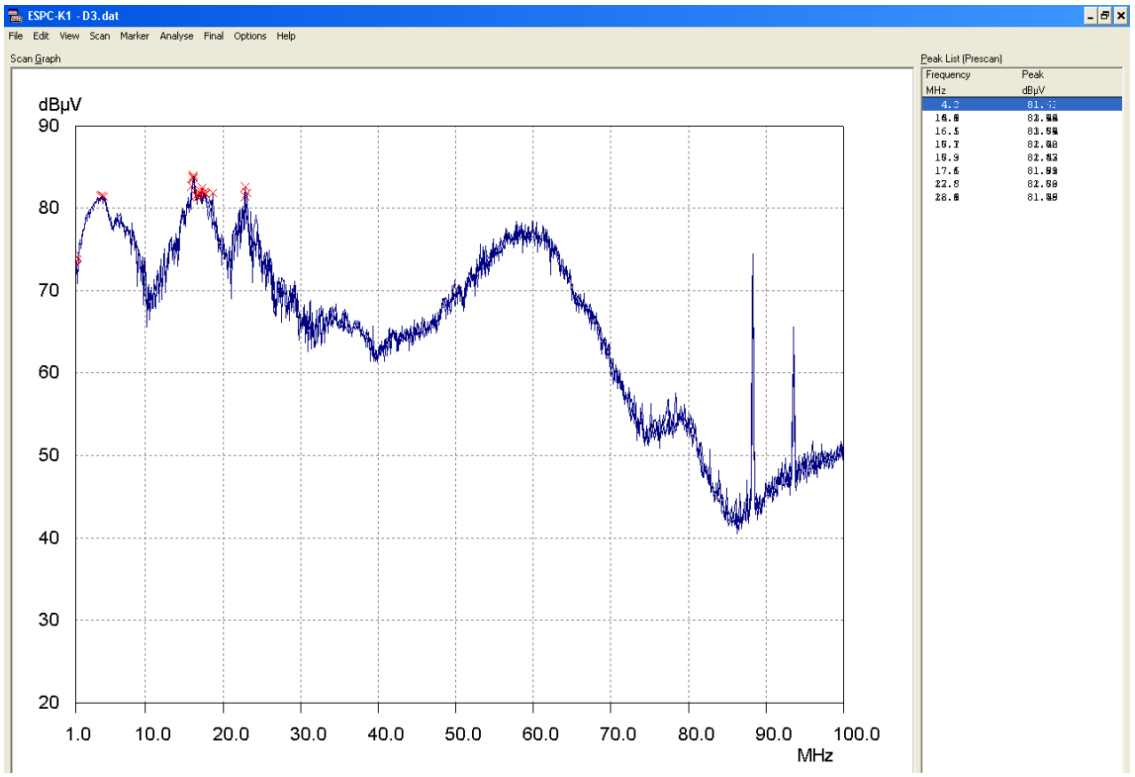

Figure B.4. *The overlaid spectrums of three repeatability tests done to transformer D3 using the small current probe.*

APPENDIX C – Standard Radiated Emissions Test Spectrum

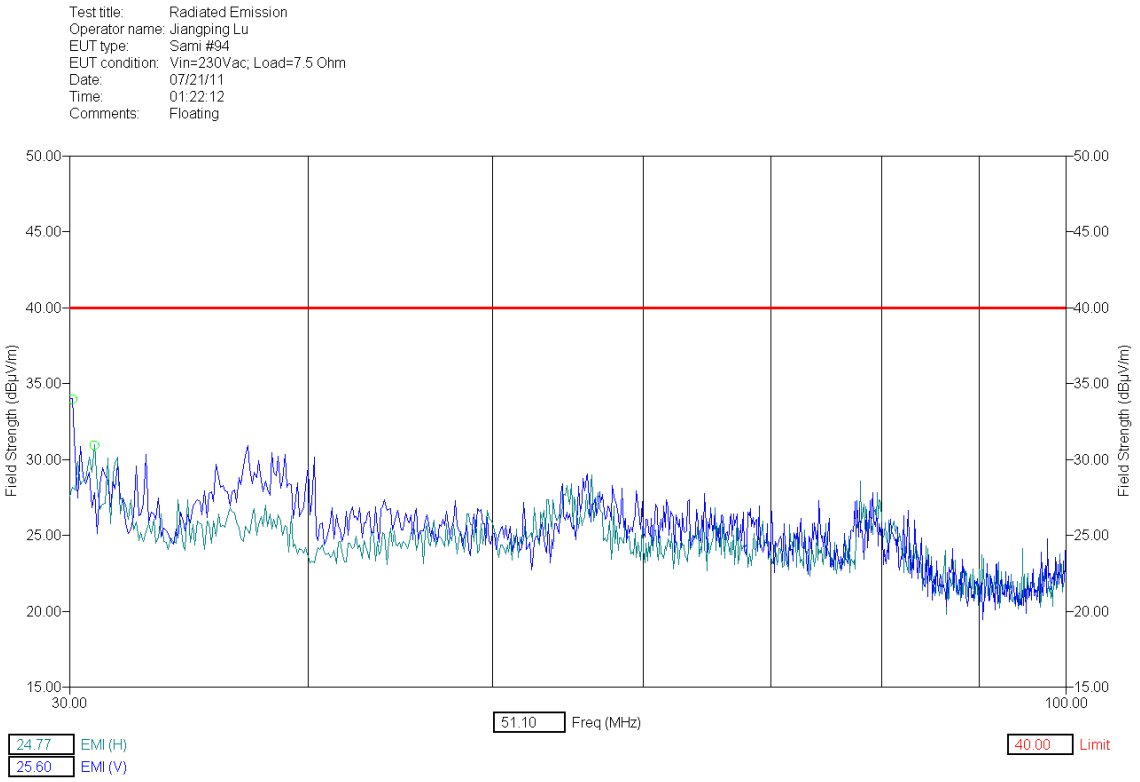

Figure C.1. *The standard radiated emissions test result spectrum for transformer A94.*

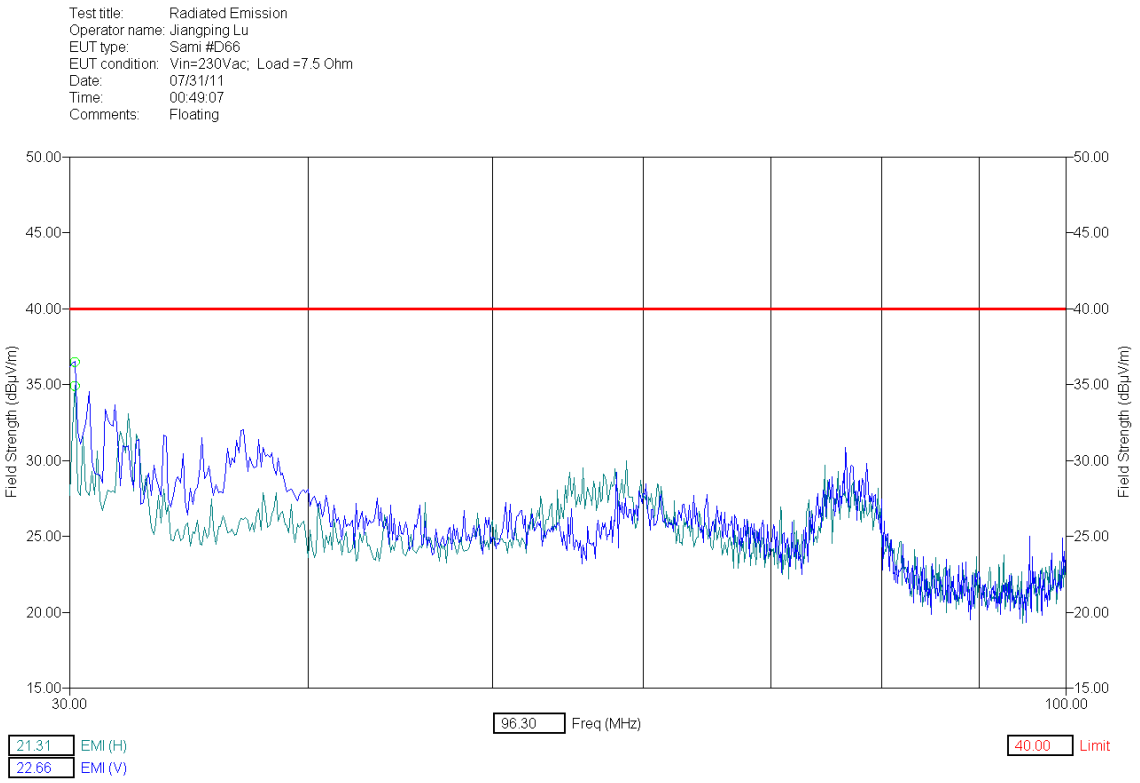

Figure C.2. *The standard radiated emissions test result spectrum for transformer D66.*

APPENDIX D – Pre-Processed and Filtered Data

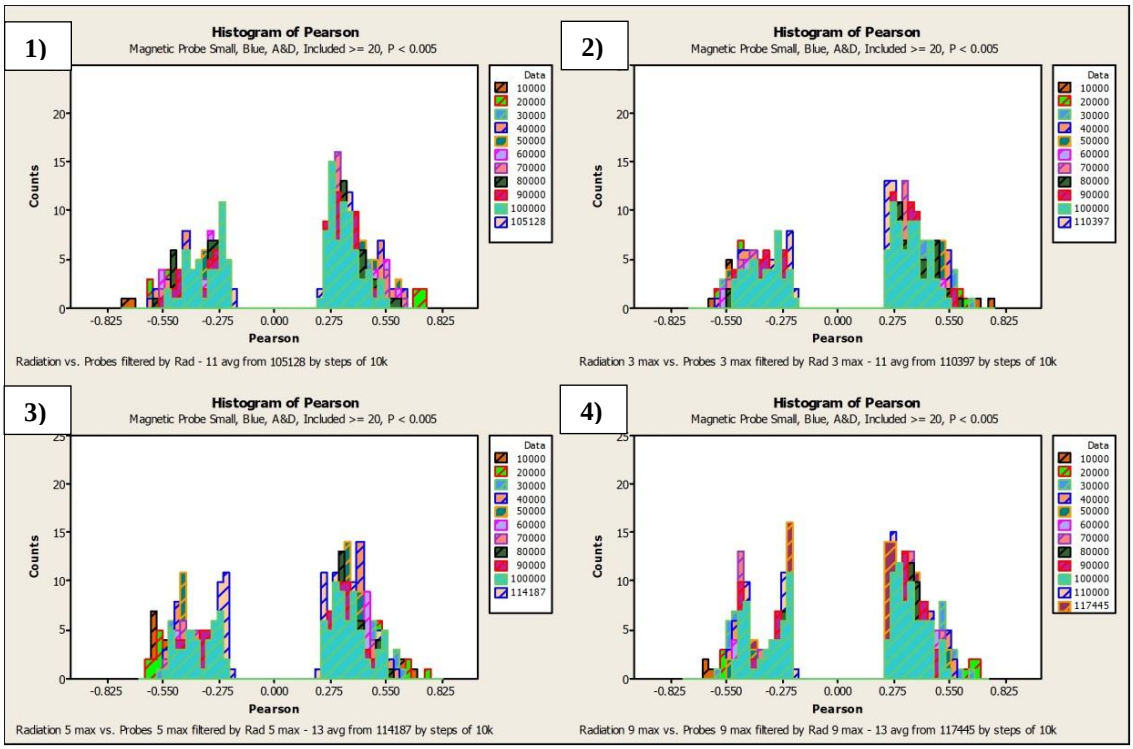

Figure D.1. *Pearson correlations between radiated emissions and small magnetic near-field probe readouts with 1) no, 2) 3 max resonance, 3) 5 max resonance, and 4) 9 max resonance detection pre-processing method, and with data filtering.*

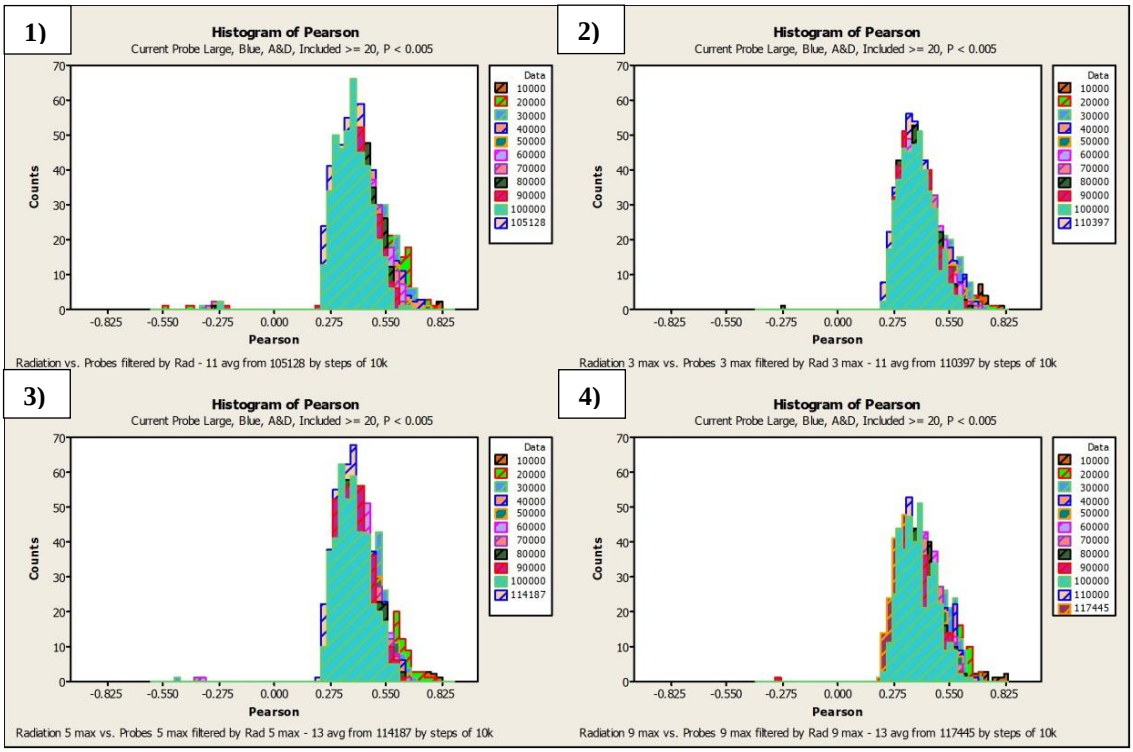

Figure D.2. *Pearson correlations between radiated emissions and large current clamp-on probe readouts with 1) no, 2) 3 max resonance, 3) 5 max resonance, and 4) 9 max resonance detection pre-processing method, and data filtering.*

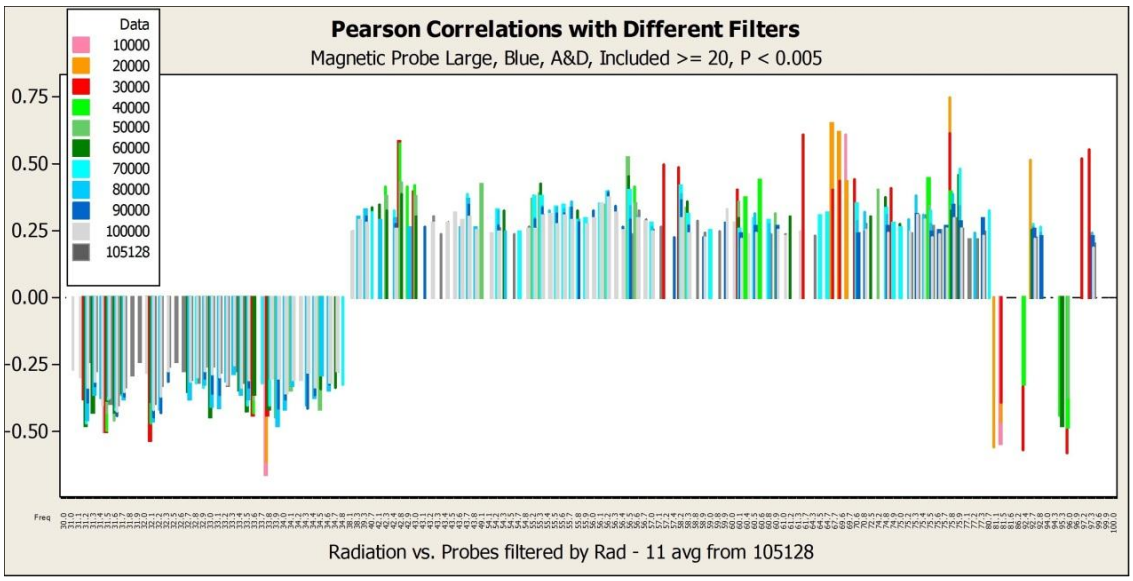

Figure D.3. *Pearson correlations between radiated emissions and large magnetic near-field probe readouts with no pre-processing method, and with filtering data at steps of 10,000 values.*

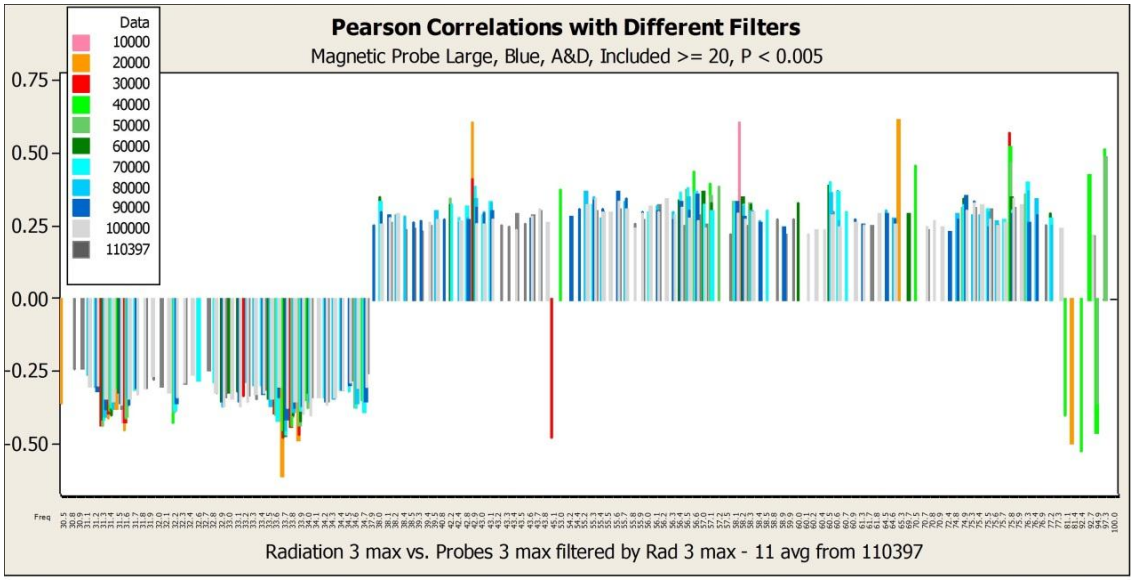

Figure D.4. *Pearson correlations between radiated emissions and large magnetic near-field probe readouts with 3 max resonance detection pre-processing method, and with filtering data at steps of 10,000 values.*

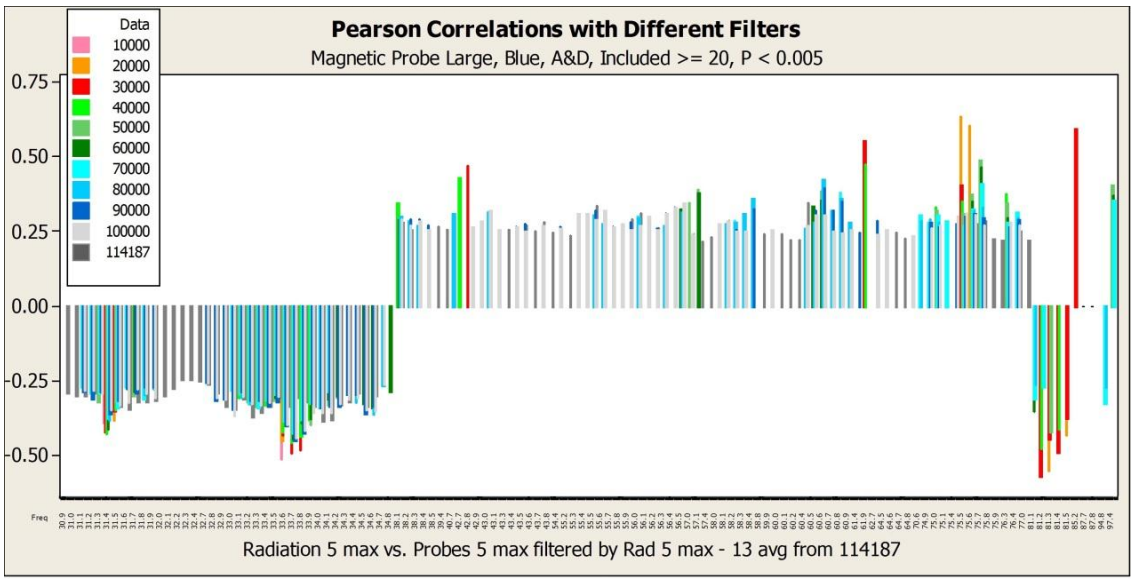

Figure D.5. *Pearson correlations between radiated emissions and large magnetic near-field probe readouts with 5 max resonance detection pre-processing method, and with filtering data at steps of 10,000 values.*

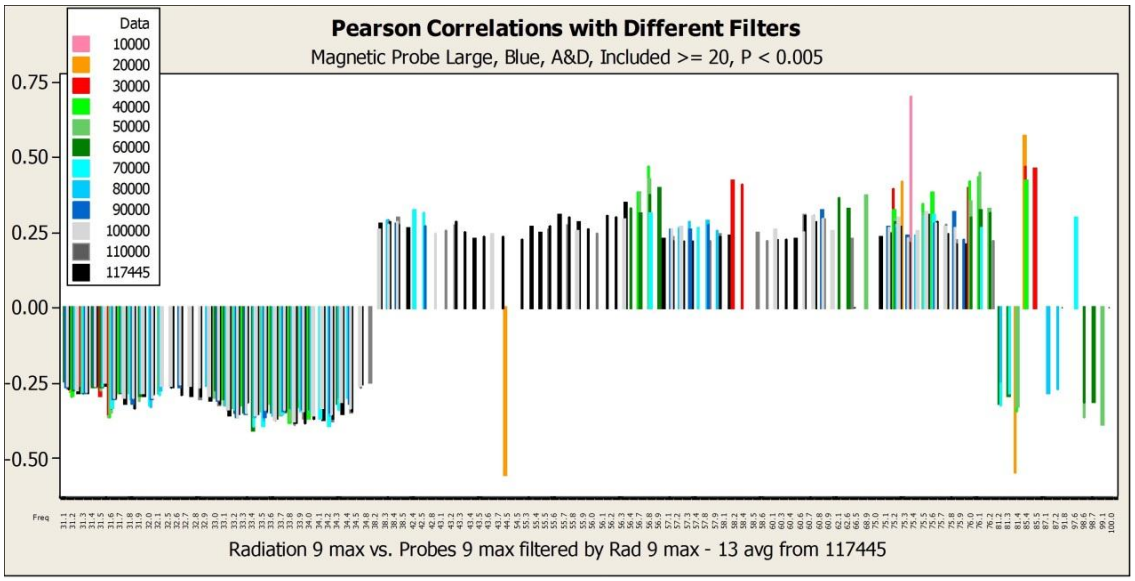

Figure D.6. *Pearson correlations between radiated emissions and large magnetic near-field probe readouts with 9 max resonance detection pre-processing method, and with filtering data at steps of 10,000 values.*

APPENDIX E – Differences between Vertical (Blue) and the Combination of Vertical and Horizontal (Blue&Green) Radiated Emissions

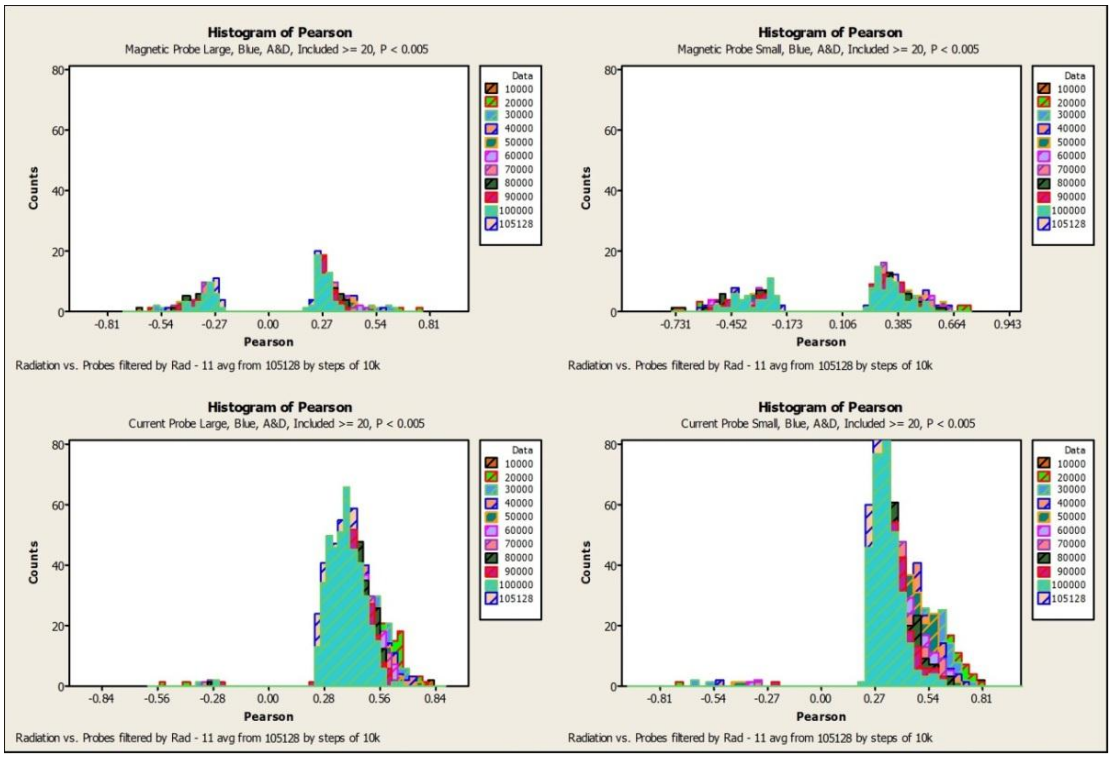

Figure E.1. *Pearson correlations of vertical (blue) radiated emissions and all four near-field probes' readouts.*

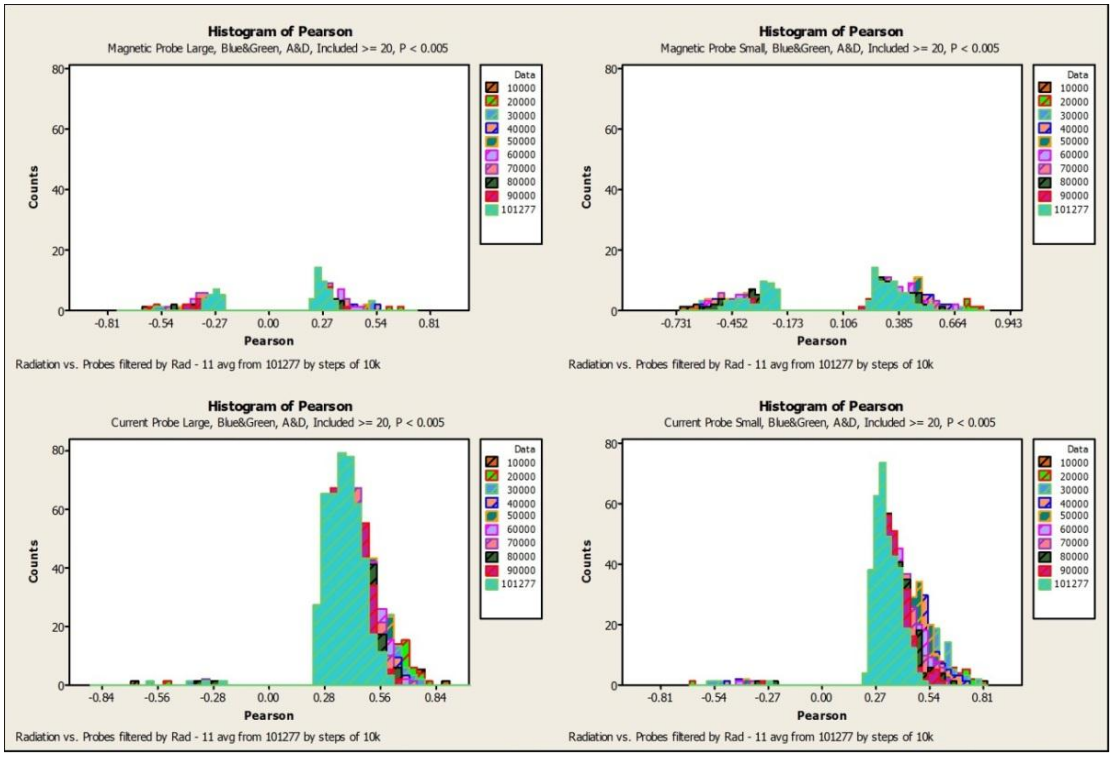

Figure E.2. *Pearson correlations of the combination of vertical and horizontal (blue&green) radiated emissions and all four near-field probes' readouts.*

APPENDIX F – "Pearson Correlation Spectrums" without Filtering or Pre-Processing

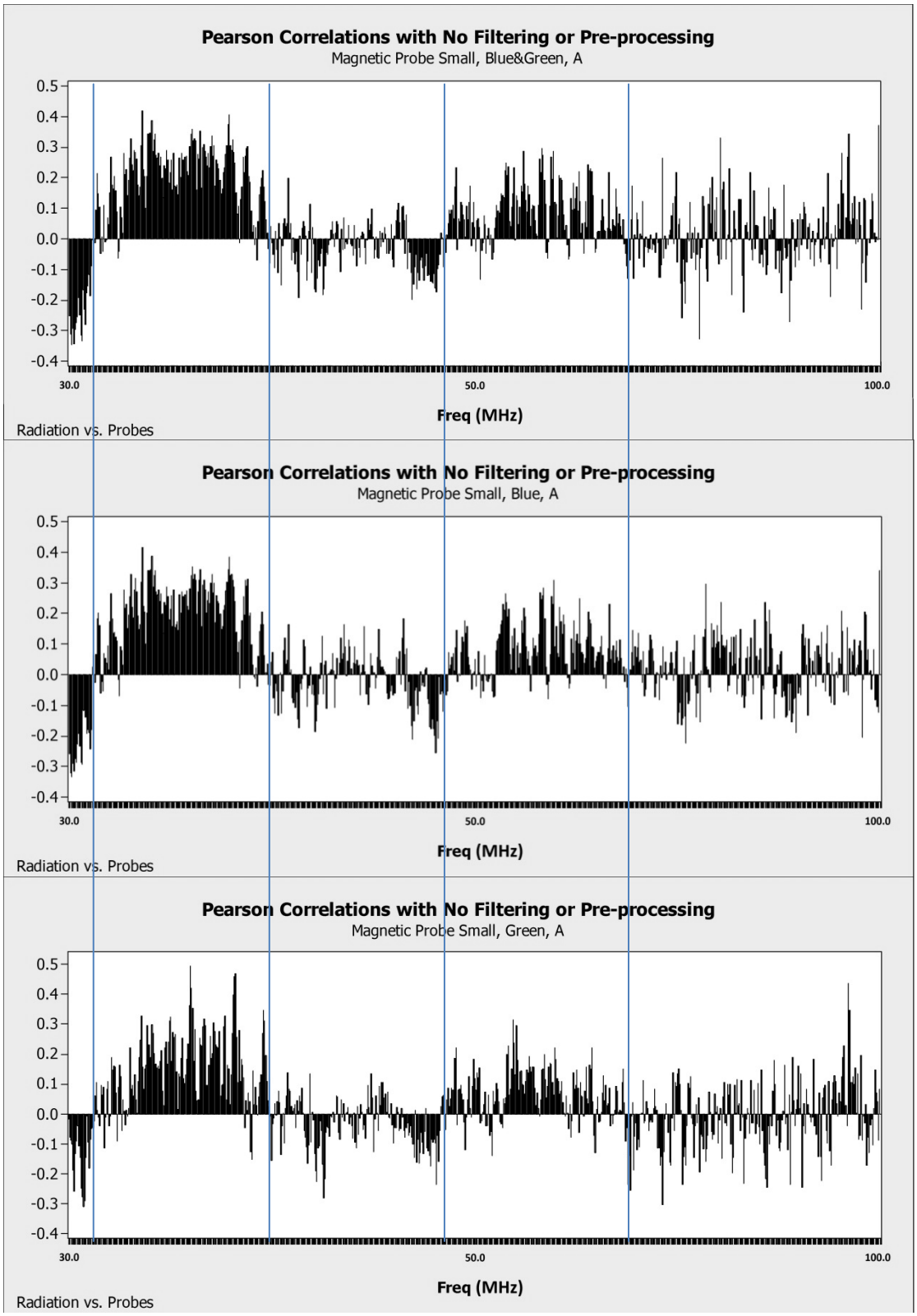

Figure F.1. *Pearson correlations of radiated emissions and small magnetic near-field probe's readouts with only supplier A's transformers.*

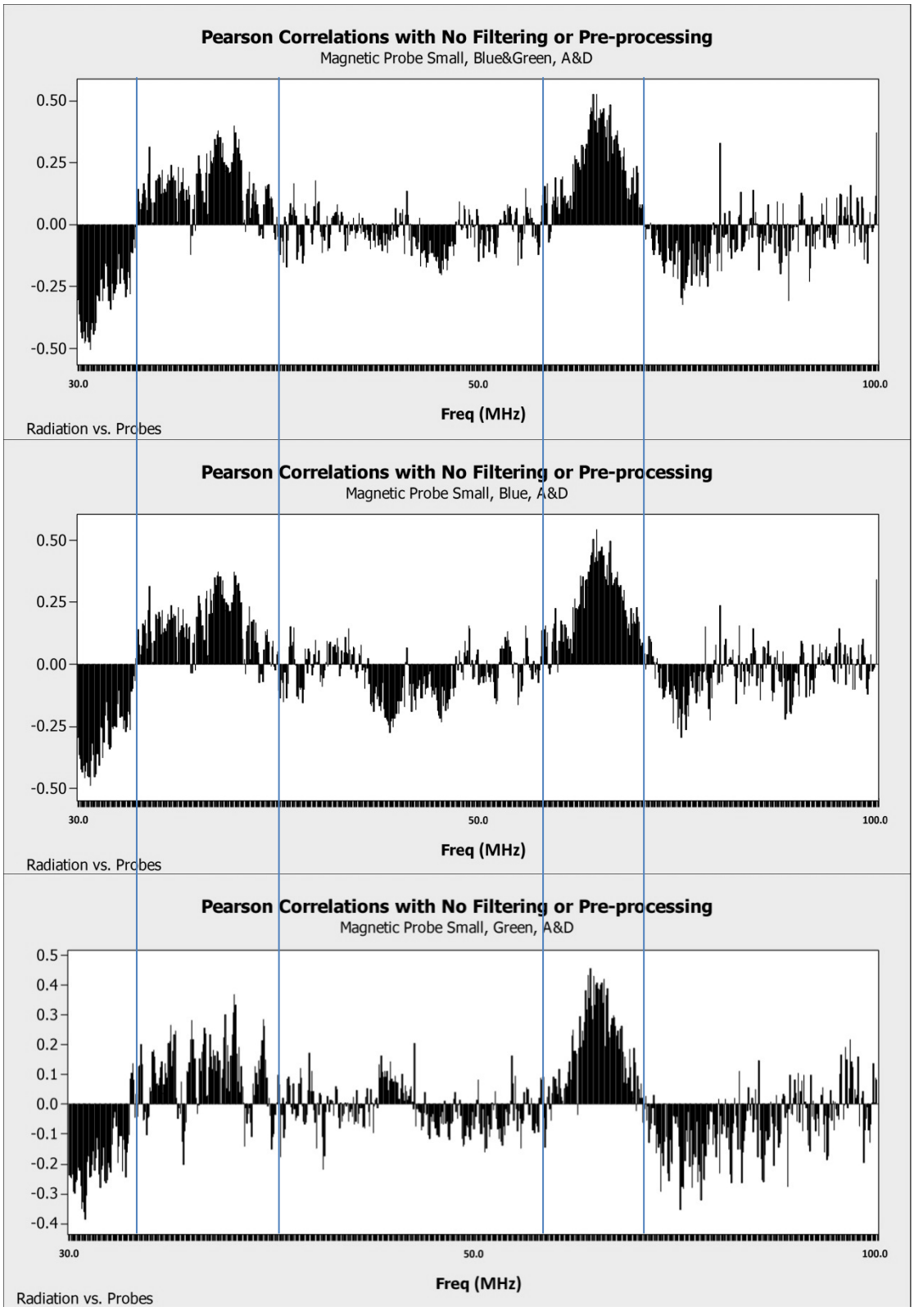

Figure F.2. *Pearson correlations of radiated emissions and small magnetic near-field probe's readouts with both supplier A's and supplier D's transformers.*

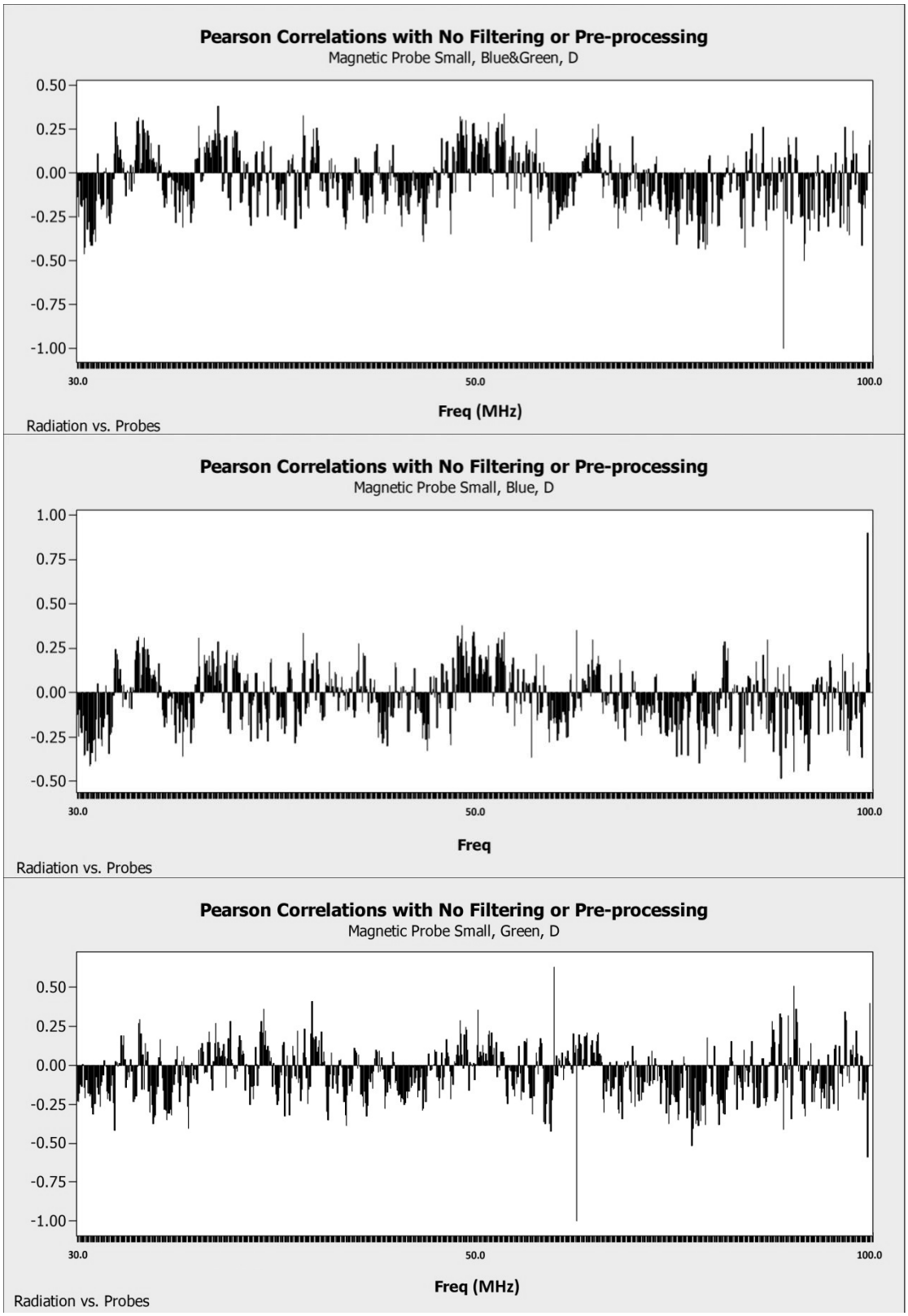

Figure F.3. *Pearson correlations of radiated emissions and small magnetic near-field probe's readouts with only supplier D's transformers.*

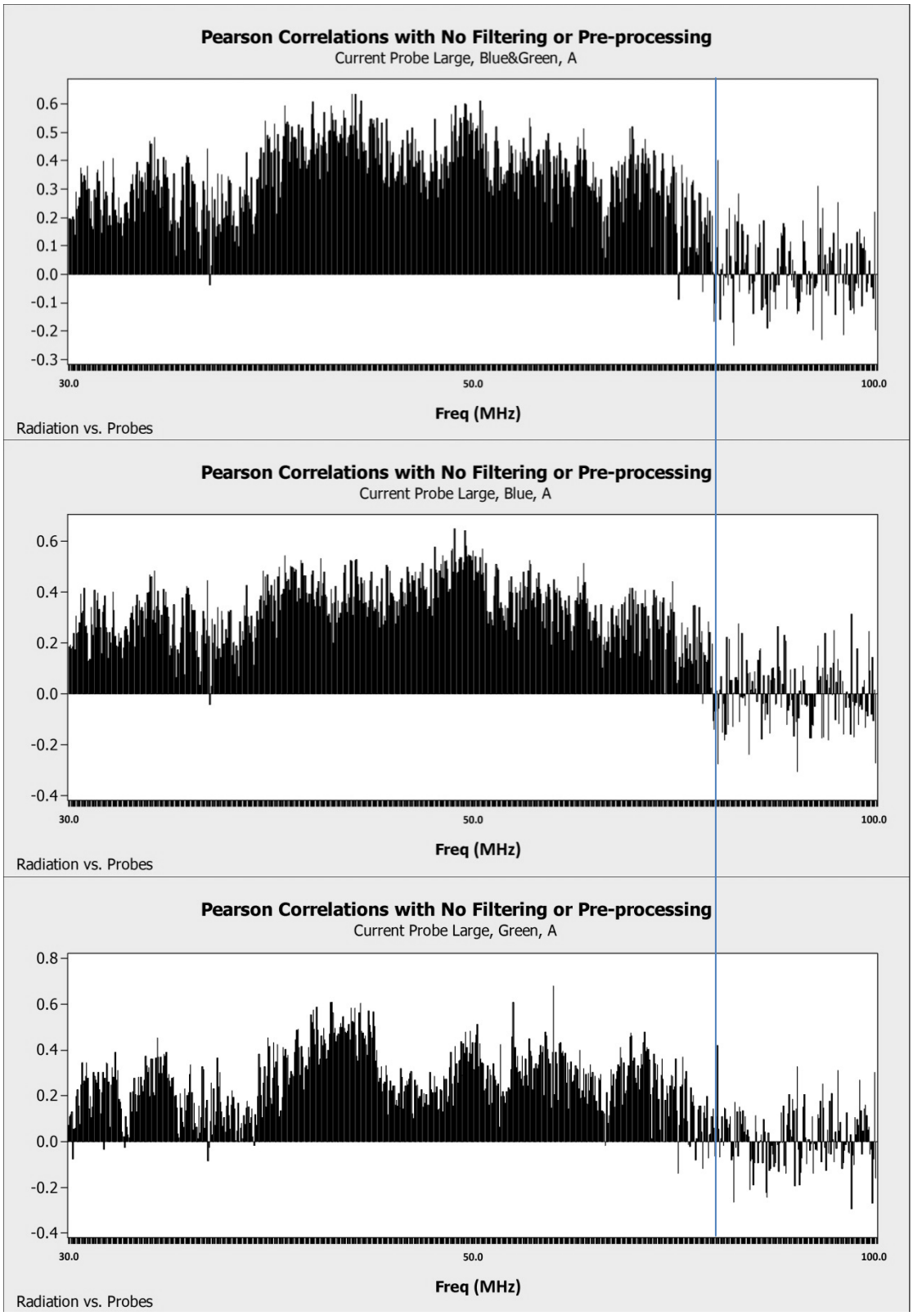

Figure F.4. *Pearson correlations of radiated emissions and large clamp-on current probe's readouts with only supplier A's transformers.*

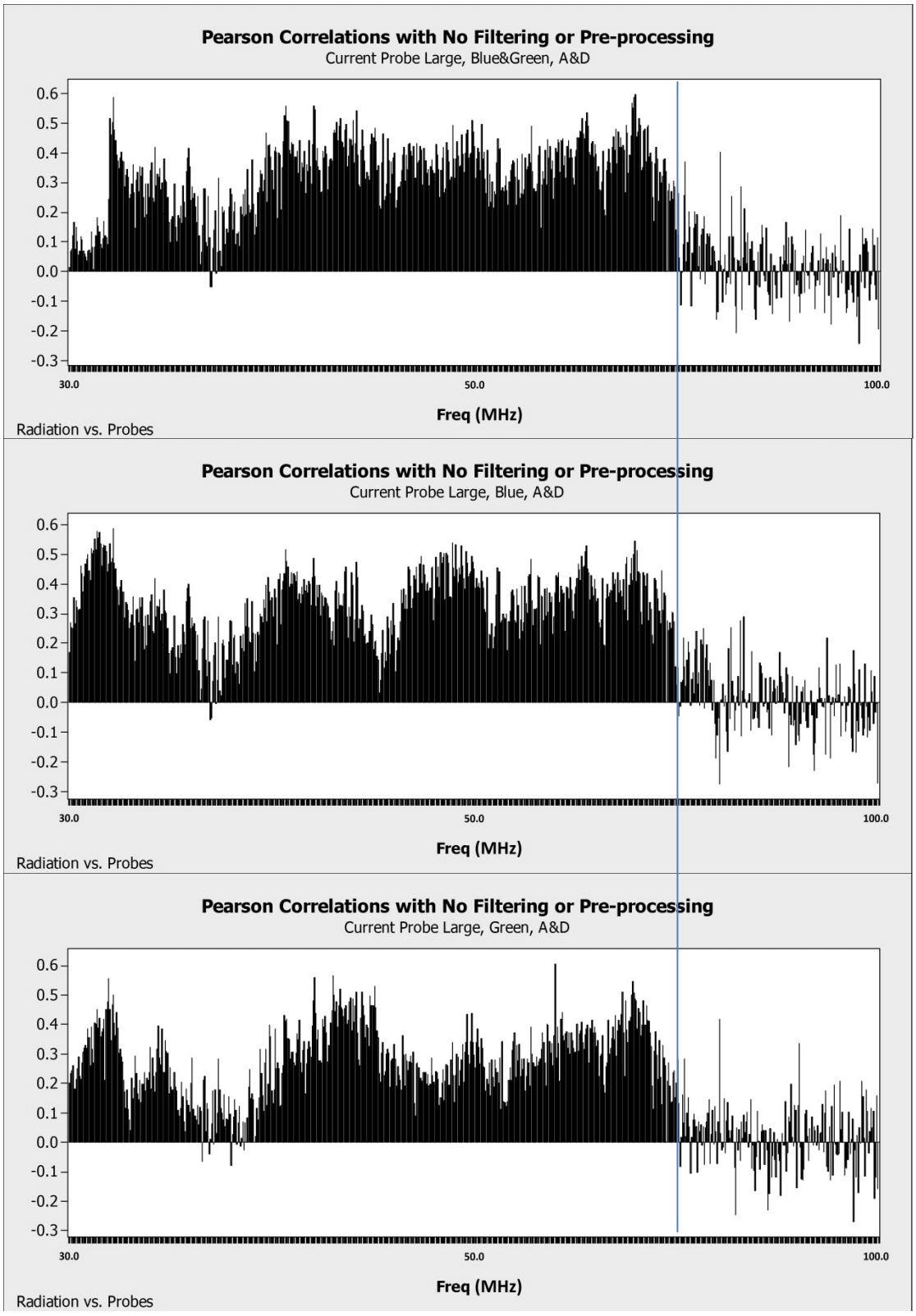

Figure F.5. *Pearson correlations of radiated emissions and large clamp-on current probe's readouts with both supplier A's and supplier D's transformers.*

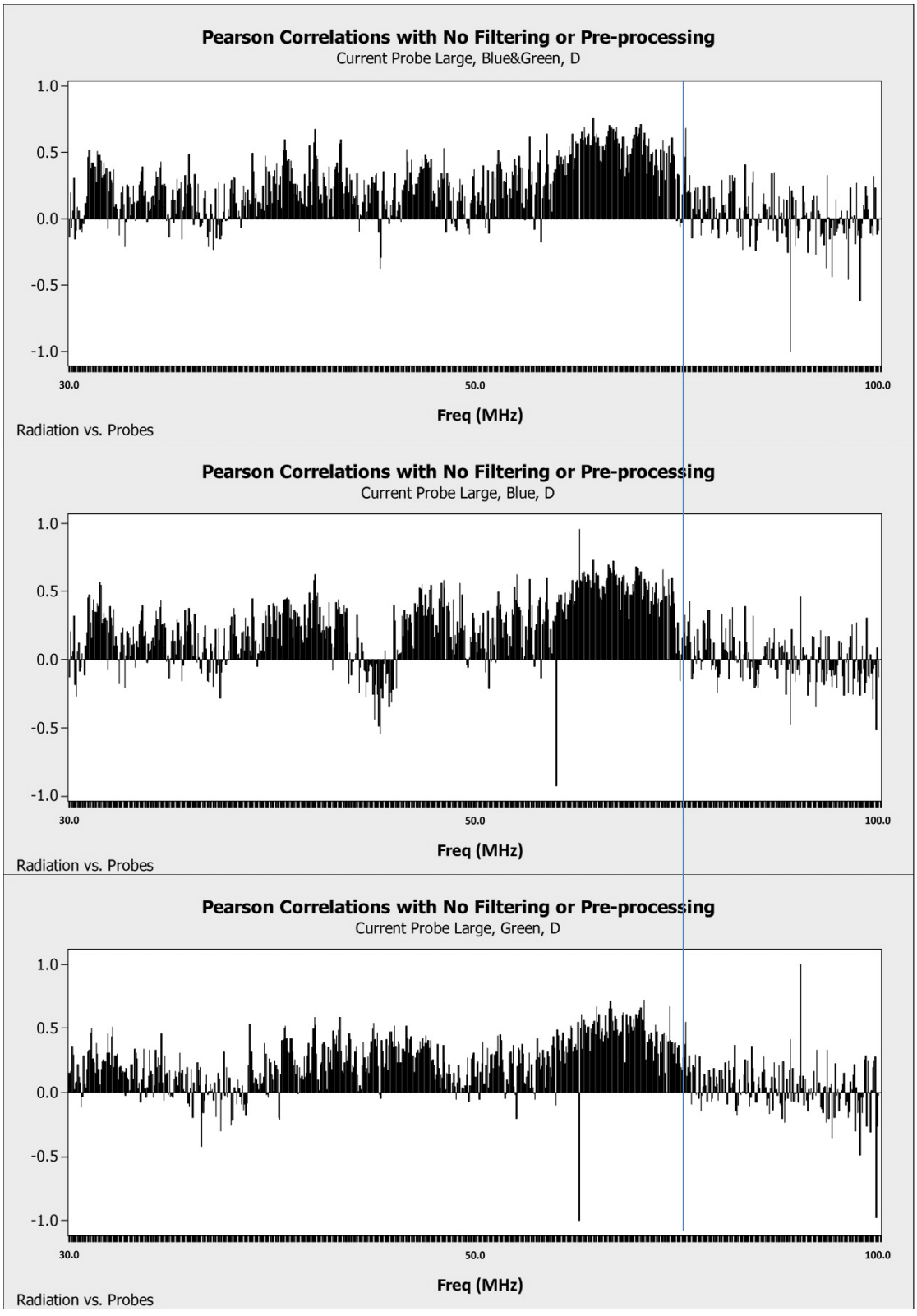

Figure F.6. *Pearson correlations of radiated emissions and large clamp-on current probe's readouts with only supplier D's transformers.*

APPENDIX G – Pearson Correlations between Radiated Emissions and Transformer Properties

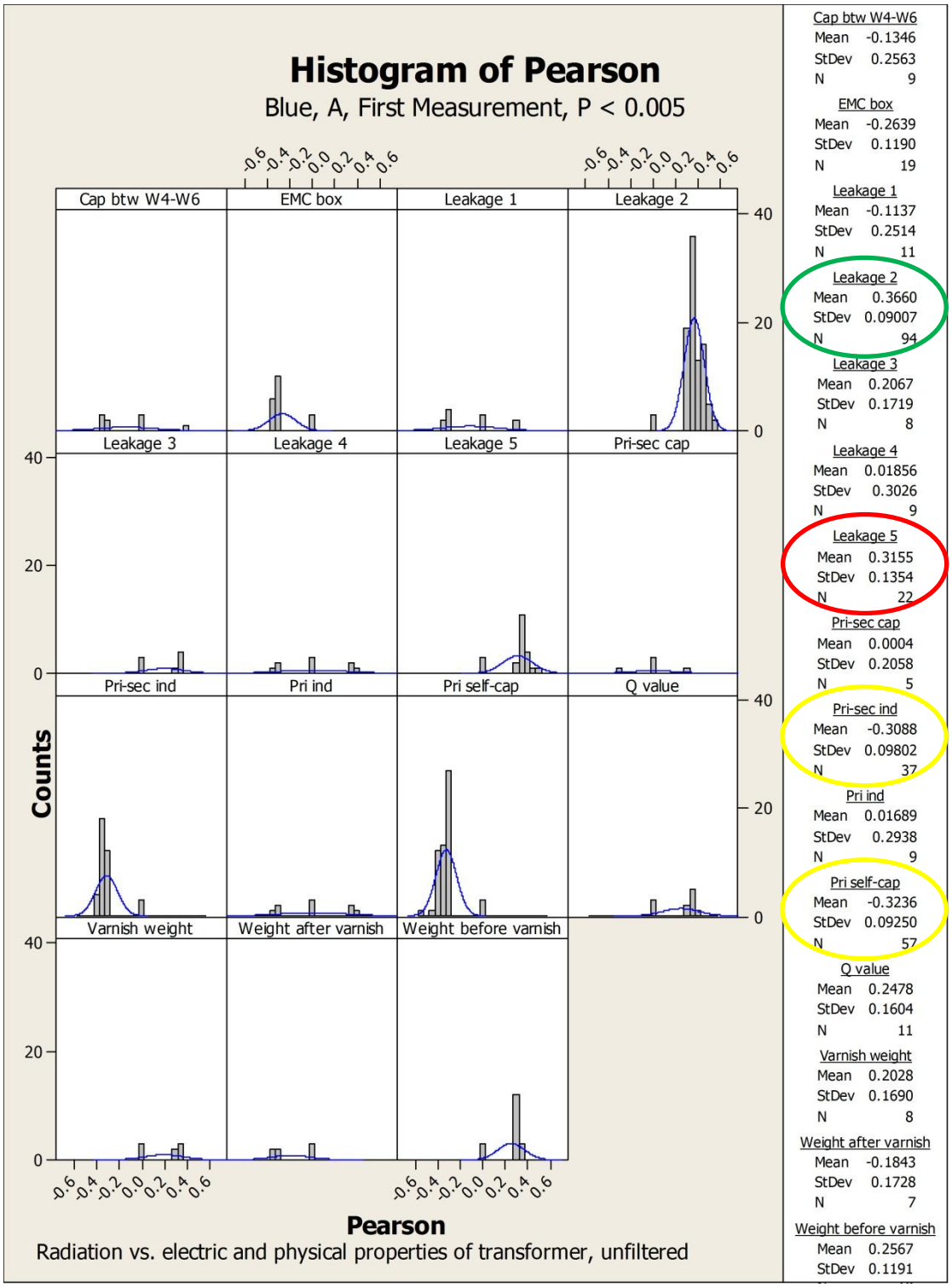

Figure G.1. *Pearson correlations between radiated emission levels and the measured transformer properties in the first measurement with only vertical orientation and supplier A's transformers, and with the condition P<0.005. Red circling highlights a property with a consistent but slight correlation, yellow circling that with a consistent and moderate correlation, and green circling that with a consistent and strong correlation.*

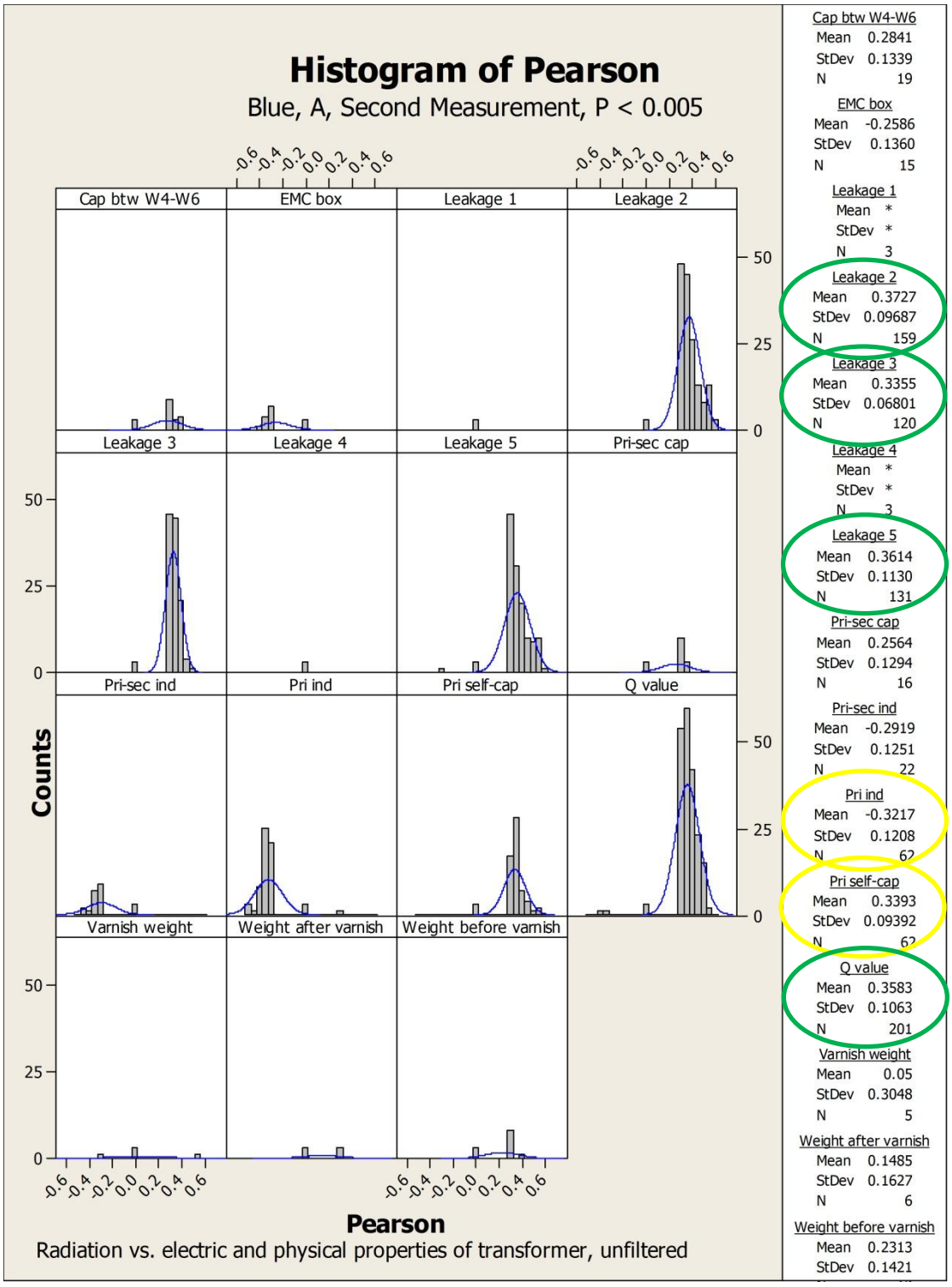

Figure G.2. *Pearson correlations between radiated emission levels and the measured transformer properties in the second measurement with only vertical orientation and supplier A's transformers, and with the condition P<0.005. Red circling highlights a property with a consistent but slight correlation, yellow circling such with a consistent and moderate correlation, and green circling such with a consistent and strong correlation.*

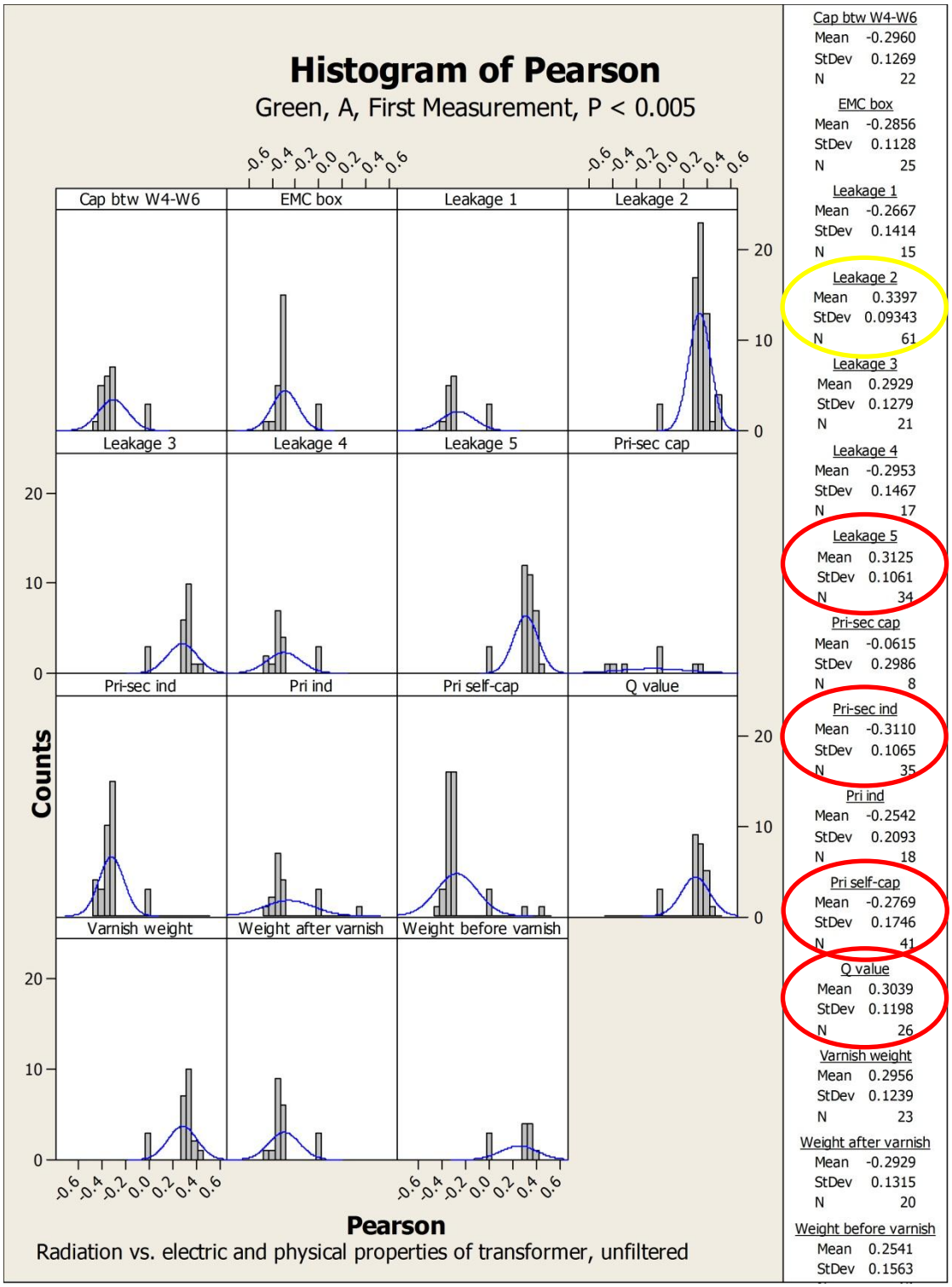

Figure G.3. *Pearson correlations between radiated emission levels and the measured transformer properties in the first measurement with only horizontal orientation and supplier A's transformers, and with the condition P<0.005. Red circling highlights a property with a consistent but slight correlation, yellow circling such with a consistent and moderate correlation, and green circling such with a consistent and strong correlation.*

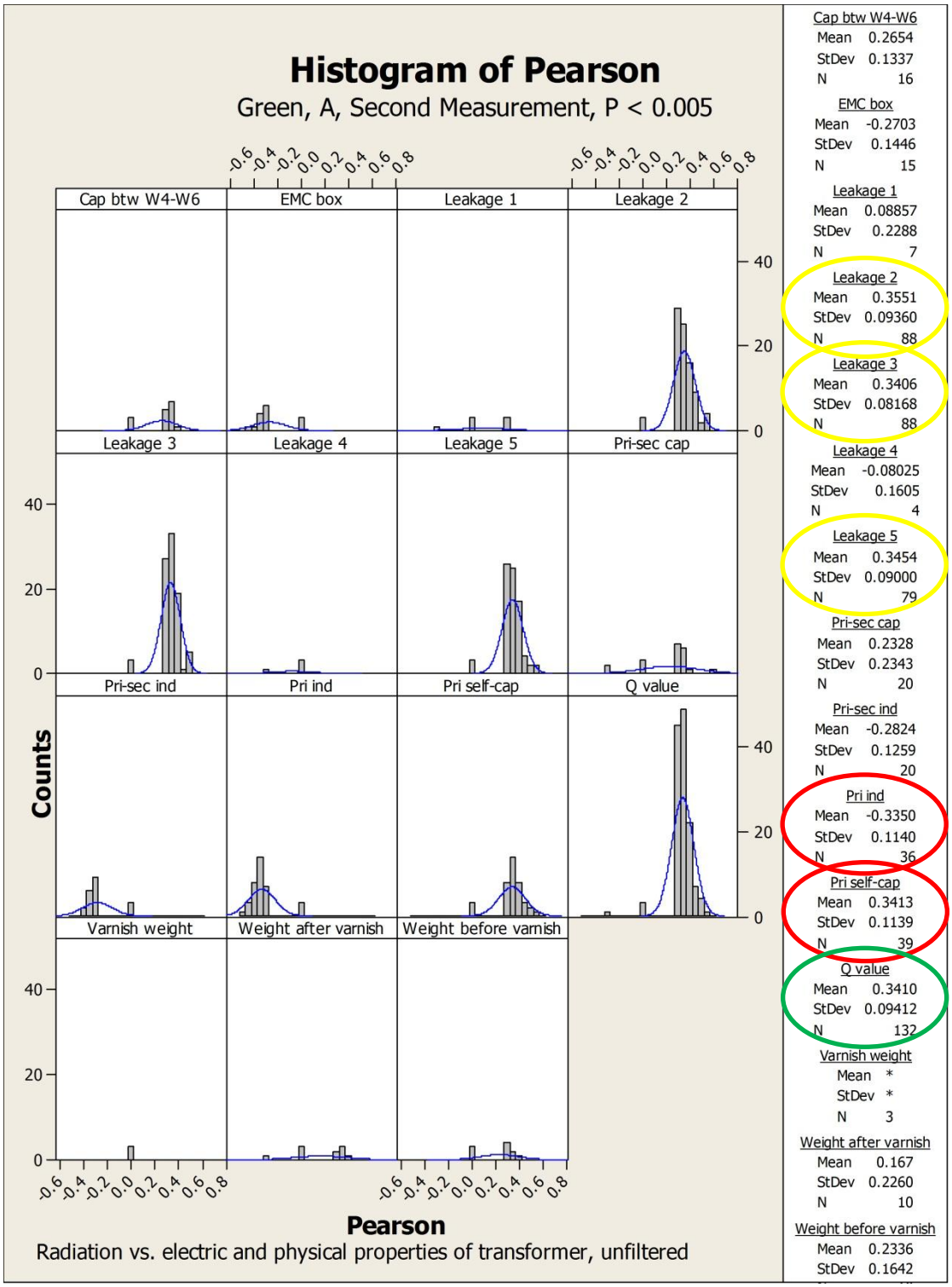

Figure G.4. *Pearson correlations between radiated emission levels and the measured transformer properties in the second measurement with only horizontal orientation and supplier A's transformers, and with the condition P<0.005. Red circling highlights a property with a consistent but slight correlation, yellow circling such with a consistent and moderate correlation, and green circling such with a consistent and strong correlation.*

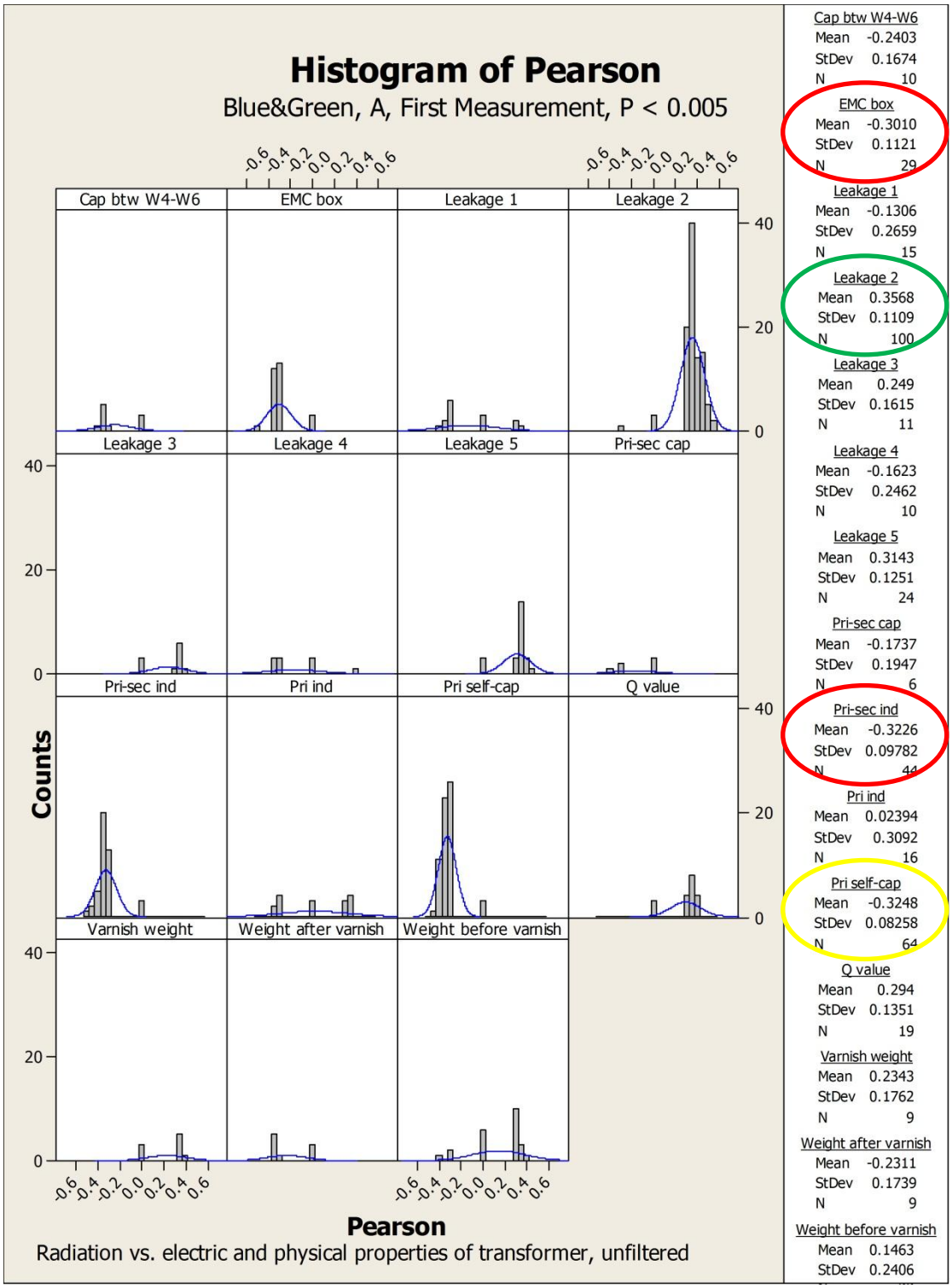

Figure G.5. *Pearson correlations between radiated emission levels and the measured transformer properties in the first measurement with both vertical and horizontal orientation but only supplier A's transformers, and with the condition P<0.005. Red circling highlights a property with a consistent but slight correlation, yellow circling such with a consistent and moderate correlation, and green circling such with a consistent and strong correlation.*

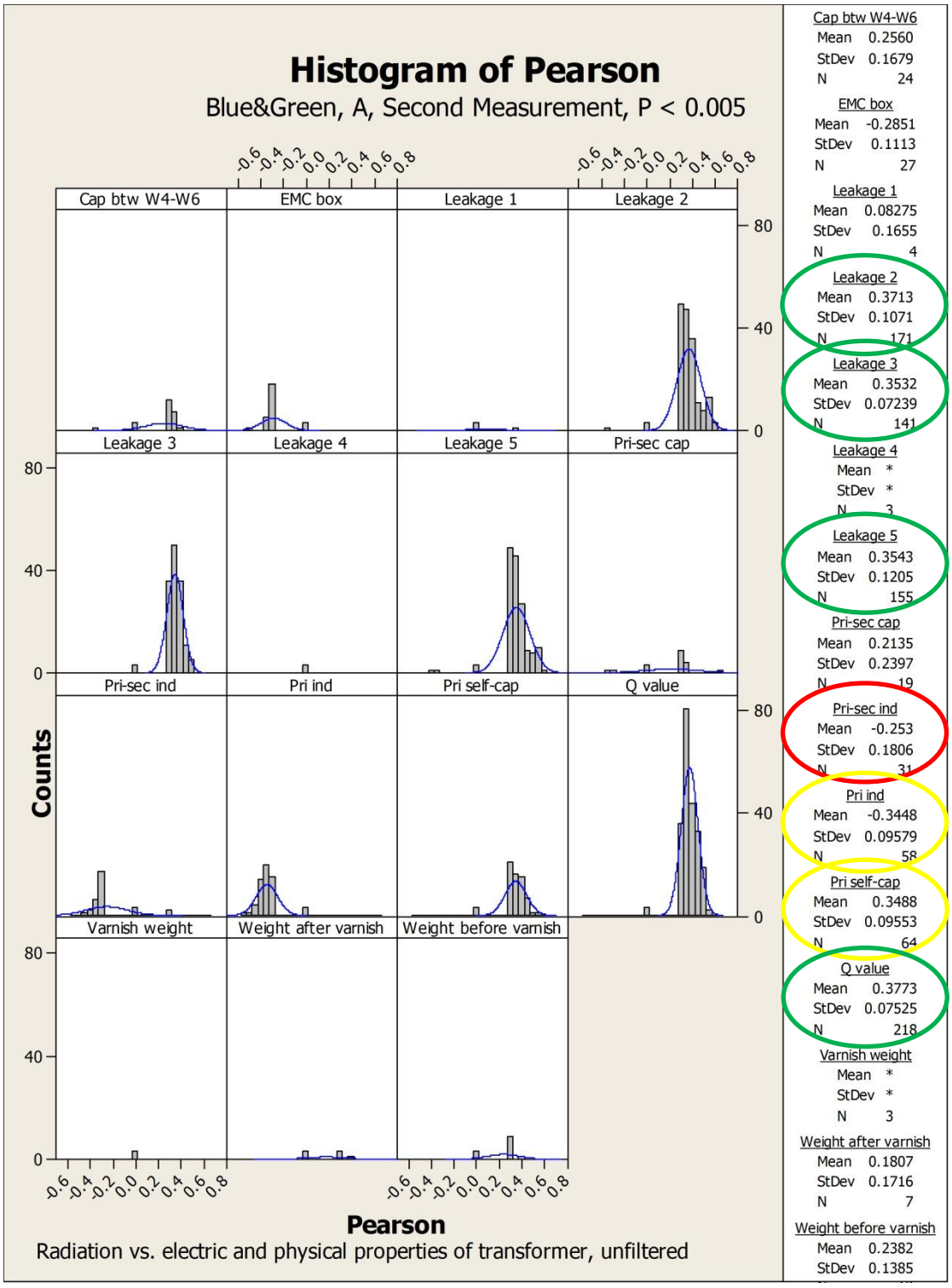

Figure G.6. *Pearson correlations between radiated emission levels and the measured transformer properties in the second measurement with both vertical and horizontal orientation but only supplier A's transformers, and with the condition P<0.005. Red circling highlights a property with a consistent but slight correlation, yellow circling such with a consistent and moderate correlation, and green circling such with a consistent and strong correlation.*

APPENDIX H – Correlations at Selected "Best" Frequency Points with Each Probe

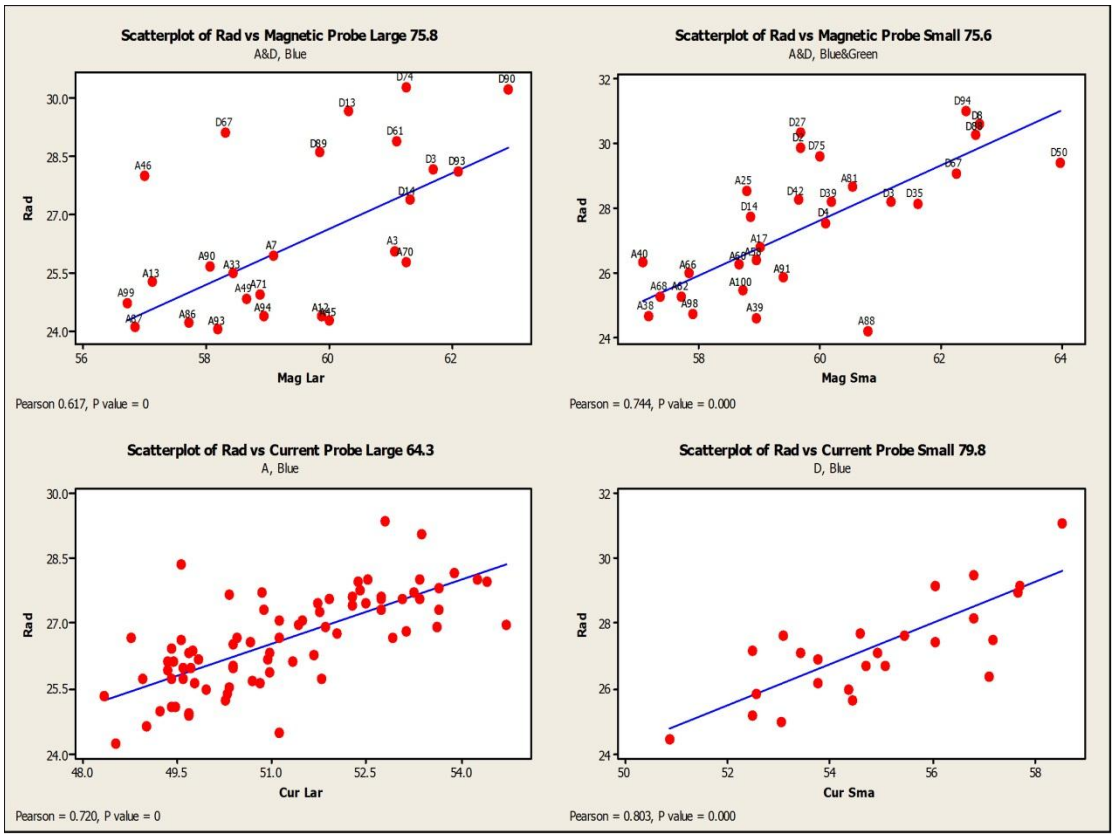

Figure H.1. *A selected well-correlating frequency point presented as a graph for each near-field probe; also filtering was used.*